TECHNISCHE UNIVERSITÄT MÜNCHEN
Lehrstuhl für Systembiologie der Pflanzen

Macrophage-Related Interaction Pathways in Tumor Stroma

Simone Salome Gusenbauer

Vollständiger Abdruck der von der Fakultät Wissenschaftszentrum Weihenstephan für Ernährung, Landnutzung und Umwelt der Technischen Universität München zur Erlangung des akademischen Grades eines

Doktors der Naturwissenschaften

genehmigten Dissertation.

Vorsitzender: Univ.-Prof. Dr. K. Schneitz

Prüfer der Dissertation: 1. Univ.-Prof. Dr. C. Schwechheimer

2. Hon.-Prof. Dr. A. Ullrich (Eberhard-Karls-Universität Tübingen)

Die Dissertation wurde am 22.03.2012 bei der Technischen Universität München eingereicht und durch die Fakultät Wissenschaftszentrum Weihenstephan für Ernährung, Landnutzung und Umwelt am 23.05.2012 angenommen.

To my family

1 INTRODUCTION 1

1.1 Composition of the tumor stroma 1
1.1.1 Tumor stroma ECM 2
1.1.2 Cells of the tumor stroma 2
1.1.2.1 Fibroblasts 3
1.1.2.2 Blood vessel cells 3
1.1.2.3 Cells of the Immune System 4

1.2 Tumor-associated macrophages 5

1.3 Inflammation and tumorigenesis 7

1.4 Tumor stroma interaction pathways 8
1.4.1 EGFR family signaling 9
1.4.2 HGF/Met signaling 12
1.4.3 STAT3 signaling 14

1.5 Targeting tumor-associated macrophages for cancer therapy 16

2 SPECIFIC AIMS 18

3 MATERIAL AND METHODS 19

3.1 Material sources 19
3.1.1 Laboratory hardware 19
3.1.2 Laboratory chemicals and biochemical 20
3.1.3 Chemicals and other material for SILAC and MS analysis 21
3.1.4 Enzymes 21
3.1.5 Kits and other materials 22
3.1.6 Growth factors and ligands 22
3.1.7 Media 23
3.1.7.1 Bacterial media 23
3.1.7.2 Cell culture media 23
3.1.8 Stock solutions and commonly used buffers 23
3.1.9 Cells 26
3.1.9.1 Human cell lines 26

3.1.9.2 Mouse cell lines 26
3.1.9.3 Primary human cells 27
3.1.9.4 Primary murine monocytes and macrophages 27
3.1.9.5 Bacterial strains 27
3.1.10 Antibodies 28
3.1.10.1 Primary antibodies for Western blot 28
3.1.10.2 Primary antibodies for immunoprecipitation 29
3.1.10.3 Secondary antibodies for Western blot 29
3.1.10.4 Antibodies for ELISA 29
3.1.10.5 Antibodies for FACS 30
3.1.10.6 Blocking antibodies 31
3.1.11 Oligonucleotides and Plasmids 31
3.1.11.1 Primary vectors 31
3.1.11.2 Constructs 32
3.1.11.3 siRNA oligonucleotides (human specific) 32
3.1.11.4 Primers for real-time PCR (human specific) 32
3.1.11.5 Primers for real-time PCR (mouse specific) 33
3.1.12 Software 34

3.2 Methods 34
3.2.1 Methods in molecular biology 34
3.2.1.1 Cultivation and maintenance of bacterial strains 34
3.2.1.2 Preparation of competent bacteria 34
3.2.1.3 Transformation of competent bacteria 35
3.2.1.4 Amplification of plasmids 35
3.2.1.5 Plasmid Purification 35
3.2.1.6 RNA isolation and cDNA synthesis 35
3.2.1.7 Quantitative real-time PCR analysis 36
3.2.2 Methods in mammalian cell culture 36
3.2.2.1 General cell culture techniques 36
3.2.2.2 Growth factor stimulation and inhibitor treatment 36
3.2.2.3 Isolation of primary human peripheral blood monocytes 37
3.2.2.4 Isolation of primary murine peritoneal macrophages 37
3.2.2.5 Isolation of primary murine spleen monocytes 38
3.2.2.6 Isolation of primary murine bone marrow monocytes 38
3.2.2.7 Treatment of human macrophages with cancer cell conditioned medium 39

3.2.2.8 Treatment of murine monocytes/macrophages with cancer cell conditioned medium....39
3.2.2.9 Coculture experiment....39
3.2.2.10 Preparation of cell culture conditioned media (CM)....40
3.2.2.11 Treatment of CM with blocking antibodies....40
3.2.2.12 Preparation of human serum....40
3.2.2.13 Heat inactivation of human serum....41
3.2.2.14 Preparation of gelatin coated plates....41
3.2.2.15 Transfection of mammalian cells....41
3.2.3 Protein analytical methods....42
3.2.3.1 Lysis of cells with Triton X-100 lysis buffer....42
3.2.3.2 Determination of protein concentration in cell lysates....42
3.2.3.3 Immunoprecipitation of proteins....42
3.2.3.4 SDS-polyacrylamide-gelelectrophoresis (SDS-PAGE)....43
3.2.3.5 Western Blotting....43
3.2.3.6 Immunoblot detection....43
3.2.3.7 Stripping....43
3.2.3.8 ELISA....44
3.2.4 Analysis of whole cell-based assays....44
3.2.4.1 Migration assay....44
3.2.4.2 MTT assay....45
3.2.4.3 FACS analyses....45
3.2.5 SILAC experiments and MS analysis....46
3.2.5.1 Cell culture in SILAC medium....46
3.2.5.2 Stable isotope labeling, cell lysis and anti-EGFR immunoprecipitation for mass spectrometry....46
3.2.5.3 Mass spectrometry analysis....46

4 RESULTS....47

4.1 HGF-mediated EGFR paracrine crosstalk....47
4.1.1 HGF-induced EGFR ligand release....47
4.1.1.1 Identification of HGF-induced EGFR ligands in SCC9 cells....47
4.1.1.2 HGF-induced EGFR ligand release is a common characteristic of cancer cells and depends on new protein synthesis....49
4.1.1.3 Metalloprotease-dependent shedding of EGFR ligands....51
4.1.1.4 CM of a monocytic cell line induces EGFR ligand induction via HGF/Met....52

4.1.1.5 Identification of the pathway underlying EGF ligand induction 52
4.1.1.6 TGFα is a strong inducer of directed cell migration in SCC9 cells 54
4.1.2 HGF-induced EGFR negative regulation 55
4.1.2.1 HGF is a paracrine inhibitor of classical EGFR activation 55
4.1.2.2 Loss of EGFR TK activity is independent of an autocrine EGFR feedback loop 55
4.1.2.3 Pathway underlying EGFR TK blockage 57
4.1.2.4 Loss of EGFR TK activity is independent of the EGFR negative regulator Mig6 57
4.1.2.5 HGF leads to impaired EGFR-mediated migration 58
4.1.2.6 HGF induces various EGFR interactions 59
4.1.2.7 HGF leads to enhanced survival upon gefitinib treatment 62
4.1.2.8 HGF-induced EGFR interactions are resistant to gefitinib treatment 63
4.1.2.9 Met TK-inhibition restores gefitinib sensitivity 64
4.1.2.10 HGF-induced EGFR TK blockage is a characteristic of cancer cells 65
4.1.2.11 Similar to EGFR, also HER2 and HER3 activation is blocked upon HGF treatment 66

4.2 Interaction pathways between breast cancer cells and macrophages in human and mouse 67
4.2.1 Interaction pathways between breast cancer cells and human macrophages 67
4.2.1.1 Characterization of human macrophages 67
4.2.1.2 HB-EGF and OSM release in tumor-educated macrophages 67
4.2.1.3 Morphology change of human macrophages after treatment with cancer cell CM 70
4.2.2 Generating an in vitro mouse model 70
4.2.2.1 Screen for mouse reporter cell lines 70
4.2.2.2 Characterization of mouse peritoneal macrophages 72
4.2.2.3 Morphology change of mouse macrophages after treatment with cancer cell CM 72
4.2.2.4 OSM release in tumor-educated mouse macrophages 72
4.2.2.5 OSM transcript and EGFR ligand transcript induction in tumor-educated macrophages 74
4.2.2.6 OSM release in bone marrow and spleen-derived monocytes 76

5 DISCUSSION 78

5.1 HGF-mediated EGFR paracrine crosstalk 78
5.1.1 HGF is a potent paracrine inducer of EGFR ligands 78
5.1.2 HGF-induced EGFR negative regulation 80

5.2 Interaction pathways between breast cancer cells and macrophages in human and mouse 82

6 SUMMARY 85

7 ZUSAMMENFASSUNG 86

8 REFERENCES 87

9 APPENDIX 96

9.1 Abbreviations 96

9.2 Acknowledgements 100

1 INTRODUCTION

Cancer is a leading cause of death in developed countries. Within the adult population, epithelial cancers are—with 83%—the most frequent cancer types (1). The deadliest cancers are in men those of lung, colon and prostate, and in women, those of breast, colon and lung (2).

Based on observations in the early twentieth century that some cancers are familial, scientists began to search for genetic changes that might underlie cancer development. Dominant gain-of-function and recessive loss-of-function alterations in critical gatekeeper genes, e.g., oncogenes and tumor-suppressor genes, have been identified and characterized during the last decades. Tumorigenesis is now recognized as a multistep process during which cancer cells accumulate multiple and sequential genetic alterations affecting intrinsic cellular programs, such as cell proliferation, cell death, differentiation, metabolism, and cell adhesion (3, 4).

During the last two decades it has been increasingly recognized that the surrounding tissue, or so-called tumor stroma, plays an important part in neoplastic growth (5, 6). Thus, tumors are regarded as complex organs consisting of two distinct but interdependent compartments: the tumor epithelial cells themselves and the stroma in which they disperse. During the neoplastic process somatic genetic alterations occur in both, tumor cells and stromal cells—also referred to as tumor stroma co-evolution (7). Stromal cells are a heterogeneous mixture of different cell lineages. It is believed, that tumorigenesis cannot proceed without active cooperation from the stroma. This cooperation influences tumor establishment, progression and dissemination (5). When viewed from this perspective, the biology of a tumor can only be understood by studying the cancer cells themselves as well as the ‘‘tumor microenvironment’’ that they construct during the multistep tumorigenesis.

1.1 Composition of the tumor stroma

The tumor stroma is mainly composed of extracellular matrix (ECM) molecules, fibroblasts, endothelial cells and inflammatory cells. Tumor cells interact with the stroma either physically or via paracrine

signaling molecules. These interactions are well-organized and follow highly regulated signaling pathways, which are involved in cell growth, survival, migration, differentiation and ECM metabolism (5).

1.1.1 Tumor stroma ECM

The extracellular matrix (ECM) is a substantial part of the extracellular space in animal tissue. Beyond providing mechanical support, the ECM also provides pathways for cellular migration, delivers essential survival signals, and sequesters important growth factors. It is mainly composed of five classes of macromolecules: collagens, elastin, proteoglycans, hyaluronan, and adhesive glycoproteins. Local cells—mainly fibroblasts and pericytes—secrete the matrix macromolecules. The basement membrane is a specialized form of ECM that separates tissue compartments and provides scaffold for all epithelial and endothelial cells (8). During tumor development ECM is altered in various ways. These modifications include basement membrane dissolution via matrix degrading enzymes, which is one of the first steps in tumor invasion and metastasis. Another modification is the synthesis of new matrix components, which results in a dense, stiff and linear accumulation of fibrillar collagens (9, 10). This dense fibrosis around the tumor—also referred to as desmoplasia—is common in several types of cancer, e.g., breast, colon, lung, pancreatic and prostate and is diagnostic of many tumors. Tumor-associated ECM also serves as a local depot for growth factors and angiogenesis factors. Vascular endothelial growth factor (VEGF), basic fibroblast growth factor (bFGF) and tumor necrosis factor (TNF) are highly expressed in developing tumors but due to the fact that they bind to ECM molecules and cell surfaces, their bioactivity is limited. The release of these growth factors is regulated by extracellular proteases, including matrix metalloproteases (MMPs) which are produced by tumor cells as well as stromal cells (5, 9).

1.1.2 Cells of the tumor stroma

Besides the ECM components, the tumor stroma is constituted of different cell types including fibroblasts, cells of the blood vasculature and inflammatory cells (5, 11).

1.1.2.1 Fibroblasts

Fibroblasts are connective-tissue cells, which synthesize components of the ECM, as well as proteases, their inhibitors, and soluble paracrine growth factors (12, 13). Fibroblasts from different regions vary in the classes of biologically active molecules that they produce (14). Tumor fibroblasts, which are also called myofibroblasts or carcinoma-associated fibroblasts (CAFs), are unique and undergo dynamic changes during tumor progression. Compared with fibroblasts in normal tissues, CAFs are characterized by a higher proliferative rate, enhanced migratory behavior and the expression of α-smooth muscle actin, fibroblast-specific protein, fibroblast-activating protein and desmin (5, 14, 15). The majority of CAFs originates from tissue-resident mesenchymal stem cells as well as from bone marrow-derived mesenchymal stem cells (16). CAFs exert an active role in promoting neoplastic programming of tissues. They are responsible for synthesis, deposition and remodeling of most of the tumor ECM (15, 16). They promote, together with immune cells, angiogenesis and cancer cell proliferation via the production of fibroblast growth factor (FGF) family members, insulin-like growth factor (IGF) family members, epidermal growth factor (EGF) family members, hepatocyte growth factor (HGF) and the STAT3 activators IL-6, leukemia inhibitory factor (LIF) and oncostatin M (OSM) (15-17). Moreover a recent study showed that CAFs are able to induce resistance to EGFR-targeted anticancer therapy in a HGF dependent mechanism (18).

During cancer progression somatic changes occur not only in tumor cells but also in CAFs, resulting in a stable phenotype of the latter. High frequencies of somatic genetic aberrations in CAFs, such as gene copy number alterations, loss of heterozygosity, microsatellite instability, and point mutations in tumor suppressor genes were found in many different cancer types including those of the breast, colon, prostate, ovary, head and neck and bladder (7).

1.1.2.2 Blood vessel cells

Angiogenesis, the growth of new blood vessels, is essential during all tissue repair and growth processes as well as during cancer development. Blood vessels are composed of endothelial cells, pericytes or smooth muscle cells and ECM. The mural cell component in capillaries and small vessels is comprised of pericytes, whereas in larger vessels it is comprised of smooth muscle cells. Angiogenesis is regulated by

local changes in the balance between soluble and insoluble molecules that induce either pro- or antiangiogenic signaling on endothelial cell and pericyte proliferation, differentiation, migration and tube formation (5).

Without the formation of new blood vessels, tumor growth is limited to 1–2 mm in size, because of insufficient supply of nutrients and oxygen (19). This theory was first proposed by Judah Folkman in 1971 (20). Tumors of this size can stay dormant for many years and are therefore clinically undetectable. A disequilibrium between pro- and antiangiogenic regulators can finally result in the construction of new blood vessels in these tumors—the so-called angiogenic switch. An important promoter of tumor angiogenesis is hypoxia, resulting in enhanced expression of proangiogenic factors, such as VEGF, bFGF and IL-8, and in decreased expression of antiangiogenic factors, such as angiostatin, platelet factor-4 and thrombospondin (19, 21).

1.1.2.3 Cells of the Immune System

Immune cells can be classified into two major subgroups: the innate immune system and the adaptive immune system. The innate immune system includes macrophages, dendritic cells, mast cells, natural killer cells, eosinophils and neutrophils, which provide an immediate but not specific response against foreign pathogens. Besides this first line of defense, the innate immune system also stimulates other cell functions like wound repair, angiogenesis and activation of the adaptive immune system. The adaptive immune system includes B and T lymphocytes which are highly specific and are able to confer long-lasting and protective immunity. Immune cells at the site of infection derive from circulating blood cells as well as from local proliferation. Recruitment of immune cells to the site of the tumor occurs actively via tumor-derived signals, such as chemoattractant cytokines (5).

Innate and adaptive inflammatory cells are found in the stroma of all solid tumors. This can be a sign of an ongoing antitumor response or represent a well-directed recruitment by the tumor for its own benefit (22). The first possibility, also known as the “immune-surveillance” theory, has shown that infiltration of tumors by subsets of B and T lymphocytes can be beneficial in retardation of tumor growth. This antitumorigenic process largely depends on new cancer-specific antigens expressed on the surface of tumor cells, but also depends on stress, necrosis and other immunostimulatory signals.

Immune-surveillance relies on CD8+ cytotoxic T cells, natural killer cells, antigen presenting dendritic cells and CD4+ Th1 cells as well as on antibody producing B cells (5, 23, 24).

However, tumors have the ability to mutate, evolve and rapidly proliferate. Hence, the cancer can easily handle the attacking immune cells through the development of low-immunogenic or resistant clones or by directly subverting the antitumor immune response and use it for tumor promotion. This process, also called “immune escape” or “tumor tolerance” is very well assured by the fact, that advanced tumors are rarely rejected, although they exhibit a high immune cell infiltration (23). Different tumor-promoting immune cells, like macrophages, mast cells, neutrophils, B cells and certain T cell subsets including Th2, Th17 and T regulatory cells (Treg) cells are frequently found to be concentrated in tumors (23-25).

The composition of cancer-associated immune cells differ depending on the tumor type and stage of tumorigenesis (5).

1.2 Tumor-associated macrophages

The normal physiological functions of macrophages are the removal of apoptotic cells, cell debris and invading microbes, remodeling of matrix components, the release of growth factors as well as T cell stimulatory cytokines and the presentation of antigens to T cells. These multifunctional cells are capable to alter their phenotype in order to suit the microenvironment in which they reside. Macrophages in tumors—usually called tumor-associated macrophages (TAMs)—mainly derive from blood monocytes which differentiate into TAMs when they migrate (extravasate) through blood vessels into the tumor. Monocyte recruitment to the site of the tumor is driven by chemoattractants secreted by both malignant and stromal cells (26-29). The main chemoattractant is CCL2 (30). TAMs are a significant component of solid tumors and are present throughout the tissue. However, only a few studies have correlated a high number of TAMs with good patient prognosis. In over 80% of published studies a high TAM number have been clinically linked to poor prognosis and malignant progression in numerous types of cancers, including carcinomas of bladder, brain, breast, cervix, lung, prostate and thyroid (26, 31-34).

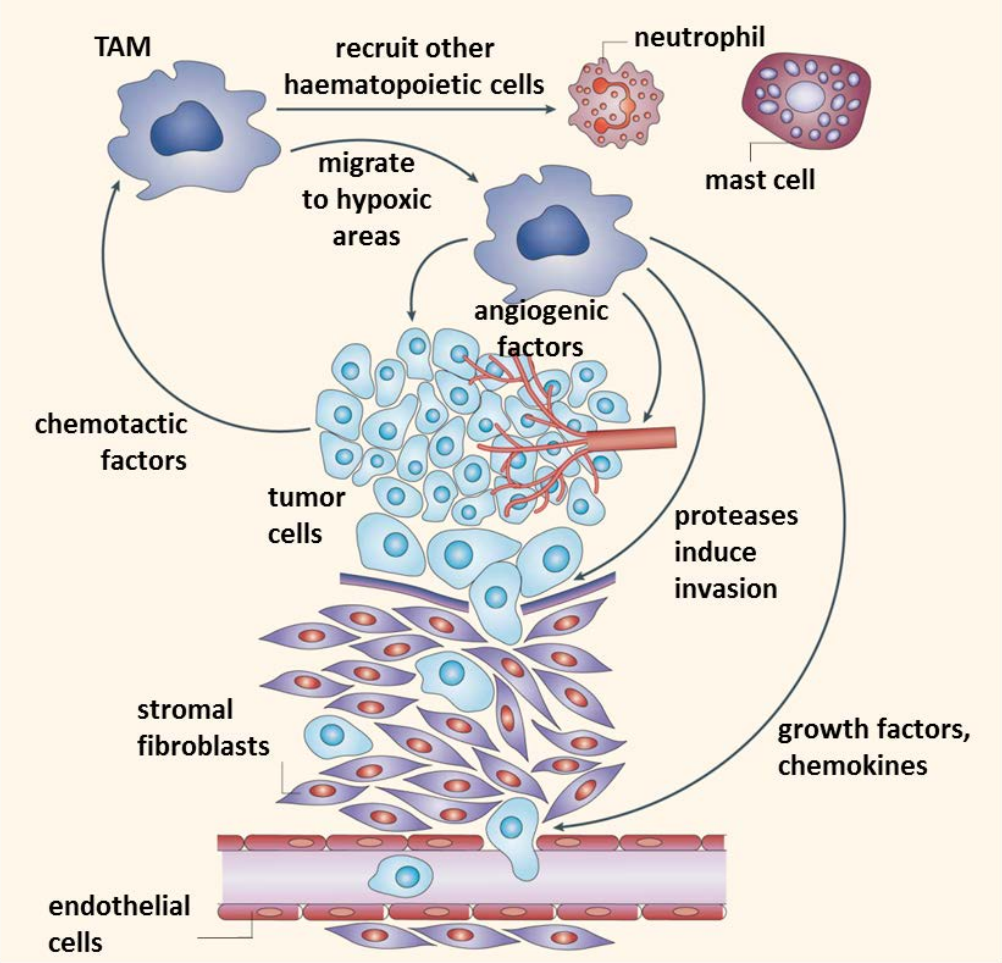

Figure 1. Tumor-promoting functions of tumor-associated macrophages. Macrophages and their precursors are recruited to the tumor site via chemoattractants, where they promote tumor development and metastasis. Tumor-associated macrophages (TAMs) migrate to hypoxic areas, where they enhance angiogenesis by the expression of proangiogenic factors such as VEGF, bFGF, TNF, angiopoietin-1, angiopoietin-2. In addition TAMs recruit other haematopoietic cells (e.g. mast cells and neutrophils) which can perform similar functions. Furthermore TAMs produce proteases that break down the basement membrane and thereby promote invasion of cancer cells. TAMs secrete different growth factors and chemokines (e.g. HGF, EGFR-family ligands, PDGF, transforming growth factor-β (TGFβ) and IL-8) that provide proliferative and anti-apoptotic signals to cancer cells and induce their migration towards blood vessels (35). The figure was adapted from Pollard, 2004 (35).

TAMs support malignant progression in many ways (Fig. 1): They reorganize the ECM by secreting matrix proteins and matrix degrading enzymes, like MMPs so that solid tumors can grow throughout the basement membrane and invasive front (27). Rodent models of breast cancer have demonstrated that TAMs promote tumor cell proliferation, invasion, metastasis and angiogenesis by synthesizing growth

factors (e.g. HGF, EGFR-family ligands, platelet-derived growth factor (PDGF) and transforming growth factor-β) and angiogenesis growth factors (e.g. VEGF, bFGF, TNF, angiopoietin-1, angiopoietin-2). Moreover TAM secreted cytokines, such as IL-10, CCL17 and CCL22 alter the composition and function of inflammatory cells in the tumor environment, making them less capable of generating an effective antitumor response (5, 27-29, 33, 35-37). TAMs further enhance the ability of tumor cells to enter blood vessels (intravasation) in an EGFR/CSF-1 dependent loop (27). And finally, the rate of mammary tumor progression and metastasis was shown to be almost completely ablated in mice harboring a homozygous null mutation of the macrophage growth factor CSF-1 (38, 39).

1.3 Inflammation and tumorigenesis

Inflammation is a protective response of the organism to injury or infection. During this complex reaction, injurious stimuli are subsequently removed and the healing process of damaged tissue is initiated. If this fundamental response goes awry, it can become a major cofactor in the pathogenesis of several chronic human diseases, including cancer.

In the nineteenth century Rudolf Virchow noted leukocytes in neoplastic tissues and made the first connection between chronic inflammation and cancer. Clear evidence has been obtained during the last decade that an inflammatory environment is an essential component of all solid tumors. It is now generally accepted that inflammation plays decisive roles in tumor development, including initiation, promotion, malignant conversion, invasion, and metastasis and that it also affects immune-surveillance and responses to therapy (40, 41).

With regard to the time of occurrence, there are three main types of cancer-associated inflammation. The first type precedes malignant transformation and thus acts as a tumor initiator. Several chronic inflammatory diseases increase the risk of cancer development. For example, persistent infection with *Helicobacter pylori* has been linked to gastric cancer. Inflammations in response to hepatitis B (HBV) or C (HCV) viruses can trigger hepatocellular carcinoma. Inhaled asbestos and tobacco smoke can induce chronic inflammations that can cause mesothelioma and lung cancer. A detailed list of cancers related to inflammation is provided in table 1. In total, pre-existing inflammatory conditions are responsible for 15–20% of cancers worldwide (40, 42-44). The mechanism underlying this first type involves the release

of cytokines as well as the release of reactive oxygen species and reactive nitrogen species (45). The second type of cancer-associated inflammatory response follows tumor development. Most, if not all solid cancers trigger an intrinsic inflammatory response, which is similar to the one that is activated during wound healing. However, in the case of the tumor, the inflammatory response is never turned off—as Dvorak suggested in 1986: “a tumor is a wound that does not heal” (46, 47). The mechanisms underlying the second type are numerous and include enhancement of proliferation and survival as well as the angiogenic-switch. In many cases oncogenes are involved that target directly or indirectly pro-inflammatory pathways. Examples are the oncogene Ras, which activates the transcription of the inflammatory cytokine interleukin-8, and the oncogenes c-myc as well as bcl-2 which inhibit apoptosis thereby leading to necrotic cancer cell death and release of damage-associated molecular pattern molecules. In both cases, the resulting host response is inflammation that promotes tumor growth and invasion (43, 48). Another major tumor-promoting mechanism is the production of cytokines by immune cells that activate transcription factors, like AP-1, STAT3 and NFκB, which induce genes that trigger proliferation and survival in tumor cells (40, 41). The third type of tumor-associated inflammation is induced by cancer therapy. As a result of chemotherapy and radiation, cancer cells and the surrounding tissue undergo necrotic cell death, which in turn can trigger inflammatory reactions, that can act either protumorigenic or antitumorigenic. It has been found, for example, that therapy-induced inflammation accelerates the re-growth of prostate cancer in mice (49). Hence, inhibition of therapy-associated inflammation may increase tumor free survival in the case of prostate cancer patients (40). An antitumorigenic immune function was shown by Zhang et al. (50); using radiation or chemotherapy in a mouse tumor model they were able to sensitize cancer stroma for destruction by T lymphocytes so that the tumors were eradicated. The chemotherapy/irradiation caused apoptosis and necrosis of cancer cells, which was sufficient for the release of antigen to activate stromal cells and for the destruction by cytotoxic T lymphocytes (50).

1.4 Tumor stroma interaction pathways

Tumor-stromal cell interactions are mediated by soluble paracrine signals or by direct cell contact to potentiate and support the survival of the tumor cells. Among the most important malignant pathways

Table 1. Chronic inflammatory conditions associated with cancer. The table was adapted from Tlsty and Coussens, 2005 (5)

Inflammatory stimulus	Malignancy
Silica, Asbestos	Mesothelioma, Lung carcinoma
Smoking (nitrosamines, peroxides)	Lung carcinoma
Reflux esophagitis, Barrett's esophagus	Esophageal carcinoma
Cystitis, bladder inflammation	Bladder cancer
Helicobacter pylori	Gastric cancer, MALT lymphoma
Hepatitis virus (B and C)	Hepatocellular carcinoma
Epstein-Barr virus	B-cell non-Hodgkin's lymphoma, Burkitts lymphoma
Pelvic inflammatory disease, chronic cervicitis	Ovarian cancer
Inflammatory bowel disease, Crohn's disease, chronic ulcerative colitis	Colorectal cancer
Human immunodeficiency virus, Human herpes virus type 8	Non-Hodgkin's lymphoma, squamous cell carcinoma, Kaposi's sarcoma

are the EGFR, the HGF/Met and the STAT3 pathway. All three of them provide promising targets for anticancer therapy (51-56).

1.4.1 EGFR family signaling

The human epidermal growth factor receptor (EGFR/HER/ErbB) family members are, with few exceptions, expressed in tissues of mesodermal and ectodermal origin and play major roles in cellular processes including cell proliferation, differentiation, migration, invasion and survival (57, 58). All four EGFR family members are receptor tyrosine kinases (RTKs). They are as follows: EGFR (ErbB1/HER1), HER2 (ErbB2/Neu), HER3 (ErbB3) and HER4 (ErbB4). The HER receptors have in common an extracellular

domain for ligand-binding, a single membrane-spanning region and a cytoplasmic kinase domain with tyrosine autophosphorylation sites (58). 13 peptide ligands, which contain a conserved EGF domain, have been identified so far: EGF, heparin-binding EGF-like growth factor (HB-EGF), amphiregulin (AR), transforming growth factor-α (TGFα), epigen, epiregulin, betacellulin and the neuregulins (57). EGFR activation upon ligand binding to the extracellular domain is followed by receptor homo- or heterodimerization, autophosphorylation and finally the initiation of cellular responses—mainly via phosphatidylinositol 3-kinase (PI3K)-Akt and mitogen-activated protein kinase (MAPK) (Fig. 2)(59).

Two members of the EGFR family, HER2 and HER3, are non-autonomous receptors. HER2 cannot bind to extracellular ligands, whereas HER3 has a defective kinase domain. Both receptors, however, form heterodimers with other HER members in order to induce cellular signaling events (60). In normal cells HER-signaling is tightly controlled; indeed, in tumor cells receptor overexpression, activating mutations within their kinase domain as well as aberrant expression of HER ligands result in receptor hyperactivation (57, 58). Overexpression of HER-receptors and their ligands is positively correlated with aggressiveness and prognosis in many epithelial cancers (61, 62).

Several studies have shown a role of the tumor microenvironment in EGFR family signaling. Cancer cell migration and proliferation, for instance, can be induced by stromal cell-derived EGFR family ligands (63, 64). Furthermore tumor endothelial cells express EGFR and blocking EGFR activity was shown to inhibit their proliferation (65). An example of indirect involvement of the stroma is the formation of new blood vessels: upon EGFR family activation on tumor cells, the secretion of several proangiogenic factors, such as VEGF, IL-8, bFGF, angiopoietin-1 andangiopoietin-2 is induced, whereas expression of antiangiogenic factors, like thrombospondin, is down regulated. Treatment with anti-EGFR or anti-HER2 agents was shown to significantly reduce the production of angiogenic growth factors in cancer cells (66).

There are currently two main strategies for targeted anti-HER treatments. The first strategy includes the use of monoclonal EGFR-targeted antibodies like cetuximab (erbitux, ImClone/Merck) and panitumumab (vectibix, Amgenix) and the HER2-targeted antibody trastuzumab (herceptin, Genentech/Roche), which bind to the extracellular domain of the receptor. These neutralizing antibodies execute their anti-tumor effect by blocking receptor-ligand interactions as well as by inducing immune reactions, like antibody-dependent cell-mediated cytotoxicity. The second anti-HER strategy comprises EGFR tyrosine kinase

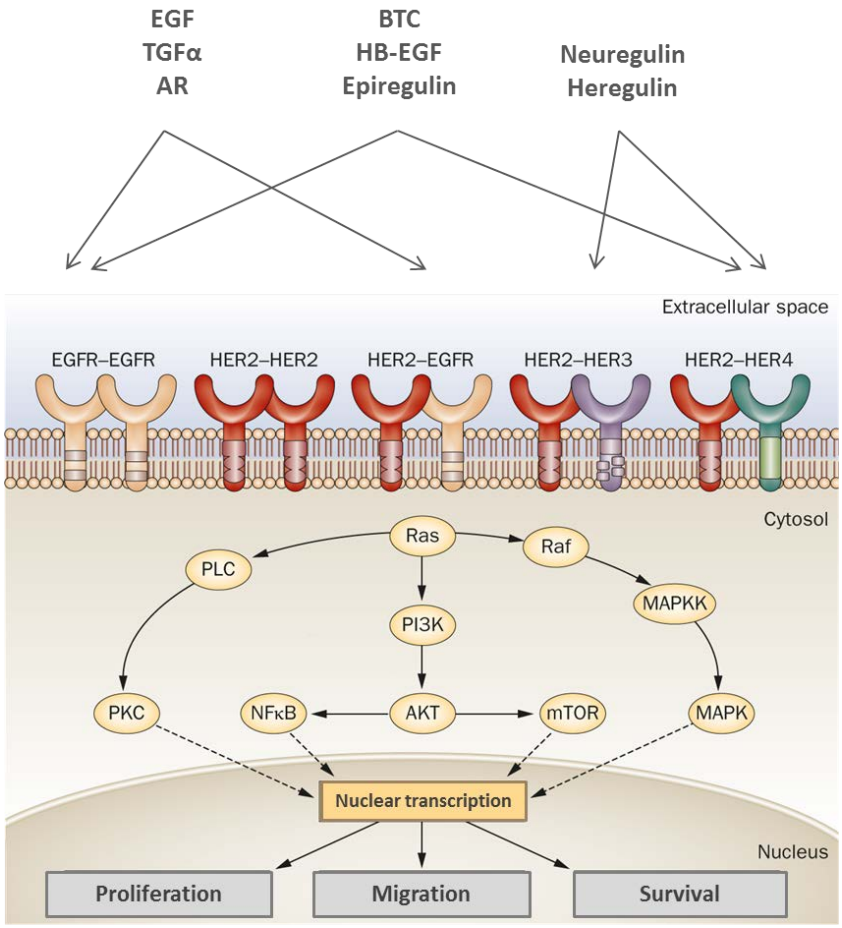

Figure 2. HER family member signaling. EGFR family ligands have different preferences for HER receptors. Ligand binding induces homo- or heterodimerization of the HER receptors and leads to the formation of several receptor combinations. The preferred dimerization partner for other HER receptors is HER2. Due to receptor dimerization, phosphorylation of the cytoplasmic tyrosine kinase domain and further activation of downstream signaling is induced. The cytoplasmic pathways consist of three major modules: PLCγ-PKC, Ras-Raf-MAPK and PI3K-Akt. Activation of these downstream cascades leads to transcriptional upregulation of genes involved in proliferation, migration and survival. Abbreviations: EGF, epidermal growth factor; TGFα, transforming growth factor α; AR, amphiregulin; BTC, betacellulin; HB-EGF, Heparin-binding EGF-like growth factor; EGFR, epidermal growth factor receptor; HER, human epidermal growth factor receptor; PLC, phospholipase C; PKC, protein kinase C; PI3K, phosphatidylinositol 3-kinase; NFκB, nuclear factor κB; mTOR, mammalian target of rapamycin; MAPK, mitogen-activated protein kinase; MAPKK, MAPK kinase. The figure was adapted from Fornaro et al., 2011 (67).

inhibitors (TKI), like gefitinib (iressa, AstraZeneca), erlotinib (tarceva, Genentech/OSI/Roche) and the dual inhibitor for EGFR/HER2 lapatinib (tykerb, GlaxoSmithKline). TKIs are competitive adenosine triphosphate analogues which prevent the binding of adenosine triphosphate to the intracellular TK domain of the HER receptors, thereby blocking TK activity and signal transduction. Anti-HER-targeted

therapies have been approved by the US Food and Drug Administration for the treatment of individual carcinomas of the head and neck (cetuximab), colorectal cancers (cetuximab, panitumumab), adenocarcinomas of the stomach or gastroesophageal junction (herceptin), breast cancers (herceptin, lapatinib) non-small-cell lung cancers (gefitinib, erlotinib) and pancreatic cancers (erlotinib) (59, 68).

The described anti-HER receptor treatments have all shown clinical efficacy. However, in several cases tumors do not show full response and some of the responders eventually develop resistance to anti-HER receptor treatment (69-71). This is why new EGFR treatment strategies such as combinatorial treatments are currently investigated in clinical trials.

1.4.2 HGF/Met signaling

HGF/Met signaling is involved in embryonic development and promotes tissue repair and regeneration (72, 73). Met belongs together with Ron to the MET proto-oncogene family, a subfamily of receptor tyrosine kinases. Hepatocyte growth factor/scatter factor (HGF/SF1) is the only known activating ligand for Met. Met is expressed primarily in cells of epithelial origin, whereas HGF expression is restricted to cells of mesenchymal origin (74-76). Met is a disulphide-linked heterodimer that is formed by proteolytic processing of a common precursor. The functional form of Met consists of an extracellular ligand-binding domain, which is constructed of the α-chain and a longer β-chain. The rest of the β-chain includes the single-pass transmembrane helix and the cytoplasmic portion. The latter contains the kinase domain with tyrosine autophosphorylation sites as well as a carboxy-terminal tail that is crucial for downstream signaling. Activation of Met upon ligand binding results in receptor homodimerization, autophosphorylation and finally in the recruitment of scaffolding proteins and signal transducers like Grb2 and Gab1 (growth-factor-receptor-bound protein 2 (Grb2)-associated binder 1)—which in turn, can bind SHP2 and PLCγ—PI3K and finally STAT3. These pathways alter gene expression of cell-cycle regulators, extracellular-matrix proteases and of cytoskeletal components thereby affecting proliferation, migration and invasion of tumor cells (Fig. 3) (74, 77).

Dysregulation of HGF/Met signaling is associated with various cancers (74). Cell lines that overexpress HGF and/or Met become tumorigenic and metastatic in athymic nude mouse models (78). HGF and/or Met overexpression often correlates with tumor invasiveness and metastatic potential and is a marker for poor patient prognosis (74, 79, 80). Notably, apart from the involvement in migratory processes, Met

activation was recently shown to confer resistance to EGFR family-targeted therapies in breast cancer, colon cancer and in non-small cell lung carcinomas (70, 81-84).

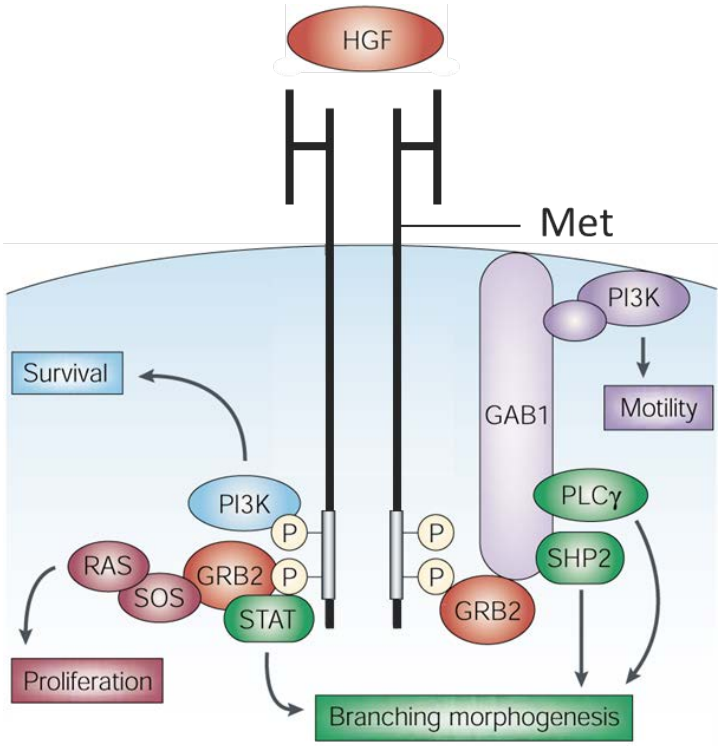

Figure 3. Met signaling pathways. After ligand-induced Met dimerization, the cytoplasmic tyrosine kinase domain phosphorylates and creates docking sites for signal transducers and for adaptor proteins that have a scaffolding function, such as Grb2-associated-binding protein 1 (Gab1). Gab1 provides additional binding sites for PI3K, SHP2 and PLCγ thereby amplifying signaling outputs. HGF stimulation induces transcriptional upregulation of genes involved in survival, migration and proliferation and branching morphogenesis. The figure was adapted from Trusolino and Comoglio, 2002 (77).

Many types of carcinomas express or overexpress Met. However, in these tumors the ligand is produced not by the tumor cells, but by the stromal cells (fibroblasts and monocytes/macrophages). Therefore Met activation in tumor cells can only occur in a paracrine manner, with the exception of a ligand-independent activation in Met overexpressing cells (74, 85). HGF expression can be induced in response to tumor-derived signals, such as inflammatory mediators (e.g. IL-1, OSM, prostaglandins (75, 86, 87)) or in response to hypoxia (36, 88).

HGF and Met as molecular targets in anticancer therapy gained extensive attention in recent years. In fact, there are yet no approved anti-cancer therapies that target the HGF/Met pathway. However 21 drugs in total are currently undergoing clinical trials to treat colon cancer, NSCLC, glioma and breast cancer (89). There are two main strategies for targeted anti-HGF/Met therapies: blocking HGF binding to Met and Met tyrosine kinase inhibitors. The first strategy includes blocking HGF antibodies, blocking Met antibodies, decoy Met as well as peptide antagonists, like the naturally occurring HGF splice variant NK4, which functions as a competitive antagonist for Met binding. The second strategy, Met TKI, compete with ATP to the receptor tyrosine kinase domain.

1.4.3 STAT3 signaling

Many cytokines regulate gene expression through STAT signaling pathways. These pathways are involved in hematopoiesis, immune responses, mammary gland development, adipogenesis and other processes (90). There are seven known mammalian STAT factors—designated as STAT1, 2, 3, 4, 5a, 5b and 6. With the exception of STAT4, STAT factors are ubiquitously expressed (91, 92). As the name indicates, all STATs act as intracellular signal transducers and activators of transcription. The STAT pathway provides one of the most direct routes from an extracellular signal into a transcriptional response. There are only three components: the plasma membrane receptor that lacks intrinsic enzymatic activity, an associated cytoplasmic tyrosine kinase called Janus kinase (JAK), and a cytoplasmic transcription factor called STAT. The first event in activation of the STAT signaling pathway is the binding of a ligand to the extracellular domain of the cytokine receptor subunits. Thereafter, the JAKs, which are associated with the cytoplasmic domains, phosphorylate the STATs. The latter are released from the receptor and form a homodimer or heterodimer with other STAT molecules. Dimerized STATs translocate to the nucleus where they activate or repress transcription of target genes (Fig. 4) (90, 91).

STAT3 activation directs genes involved in proliferation, survival, migration and immune responses (91, 93). It transduces signals for the entire IL-6 (e.g. IL-6, IL-11, LIF, OSM) and IL-10 (e.g. IL-10, IL-19, IL-20, IL-22) families and in addition, STAT3 can be activated by several growth factor receptors, such as EGFR, HER2, fibroblast growth factor receptor (FGFR), insulin-like growth factor receptor (IGFR), Met, Platelet-derived growth factor receptor (PDGFR) and vascular endothelial growth factor receptor (VEGFR) (94, 95).

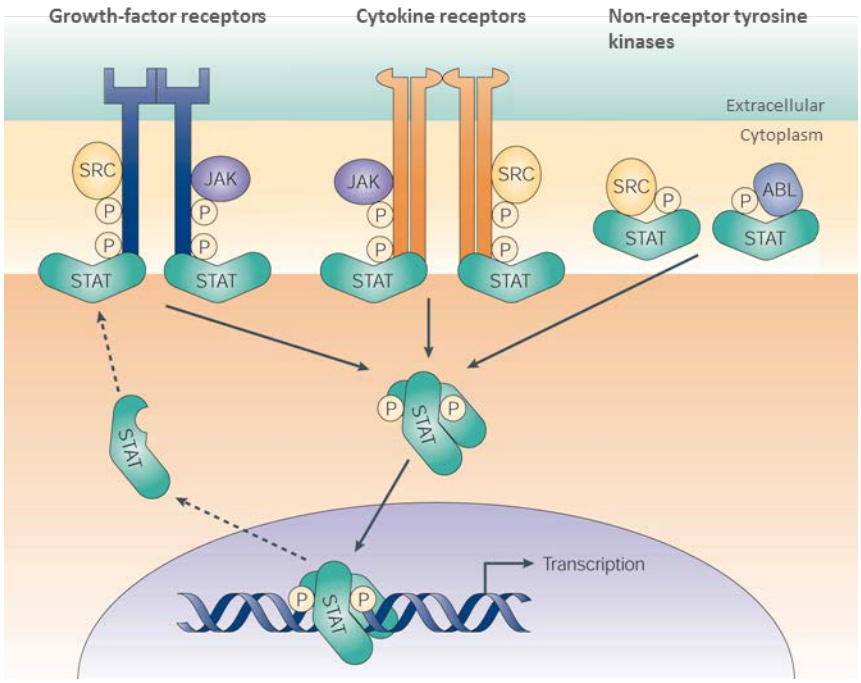

Figure 4. The STAT signaling pathway. Binding of cytokines or growth factors to their receptors results in the activation of receptor-associated kinases, such as the JAKs or Src tyrosine kinases. Receptor bound JAK and Src kinases provide docking sites for monomeric STATs. As soon as they have been recruited, STATs are phosphorylated. Non-receptor tyrosine kinases, such as the oncoproteins Src and Bcr-Abl, can activate STAT proteins without receptor engagement. Phosphorylated STATs form dimers that translocate to the nucleus, where they directly regulate gene expression. The figure was adapted from Yu and Jove, 2004 (96).

A link between STAT3 activity and cancer was made in the 1990s, when it was discovered, that STAT3 regulates Src dependent transformation of fibroblasts (97). In another study, a constitutively activated STAT3 mutant has been shown to potentate tumorigenesis (98). Since then, constitutive phosphorylation of STAT3 by aberrant upstream tyrosine kinase activities has been implicated in a broad spectrum of human cancers (96, 99, 100).

There is a tremendous effect of dysregulated STAT3 signaling on immune cells of the tumor microenvironment: STAT3 is essential for the differentiation of the Th17 cells, a subset of T lymphocytes which are frequently found in a protumorigenic environment and which can promote tumor growth and angiogenesis via the secretion of IL-17 (101). Another immune modulating function of STAT3, together with STAT5, is the expansion of T regulatory cells (Tregs) in tumors (102). Tregs are important negative regulators of Th1 anticancer responses. In addition, STAT3 antagonizes STAT1/NFκB dependent Th1

antitumor immune responses (94, 95, 103). And finally, recent studies have shown that STAT3 phosphorylation in tumor cells triggers secretion of the immunosuppressive cytokines TGFβ and IL-10, which inhibit the proliferation and function of tumor-specific cytotoxic T cells (104). Taken together, STAT3 drives tumor-promoting inflammatory conditions, and at the same time suppresses antitumor immunity (95).

STAT3 represents a promising therapeutic target for treating cancers that require STAT3 overactivity as well as for converting cancer-promoting inflammation to antitumor immunity (56, 105-107). Currently there are no STAT3 inhibitors on the market; however some are in clinical trials for the treatment of solid tumors and lymphomas (108). Strategies to target STAT3 are decoy STAT3 and small molecule inhibitors, which block the phosphorylation and thus impede STAT3 from translocating from the cytoplasm to the nucleus resulting in the inhibition of STAT3-mediated transcription (109). In addition, upstream molecules like JAK1 and JAK2 represent promising targets to block STAT3 activity (110-113).

1.5 Targeting tumor-associated macrophages for cancer therapy

Targeting cancer-promoting inflammation as therapeutic approach is at a very early stage. However, evidence has been provided—especially from genetic mouse carcinogenesis models—that TAMs can be valuable targets for new therapeutic strategies e.g. by targeting recruitment of TAMs, targeting transcription factors which control TAM activation and finally by targeting TAM produced protumorigenic factors (114, 115). Since some of these targeted proteins are also expressed by tumor cells and other stromal cells, it still has to be determined whether macrophages are the site of action.

TAMs derived from circulating monocytes are attracted into tumors in response to chemoattractant cytokines. It was shown in mouse tumor models, that inhibition of monocyte recruitment by blocking certain chemokines such as CCL2, CCL5 or CSF-1, can retard tumor growth (35, 114, 116).

An additional approach to target TAMs, is the inhibition of effector molecules which are responsible for the establishment of a protumorigenic environment. One such molecule could be MMP-9 that is predominantly secreted by TAMs, and indeed suppression of MMP-9 in TAMs was shown to result in a slower tumor growth in mouse models (117-119). Cyclooxygenase-2 (COX-2) represents another TAM

produced target (35, 114, 120). It is a key enzyme in the synthesis of prostaglandins and has an important role in inflammatory responses. The usage of COX-2 inhibitors in the form of nonsteroidal antiinflammatory drugs, such as aspirin, was shown to significantly lower human colon cancer risk and cancer-associated mortality (121). The potential TAM-related anticancer targets, which are involved in EGFR, HGF/Met and STAT3 pathways, were already discussed earlier in this work.

Importantly, recent work suggests that TAMs contribute to chemotherapy resistance. A pharmacological blockade of TAM recruitment was shown to significantly improve the anticancer effect of chemotherapeutics (122). Thus, established anticancer agents in combination with targeted anti-TAM treatment may provide novel opportunities towards the extended treatment of cancer.

2 SPECIFIC AIMS

During the past 20 years it became increasingly clear that the tumor microenvironment plays a significant role in neoplastic growth. Paracrine factors secreted either by tumor-associated stromal cells or by malignant cells act as extracellular signal transductors, thereby driving tumor progression. Importantly, stromal cells and their induced pathways could be promising molecular targets for novel anticancer therapies.

Several tumor-driving EGFR transactivation mechanisms have been described in recent years (123-126). HGF is a frequently found ligand in the tumor stroma and is produced by tumor-associated macrophages (TAMs) and by stromal fibroblasts. In the first part of this study we aimed to investigate HGF/Met-mediated EGFR transactivation in human epithelial cancer cell lines. Interestingly, HGF treatment induced not only EGFR ligand induction, but also an inhibition of EGFR tyrosine kinase (TK) activity in these cell lines. Based on this observation we further aimed to analyze the TK inactive EGFR.

The second part deals with the capability of tumor cells to educate macrophages and monocytes, so that they, in turn, release protumorigenic factors. We focused on the potency of these TAMs to activate two crucial tumorigenic signaling pathways, namely, STAT3 and EGFR signaling. We have established an in vitro model for human and mouse TAMs, in order to study their effect on breast cancer cell lines.

3 MATERIAL AND METHODS

3.1 Material sources

3.1.1 Laboratory hardware

Balances	Kern 572, Kern & Sohn GmbH (Balingen) Mettler AE200, Mettler Toledo (Giessen, Germany)
Centrifuges	Biofuge pico, Heraeus (Hanau, Germany) Universal 320, Hettich, Thermo Fisher Scientific (Schwerte, Germany) Sorvall super T21
Coulter Counter®, Beckman Coulter - Z1™	Beckman Coulter GmbH (Krefeld, Germany)
ELISA reader	Bio Tek, USA
FACScan flow cytometer	BD Biosciences (Heidelberg, Germany)
Film processor, Optimax® 2010	Protec (Oberstenfeld, Germany)
Heating block	Liebisch (Bielfeld, Germany)
HPLC, Proxeon Easy-nLC VI 2.0	Proxeon, Denmark
IDA gel documentation system	Raytest (Straubenhardt, Germany)
Incubator HERAcell® 150	Thermo Scientific (Munich, Germany)
LightCycler, StepOnePlus	Applied Biosystems (Darmstadt, Germany)
Mass spectrometer, LTQ-Orbitrap MS 2.2	Thermo Electron, Dreieich
Microscopes	Zeiss Axio Observer.A1 (Jena, Germany) Zeiss ID 02 (Jena, Germany)
Microwave	Siemens (Munich, Germany)
Multichannel pipette, eline®1200	Biohit (Rosbach, Germany)
Orbital shaker, Red Rotor	Hoefer Scientific (Kehl/Rhein, Germany)
Pipetboy	INTEGRA Biosciences GmbH (Fernwald, Germany)
Polyacrylamide gel electrophoresis system	ATTO, Japan
Power supply	Consort EV 261, Belgium
Spectrophotometer, Nanodrop ND 1000	Thermo Fisher Scientific (Schwerte, Germany)
Vacuum Concentrator 5301	Eppendorf, Wesseling-Berzdorf
Sterile laminar air hood	Biogard hood (Sanford, USA)
Thermocycler	Eppendorf, Wesseling-Berzdorf
Vortex Genie 2TM	Bender and Hobein, Swizerland
Western blotting chamber, “semidry” system	Workshop MPI of Biochemistry (Martinsried, Germany)

3.1.2 Laboratory chemicals and biochemical

Acrylamide solution (30/0,8%) 30% (w/v) Acrylamide 0.8% (w/v) Bisacrylamide	Serva (Heidelberg, Germany)
Agar	Difco, USA
Ampicillin	Roche (Mannheim, Germany)
Aprotinin	Sigma (Taufkirchen, Germany)
APS (ammonium peroxodisulfate)	Bio-Rad (Munich, Germany)
Batimastat	British Biotech, UK
Bisacrylamide	Roth (Karlsruhe, Germany)
Bromphenol blue	Sigma (Taufkirchen, Germany)
BSA (bovine serum albumin)	Sigma (Taufkirchen, Germany)
2-butanol	Sigma (Taufkirchen, Germany)
Coomassie G250	Serva (Heidelberg, Germany)
Chloroquin	Biotrend Chemikalien (Cologne, Germany)
Crystal Violet	Sigma (Taufkirchen, Germany)
Cycloheximide	Sigma (Taufkirchen, Germany)
Deoxynucleotides (dG/A/T/CTP)	Pharmacia Biotech (Freiburg, Germany)
Ethidium bromide	Sigma (Taufkirchen, Germany)
Ficoll-Paque™ PLUS	GE Healthcare (Munich, Germany)
Geneticin (G418)	Invitrogen (Eggenstein, Germany)
Gefitinib	LC Laboratories, USA
HEPES (N-(2-hydroxyethyl)piperazine-N'-(2-ethanesulfonic acid))	Serva (Heidelberg, Germany)
IPTG (isopropyl β-D-1-thiogalactopyranoside)	Biomol (Hamburg, Germany)
L-Glutamine (GibCo)	Invitrogen (Eggenstein, Germany)
LipofectamineTM 2000	Invitrogen (Eggenstein, Germany)
LipofectamineTM RNAiMAX	Invitrogen (Eggenstein, Germany)
LPA (lysophosphatidic acid)	Sigma (Taufkirchen, Germany)
MnCl2	Sigma (Taufkirchen, Germany)
MTT (Thiazolyl blue formazan)	Sigma (Taufkirchen, Germany)
PD98059	Calbiochem, UK
PHA665752	Tocris Bioscience, USA
PIPES	Sigma (Taufkirchen, Germany)
PMSF (phenylmethanesulfonyl fluoride)	Sigma (Taufkirchen, Germany)
Polybrene (hexadimethrine bromide)	Sigma (Taufkirchen, Germany)
Ponceau S	Sigma (Taufkirchen, Germany)
Protein marker, PageRuler™ Prestained Protein Ladder	Fermentas (St. Leon-Rot, Germany)
Random primer p(dN)6	Roche (Mannheim, Germany)
RNase inhibitor	Fermentas (St. Leon-Rot, Germany)
SDS (sodium dodecyl sulfate)	Roth (Karlsruhe, Germany)
Sodium azide	Serva (Heidelberg, Germany)
Sodium fluoride	Sigma (Taufkirchen, Germany)
Sodium orthovanadate	Sigma (Taufkirchen, Germany)
TEMED (N,N,N',N'-tetramethylethylenediamine)	Serva (Heidelberg, Germany)

TMB (3,3’,5,5’-tetramethylbenzidine)	Calbiochem, UK
TPA (tetradecanoyl-phorbol-13-acetate)	Sigma (Taufkirchen, Germany)
Trifluoperazine	Sigma (Taufkirchen, Germany)
Triton X-100	Serva (Heidelberg, Germany)
Tween 20	Sigma (Taufkirchen, Germany)
UO126	Calbiochem, UK
Wortmannin	Sigma (Taufkirchen, Germany)

All other chemicals were purchased in analytical grade from Merck (Darmstadt, Germany).

3.1.3 Chemicals and other material for SILAC and MS analysis

Acetonitrile for HPLC	Sigma (Taufkirchen, Germany)
ABC (Ammoniumbicarbonate)	Sigma (Taufkirchen, Germany)
Ammonium hydroxide	Merck (Darmstadt, Germany)
DTT (DL-Dithiothreitol)	Sigma (Taufkirchen, Germany)
Fetal bovine serum, dialyzed	Gibco, USA
IAA (Iodoacetamide), crystalline	Sigma (Taufkirchen, Germany)
L-Arginine	Gibco, USA
L-Arginine: HCl, U-13C614N4	Cambridge Isotope Laboratories, USA
L-Arginine: HCl, U-13C615N4	Cambridge Isotope Laboratories, USA
L-Glutamine	Gibco, USA
L-Lysine	Gibco, USA
L-Lysine: 2 HCl, 2H4	Cambridge Isotope Laboratories, USA
L-Lysine: 2 HCl, U-13C615N2	Cambridge Isotope Laboratories, USA
Lys-C	WAKO (Neuss, Germany)
NuPAGE® Novex® 4–12% Bis-Tris mini gels 1 mm, 10 well	Invitrogen (Eggenstein, Germany)
NuPAGE® LDS sample buffer 4×	Invitrogen (Eggenstein, Germany)
NuPAGE® antioxidance	Invitrogen (Eggenstein, Germany)
NuPAGE® Tris-glycine-SDS buffer	Invitrogen (Eggenstein, Germany)
Colloidal Blue Staining Kit	Invitrogen (Eggenstein, Germany)
SILAC DMEM (high glucose) /F12	Gibco, USA
Trypsin (seq. grade modified)	Promega, USA

3.1.4 Enzymes

AMV reverse transcriptase	Roche (Mannheim, Germany)
REDTaq™ ReadyMix™ PCR Reaction Mix	Sigma (Taufkirchen, Germany)
Trypsin (GibCo)	Invitrogen (Eggenstein, Germany)
Fast SYBR® Green Master Mix	AB Applied Biosystems (Darmstadt, Germany)
Streptavidin, peroxidase-conjugated	Jackson ImmunoResearch, USA

3.1.5 Kits and other materials

Cell culture materials	BD Falcon (Heidelberg, Germany) Greiner (Solingen, Germany) Nunc, Denmark Falcon, UK
Cell strainer, 70 µm nylon	BD Falcon (Heidelberg, Germany)
Companion plates, 24-well (for transwells)	BD Falcon (Heidelberg, Germany)
Nitrocellulose transfer membrane, PROTAN® BA85 0.45 µm	Whatman (Dassel, Germany)
CryoTubeTM vials	Nunc, Denmark
ECL, Western LightingTM Chemoluminescence Reagent Plus	PerkinElmer, USA
Micro BCA Protein Assay Kit	Pierce (Sankt Augustin, Germany)
Needle (26G, 27G)	Terumo Neolus, Japan
Nunc MaxiSorpTM flat-bottom 96 well	Nunc, Denmark
Parafilm	Dynatech (Denkendorf, Germany)
PCR tube, 0.2 ml Thermo TubeTM	Peqlab (Erlangen, Germany)
Protein A-Sepharose	Amersham Pharmacia (Freiburg, Germany)
QIAquick PCR Purification Kit	Qiagen (Hilden, Germany)
QIAGEN Plasmid Maxi Kit	Qiagen (Hilden, Germany)
QIAGEN RNase Mini Kit	Qiagen (Hilden, Germany)
SmartLadder DNA marker, 200–10 000 bp	Eurogentec (Cologne, Germnay)
Sterile filter (0.22, 0.45 µm pore size), MCE membrane	Millipor (Schwalbach, Germnay)
Syringe Norm-Ject (2 ml, 5 ml, 12 ml, 50 ml)	BD Falcon (Heidelberg, Germnay) Henke-Sass Wolf (Tuttlingen, Germany)
Transwell inserts, 8 µm pore size	Becton Dickinson, France
Whatman 3MM, chromatography paper	Whatman (Rotenburg/Fulda, Germany)
MicroAmp® Fast Optical 96-Well Reaction Plate	AB Applied Biosystems (Darmstadt, Germany)
X-ray films, HyperfilmTM MP	Amersham Pharmacia (Freiburg, Germnay)

3.1.6 Growth factors and ligands

Amphiregulin (human)	R&D Systems (Wiesbaden, Germany)
EGF (human)	Peprotech, USA
HB-EGF (human)	R&D Systems (Wiesbaden, Germany)
Heregulin beta-1 (human)	R&D Systems (Wiesbaden, Germany)
HGF (human)	R&D Systems (Wiesbaden, Germany)
Oncostatin M (human)	R&D Systems (Wiesbaden, Germany)
TGFα (human)	R&D Systems (Wiesbaden, Germany)
Amphiregulin (mouse)	R&D Systems (Wiesbaden, Germany)
EGF (mouse)	Paesel + Lorei (Duisburg, Germany)
Oncostatin M (mouse)	R&D Systems (Wiesbaden, Germany)
TGFα (mouse)	R&D Systems (Wiesbaden, Germany)

3.1.7 Media

3.1.7.1 Bacterial media

Luria-Bertani (LB) broth was used for cultivation of all Escherichia coli strains. If required 100 µg/ml ampicillin were added to media after autoclavation. For the preparation of LB-plates 1.5% Agar was added.

LB-medium	1.0% Tryptone
	0.5% yeast extract
	1.0% NaCl
	pH 7.2

3.1.7.2 Cell culture media

All cell lines used in this study were cultured according to ATCC and DKFZ guidelines. Cell culture media were supplemented to the requirements of each cell line. The media and the additives (apart from NHS) were obtained from GibcoTM (Invitrogen, Eggenstein). Unless otherwise indicated, all cell lines were grown in the presence of 10% fetal calf serum (FCS), all human primary monocytes and primary macrophages were grown in the presence of 5% normal human serum (NHS) blood group AB (Sigma, Taufkirchen) and finally all primary mouse-derived monocytes and macrophages were grown in the presence 5% FCS. Unless otherwise indicated, 50 U/ml penicillin and 50 µg/ml streptomycin were further supplemented to the medium. Freeze medium contained 90% FCS and 10% DMSO.
FCS and NHS were heat inactivated for 30 minutes at 56 °C and then filtered through a sterile 0.22 µm pore size filter before use.

3.1.8 Stock solutions and commonly used buffers

All solutions and buffers were prepared with Millipore water, unless indicated otherwise.

ABC buffer	500 mM	ammoniumbicarbonat
	aliquots were stored at -20 °C	
Collecting gel buffer (4×)	0.5 M	Tris/HCl, pH 6.8
	0.4%	SDS
EDTA	0.5 M	EDTA, pH 8
DTT	1 M	DL-Dithiothreitol
	dissolve in ABC buffer; aliquots were stored at -20 °C	

HNTG	20 mM	HEPES, pH 7.5
	150 mM	NaCl
	0.1%	Triton X-100
	10%	glycerol
	10 mM	Na4P2O7
IAA	550 mM	Iodoacetamide
	dissolve in ABC buffer; aliquots were stored at -20 °C	
Laemmli buffer (3×)	100 mM	Tris/HCl, pH 6.8
	3%	SDS
	45%	glycerol
	0.01%	Bromphenol blue
	7.5%	β-mercaptoethanol
MTT solution	5 mg/ml in PBS	
	protect from light, aliquots were stored at 4 °C	
MTT stop solution	190 ml	10% SDS
	10 ml	2-butanol
	1.2 ml	2N HCl
NET-gelatin	50 mM	Tris/HCl, pH 7.5
	5 mM	EDTA, pH 8.0
	0.05%	Triton X-100
	150 mM	NaCl
	0.25%	gelatin
PBS	137 mM	NaCl
	27 mM	KCl
	80.9 mM	Na2HPO4
	1.5 mM	KH2PO4
	pH 7.4	
TB for competent cells	10 mM	PIPES
	250 mM	KCl
	15 mM	CaCl2
	pH 6.7 (adjust with KOH)	
	after pH adjustment, MnCl2 is added, and the solution is sterile filtered	
	55 mM	MnCl2
Transblot-SD buffer	50 mM	Tris/HCl, pH 7.5
	40 mM	glycine
	20%	methanol
	0.004%	SDS

Separating gel buffer (4×)	0.5 M	Tris/HCl, pH 8.8
	0.4%	SDS
Staining buffer	20%	methanol
	0.5%	crystal violet
Stripping buffer	62.5 mM	Tris/HCl pH, 6.8
	2%	SDS
	added shortly before use:	
	100 mM	β-mercaptoethanol
TAE	40 mM	Tris/acetate pH, 8.0
	1 mM	EDTA
TE (10/0.1)	10 mM	Tris/HCl, pH 8.0
	0.1 mM	EDTA, pH 8.0
Tris-glycine-SDS buffer	25 mM	Tris/HCl, pH 7.5
	200 mM	glycine
	0.1%	SDS
Triton X-100 lysis buffer	50 mM	HEPES, pH 7.5
	150 mM	NaCl
	1 mM	EDTA
	10%	glycerol
	1%	Triton X-100
	10 mM	Na4P2O7
	added shortly before use:	
	2 mM	VaO5
	10 mM	NaF
	1 mM	PMSF
	100 µg/l	aprotinin

3.1.9 Cells

3.1.9.1 Human cell lines

Table 2

Name	Description	Origin/Reference
A498	Renal cell carcinoma	SUGEN, USA
Ac745	Mammary epithelial cells	SUGEN, USA
Caki-1	Metastatic renal cell carcinoma	SUGEN, USA
Caki-2	Renal cell carcinoma	ATCC, USA
HepG2	Hepatocellular carcinoma	ATCC, USA
Hs578T	Mammary carcinoma	ECACC, UK
HT29	Colorectal adenocarcinoma	ATCC, USA
Huh7	Hepatocellular carcinoma	A. Ullrich, MPI Biochemistry (Martinsried, Germany)
MAD-NT	Myeloid leukemia, semi-adherent subclone of HL-60 cells	P. Knyazev, MPI Biochemistry (Martinsried, Germany)
MCF7	Mammary carcinoma	ATCC, USA
MCF10A	Mammary epithelial cells	ATCC, USA
MDA-MB-231	Mammary carcinoma	ATCC, USA
MDA-MB-435s	Mammary carcinoma	ATCC, USA
MDA-MB-468	Mammary carcinoma	ATCC, USA
SCC4	Squamous cell carcinoma of the tongue	ATCC, USA
SCC9	Squamous cell carcinoma of the tongue	ATCC, USA
SCC25	Squamous cell carcinoma of the tongue	ATCC, USA
Sk-Hep-1	Hepatocellular carcinoma	DKFZ, Germany
T47D	Mammary carcinoma	ATCC, USA

3.1.9.2 Mouse cell lines

Table 3

Name	Description	Origin
Mm5mt	Mammary gland carcinoma	SUGEN, USA
Mm2mt	Mammary gland carcinoma	SUGEN, USA
RIIImt	Mammary gland carcinoma	SUGEN, USA
L8A	Mammary gland carcinoma	SUGEN, USA
1209-PmT-T-breast	Mammary, transgene for PmT (polyomavirus middle T antigen)	A. Ullrich, MPI Biochemistry (Martinsried, Germany)

Name	Description	Origin
Mmt060562	Mammary gland, tumor	ATCC, USA
EpH4	Mammary epithelial cells	A. Ullrich, MPI Biochemistry (Martinsried, Germany)
MEFs	Embryonic fibroblasts, wild type	R. Faessler, MPI Biochemistry (Martinsried, Germany)
NMUMG	Mammary gland, normal epithelial	ATCC, USA

ATCC, American Type Culture Collection, Manassas, USA
DKFZ, Deutsches Krebsforschungszentrum, Heidelberg
ECACC, European Collection of Cell Cultures, UK

3.1.9.3 Primary human cells

Table 4

Name	Description	Origin
HMEC	Human mammary epithelial cells	ATCC, USA
PBMCs	Human peripheral blood monocytes; derived from venous blood of healthy donors	Bavarian Red Cross (Herzog-Heinrich-Str. 2, D-80336 Munich)

3.1.9.4 Primary murine monocytes and macrophages

Mouse monocytes and macrophages were isolated from peritoneum, spleen and bone marrow of 8–9 week old female C57BL/6 (breeding line: C57BL/6NCrlMpi) mice. The animals used in this study were kept in a barrier facility at the Max Planck Institutes in Martinsried, Germany.

3.1.9.5 Bacterial strains

The Escherichia coli (E. coli) DH5α strain was used for transformations to amplify plasmids.

Table 5

Name	Genotype Description	Origin/Reference
DH5αF’	F’ endA1 hsd17 (rk-mk+) supE44 recA1 gyrA (Nal) thi-1 Δ(lacZYA-argF196)	Genentech, USA

3.1.10 Antibodies

3.1.10.1 Primary antibodies for Western blot

Table 6

Recognized protein	Description	Origin/Reference
pAkt	Rabbit, polyclonal; recognizes endogenous Akt1 phosphorylated at Ser473	Cell Signaling, MA
Axl	Goat, polyclonal; recognizes C-terminus of human Axl	Santa Cruz, USA
CDCP1	Rabbit, polyclonal; recognizes C-terminus of endogenous human CDCP1	Cell Signaling, MA
EGFR	Rabbit, polyclonal; recognizes C-terminus of the human and mouse EGFR u	Cell Signaling, MA
pEGFR	Rabbit, monoclonal; recognizes endogenous human and mouse EGFR phosphorylated at Tyr1173	Cell Signaling, MA
EphA2	Mouse monoclonal; recognizes human and mouse EphA2	Millipore (Schwalbach, Germany)
Erk1	Rabbit, polyclonal; recognizes C-terminus of Erk1	Santa Cruz, USA
pErk1/2	Rabbit, polyclonal; recognizes phospho-p44/ p42	Cell Signaling, MA
HER2	Rabbit, polyclonal; recognizes cytoplasmic domain of human HER2	Millipore (Schwalbach, Germany)
HER3	Mouse, monoclonal, clone 2F12; recognizes cytoplasmic domain of human HER3	Millipore (Schwalbach, Germany)
Integrin β4	Mouse, monoclonal, clone M126; recognizes all three isoforms of integrin β4 (4A, 4B, 4C)	Abcam, UK
JAK1	Rabbit, polyclonal; recognizes human and Mouse JAK1	Cell Signaling, MA
Mig6	Rabbit, polyclonal; recognizes amino acids 395–410 of rat Mig6	Sigma (Taufkirchen, Germany)
pp38 MAPK	Rabbit, polyclonal; recognizes phosphorylation at Thr180/Tyr182	Cell Signaling, MA
pSAPK/JNK	Rabbit, polyclonal; recognizes endogenous p46 and p54 SAPK/JNK phosphorylated at Thr183/Tyr185	Cell Signaling, MA
pSTAT3	Rabbit, polyclonal; recognizes endogenous human and mouse STAT3 phosphorylated at Tyr705	Cell Signaling, MA
pY	Mouse, monoclonal, clone 4G10; recognizes phospho-tyrosine residues	A. Ullrich, MPI Biochemistry Martinsried
α-tubulin	Mouse, monoclonal, ascites	Sigma (Taufkirchen, Germany)

3.1.10.2 Primary antibodies for immunoprecipitation

Table 7

Recognized protein	Description	Origin/Reference
EGFR	Mouse, monoclonal, clone 108.1, homemade; recognizes ectodomain of the human EGFR	A. Ullrich, MPI Biochemistry Martinsried, Germany/ Daub et al., 1997
HER2	Mouse, monoclonal, clone 13D1B1, homemade; recognizes human HER2	A. Ullrich, MPI Biochemistry Martinsried, Germany/ Ruschel et al., 2004
HER3	Mouse, monoclonal, clone 2F12; recognizes cytoplasmic domain of human HER3	Millipore (Schwalbach, Germany)

3.1.10.3 Secondary antibodies for Western blot

For immunoblot analysis corresponding secondary antibodies conjugated with horseradish peroxidase (HRP) were utilized.

Table 8

Recognized protein	Description	Origin/Reference
Mouse IgG	Goat polyclonal, HRP-conjugated	Sigma (Taufkirchen, Germany)
Rabbit IgG	Goat polyclonal, HRP-conjugated	BioRad, Munich
Goat IgG	Goat polyclonal, HRP-conjugated	Jackson ImmunoResearch, USA

3.1.10.4 Antibodies for ELISA

The following antibodies were used for sandwich ELISA.

Table 9

Recognized protein	Description	Origin/Reference
Amphiregulin	Mouse, monoclonal, capture antibody; recognizes human (h) amphiregulin	R&D Systems (Wiesbaden, Germany)
	Goat, polyclonal, biotinylated detection antibody; recognizes human amphiregulin	R&D Systems, Wiesbaden, Germany)

Recognized protein	Description	Origin/Reference
Amphiregulin	Goat, polyclonal, capture antibody; recognizes mouse amphiregulin	R&D Systems (Wiesbaden, Germany)
	Goat, polyclonal, biotinylated detection antibody; recognizes mouse amphiregulin	R&D Systems (Wiesbaden, Germany)
HB-EGF	Mouse monoclonal (clone 1.19.3), capture antibody; recognizes human HB-EGF	U3 Pharma (Martinsried, Germany)
	Goat, polyclonal, biotinylated detection antibody; recognizes human HB-EGF	R&D Systems (Wiesbaden, Germany)
Oncostatin M	Goat, polyclonal, capture antibody; recognizes mouse oncostatin M	R&D Systems (Wiesbaden, Germany)
	Goat, polyclonal, biotinylated detection antibody; recognizes mouse (m) oncostatin M	R&D Systems (Wiesbaden, Germany)
TGFα	Goat, polyclonal, capture antibody; recognizes human TGFα	R&D Systems (Wiesbaden, Germany)
	Goat, polyclonal, biotinylated detection antibody; recognizes human TGFα	R&D Systems (Wiesbaden, Germany)

3.1.10.5 Antibodies for FACS

Table 10

Recognized protein	Description	Origin/Reference
CD14	Rat IgG2a, monoclonal, FITC-labeled; recognizes mouse CD14	Abcam, UK
CD14/CD64	Mouse IgG2b, monoclonal, FITC/PE labeled recognizes human CD14 and CD64	BD Biosciences (Heidelberg, Germany)
EGFR	Mouse, monoclonal, clone 108.1, homemade; recognizes ectodomain of the human EGFR	A. Ullrich, MPI Biochemistry Martinsried, Germany/ Daub et al., 1997
F4/80	Rat IgG2a, monoclonal, FITC-labeled; recognizes mouse F4/80	Abcam, UK
-	Mouse IgG monoclonal, clone 4H1A7; isotype control	U3 Pharma (Martinsried, Germany)

Recognized protein	Description	Origin/Reference
Mouse IgG	Donkey, polyclonal, PE-labeled detection antibody; recognizes mouse IgG (H+L)	Jackson ImmunoResearch, USA
Rat IgG2a	Rat, monoclonal FITC-labeled isotype Control	Abcam, UK

3.1.10.6 Blocking antibodies

Table 11

Recognized protein	Description	Origin/Reference
HGF	Mouse, monoclonal; recognizes human (h) HGF	R&D Systems (Wiesbaden, Germany)
Amphiregulin	Goat, polyclonal; recognizes human amphiregulin	R&D Systems (Wiesbaden, Germany)
Goat IgG	Polyclonal goat IgG; isotype control	R&D Systems (Wiesbaden, Germany)
HB-EGF	Goat, polyclonal; recognizes human HB-EGF	R&D Systems (Wiesbaden, Germany)
Oncostatin M	Monoclonal Mouse IgG2 A, recognizes human oncostatin M	R&D Systems (Wiesbaden, Germany)
Oncostatin M	Goat, polyclonal; recognizes (m) mouse oncostatin M	R&D Systems (Wiesbaden, Germany)
TGFα	Goat, polyclonal; recognizes human TGFα	R&D Systems (Wiesbaden, Germany)

3.1.11 Oligonucleotides and Plasmids

3.1.11.1 Primary vectors

Table 12

Name	Description	Origin/Reference
pcDNA3	Mammalian expression vector, Ampr, Neor, CMV promotor, BGH poly A, high copy number plasmid, F1+ origin	Invitrogen, USA

3.1.11.2 Constructs

Table 13

Name	Insert description	Origin/Reference
pcDNA3-VSV-proAR	cDNA of human pro-amphiregulin	A. Ullrich, MPI Biochemistry Martinsried, Germany/ Andreas Gschwindt

3.1.11.3 siRNA oligonucleotides (human specific)

20 µM Stock with Millipore water. Aliquots were stored at -20 °C.

Table 14

Target/name	Sequence (description)	Origin/Reference
Gl2	directed against firefly luciferase CGUACGCGGAAUACUUCGAdTdT	Dharmacon Research, USA
MAPK3 (Erk1)	AGACUGACCUGUACAAGUU (target sequence)	Dharmacon Research, USA
MAPK1 (Erk2) #1	CACCAACCAUCGAGCAAAU (target sequence)	Dharmacon Research, USA
MAPK1 (Erk2) #2	ACACCAACCUCUCGUACAU (target sequence)	Dharmacon Research, USA
Mig6 #2	GCUAUGUGUCUGACCAAAAtt (sense) UUUUGGUCAGACACAUAGCtg (antisense)	AB Applied Biosystems (Darmstadt, Germany)

3.1.11.4 Primers for real-time PCR (human specific)

Primers for real-time PCR were diluted in Millipore water to final concentration of 100 pmol/µl. Aliquots were stored at -20 °C.

Table 15

Target	Sequence (description)	Name
Cyclophilin A	GCCG-CGTCTCCTTTGAGCT (forward primer, Pjotr K.)	CYCLO Fw
	CACCACATGCTTGCCATCC (reverse primer, Pjotr K.)	CYCLO Rev
Amphiregulin	TGGTGCTGTCGCTCTTGATA (forward primer, Gschwind A.)	AREG Fw
	GCCAGGTATTTGTGGTTCGT (reverse primer, Gschwind A.)	AREG Rev

Target	Sequence (description)	Name
EGF	GCCAAGCAGTCTGTGATTGA (forward primer, Vlaicu P.)	EGF Fw
	CTGATGGCATAGCCCAATCT (reverse primer, Vlaicu P.)	EGF Rev
HB-EGF	TTATCCTCCAAGCCACAAGC (forward primer, Gschwind A.)	HB-EGF Fw
	TGACCAGCAGACAGACAGATG (reverse primer, Gschwind A.)	HB-EGF Rev
TGFα	TGTGTCTGCCATTCTGGGTA (forward primer, Vlaicu P.)	TGFA Fw
	GACCTGGCAGCAGTGTATCA (reverse primer, Vlaicu P.)	TGFA Rev

3.1.11.5 Primers for real-time PCR (mouse specific)

Primers for real-time PCR were diluted in Millipore water to final concentration of 100 pmol/µl. Aliquots were stored at -20 °C.

Table 16

Target	Sequence (description)	Name
Amphiregulin	GACTCACAGCGAGGATGACA (forward primer)	AREG-3 Fw
	GGCTTGGCAATGATTCAACT (reverse primer)	AREG-3 Rev
β-actin	GTCCACACCCGCCACCAGT (forward primer)	ACTB-2 Fw
	GATCTTCTCCATGTCGTCCCAGTT (reverse primer)	ACTB-2 Rev
Oncostatin M	CTCACGGGGAACACAGAATCACTC (forward primer)	OSM-2 Fw
	GCCGGGCCATGCAGAAAACA (reverse primer)	OSM-2 Rev
HB-EGF	AGACCCATGCCTCAGGAAATACAA (forward primer)	HBEGF-2 Fw
	ACTACAGCCACCACAGCCAAGACT (reverse primer)	HBEGF-2 Rev
TGFα	TGGCGGCTGCAGTGGTGTCTC (forward primer)	TGFA-1 Fw
	AGGGCGCTGGGCTTCTCAT (reverse primer)	TGFA-1 Rev
	CTCTGCTAGCGCTGGGTATCCTG (forward primer)	TGFA-2 Fw
	GACACATGCTGGCTTCTCTTCCTG (reverse primer)	TGFA-2 Rev
EGF	GGCTTGGAACTTTCCATCAA (forward primer)	EGF Fw
	CAGGTCCTTCTGCACCTCTC (reverse primer)	EGF Rev

3.1.12 Software

CellQuest software	BD Biosciences (Heidelberg, Germany)
MetaVue™ imaging software	MetaVue, Universal Imaging Corporation, USA
Photoshop CS3	Adobe Systems Inc (San Jose, USA)
ImageJ	National Institutes of Health (USA)
MaxQuant 1.1.1.21	MPI of Biochemistry dept. Mann

3.2 Methods

3.2.1 Methods in molecular biology

3.2.1.1 Cultivation and maintenance of bacterial strains

E. coli strains were grown at 37 °C for 12–16 hours in LB-medium supplemented with antibiotics for selection. For short-term storage E. coli cultures were kept on LB agar plates at 4 °C. For long-term storage 1 ml glycerol stocks containing 50% (v/v) glycerol in LB-medium were stored in screw-top vials at -80 °C.

3.2.1.2 Preparation of competent bacteria

To generate competent bacteria, DH5αF' cells were taken from the -80 °C glycerol stock, streaked on a LB-agar plate and incubated at 37 °C overnight. A single bacterial colony was inoculated in 3 ml LB-medium and incubated shacking (180 rpm) for 6 hours at 37 °C. The 6 hour culture was diluted in 500 ml fresh LB-medium and incubated shacking at 18–22 °C until the cell density reached the optical density of 0.4–0.6 at 600 nm (approx. 24 hours). At this point bacteria were incubated for 10 minutes on ice before they were harvested by centrifugation at 2500 × g, 4 °C, 10 minutes. The supernatant was decanted and the bacteria were resuspended in 160 ml of sterile ice-cold TB for competent cells. Again the bacteria were incubated for 10 minutes on ice before they were pelleted as before and resuspended in 40 ml of ice cold TB for competent cells and 2.8 ml of DMSO. The now competent bacteria were incubated for 10 minutes on ice, shock frozen as 100 µl aliquots in liquid nitrogen and stored at -80 °C. Newly generated competent bacteria were tested for efficiency by transformation of 0.1 ng of known plasmid, which should result in 108-109 colonies per µg DNA.

3.2.1.3 Transformation of competent bacteria

Competent bacteria were transformed by heat shock. For each sample a 30 µl aliquot of competent bacteria was thawed on ice and supplemented with 0.5 µl of plasmid DNA. The mixture was incubated on ice for 30 minutes followed by a heat shock at 42 °C for 45 seconds. Then, 900 µl LB-medium were added and samples were incubated for 50 minutes at 37 °C with rotation. 100 µl aliquots of bacteria (in 1:10, 1:100 and 1:1000 dilutions) were streaked out per agar plate containing ampicillin for the selection of transformants. The plates were incubated overnight at 37 °C and then stored at 4 °C until further use.

3.2.1.4 Amplification of plasmids

For plasmid amplification one colony per plasmid was picked and was incubated with 3 ml LB-medium containing ampicillin shacking (180 rpm) at 37 °C for 5–8 hours. The culture was transferred into 200 ml of LB-medium containing ampicillin and incubated shacking (180 rpm) at 37 °C overnight (12–16 hours).

3.2.1.5 Plasmid Purification

Plasmid DNA was prepared using the QIAfilter Plasmid Maxi Kit mainly following the manufacturer's instructions. Modification from the manufacturer's protocol were as follows: for DNA precipitation, samples were centrifuged at 4300 rpm (ST-H750 rotor: 4300 rpm MAX, Sorvall super T21 centrifuge) for 1 hour (instead of 15 000 g for 30 minutes) in 50 ml falcon tubes and for washing the DNA pellet samples were centrifuged at 4300 rpm for 45 minutes (instead of 15 000 g for 10 minutes). The DNA pellet was finally diluted in 250 µl of TE (10/0.1) buffer at 4 °C overnight. On the following day plasmid concentration was measured with a spectrophotometer (Nanodrop) and the plasmids were diluted with TE (10/0.1) buffer to a final concentration of 1 µg/µl. Aliquots were stored at -20 °C.

3.2.1.6 RNA isolation and cDNA synthesis

Total RNA out of one 12-well was isolated using RNeasy Mini Kit (Qiagen, Hilden). The isolated RNA was eluted in 20 µl of Millipore water and reverse transcribed into cDNA using AMV Reverse Transcriptase (Roche, Mannheim). Therefore 1 µl random primer [1 mM] were added to 20 µl of mRNA and incubated for 3 minutes at 68 °C. Then 6.25 µl 5× AMV-buffer, 1 µl RNase inhibitor cocktail, 1 µl AMV reverse transcriptase and 2 µl dNTPs [10 mM] were added and incubated for minimum of 2 hours at 42 °C. cDNA was isolated using QIAquick PCR Purification Kit (Qiagen, Hilden) and concentration was measured with a spectrophotometer (Nanodrop). cDNA was diluted in Millipore water to a final concentration of 16 ng/µl and analyzed via standard PCR analysis or by quantitative real-time PCR. cDNA was stored at -20 °C.

3.2.1.7 Quantitative real-time PCR analysis

cDNA levels were analyzed via quantitative real-time PCR (RT-PCR). Fast SYBR® Green Master Mix (AB Applied Biosystems, Darmstadt) was used for cDNA amplification. The PCR reaction was performed in a final volume of 15 µl composed of 2 µl of cDNA [16 ng/µl], 0.38 µl (0.5 µM) of forward and of reverse gene specific primers, 7.5 µl of Fast SYBR® Green Master Mix and 4.74 µl of Millipore water in 96-well MicroAmp® Fast Optical Reaction Plates (AB Applied Biosystems, Darmstadt). The PCR was carried out on a StepOnePlus instrument (AB Applied Biosystems, Darmstadt), according to the manufacturer's instructions. Calculations were done using the ΔΔCt method (Winer et al., 1999). Gene-specific primers are listed in table 15 and 16. RT-PCR was performed in duplicates.

3.2.2 Methods in mammalian cell culture

3.2.2.1 General cell culture techniques

All cell lines (see table 2 and 3) and primary cells were cultivated in a humidified HERAcell® 150 incubater in a 93% air, 7% CO2 atmosphere at 37 °C. Cell lines were routinely assayed for mycoplasma contamination using a bisbenzimidestaining kit (Sigma). All working steps were carried out in sterile laminar air hoods (Biogard hood; Maine, USA). Before seeding, cells were counted with a Coulter Counter®. All of the cell lines (American Type Culture Collection, USA) were routinely grown according to the supplier's instructions.

3.2.2.2 Growth factor stimulation and inhibitor treatment

Unless otherwise indicated, ligands and growth factors were used in the following concentrations: HGF 50 ng/ml, amphiregulin (AR) 50 ng/ml, human and mouse EGF 10 ng/ml, heregulin beta-1 (HRGβ1) 10 ng/ml and human and mouse OSM 10 ng/ml. Chemical inhibitors, except gefitinib, were added 15 min prior to HGF treatment and were present during the entire period of the experiment. The inhibitors, dissolved in dimethyl sulfoxide (DMSO), were used in the following concentrations: metalloprotease inhibitor batimastat BB94 [5 µM] (British Biotech), Met inhibitor PHA665752 [100 nM] (Tocris Bioscience), MEK inhibitors UO126 [5 µM] and PD98059 [50 µM] (Calbiochem), PI3K inhibitor wortmannin [50 nM] (Sigma). Gefitinib [2 µM] (LC Laboratories) was present during the last 2 h of the 24 h HGF treatment. Control cells were subjected to DMSO only.

The translation inhibitors were used in the following concentrations: cycloheximide (CHX) 1 µg/ml, geneticin (G418) 1 mg/ml. The inhibitors were added 15 min prior to HGF treatment and were present during the entire period of the experiment.

3.2.2.3 Isolation of primary human peripheral blood monocytes

Human monocytes were isolated and purified from 500 ml blood from healthy donors. Blood was concentrated by centrifugation (1400 rpm, 15 min, 18 °C, break off) and 25 ml of plasma was collected in a new 50 ml Falcon tube, clarified by centrifugation (2 × 3500 rpm, 15 min, 18 °C) diluted 1:1 with PBS and kept on ice until further use. The blood concentration was repeated again; the plasma was removed unless 1 cm above the red blood phase; the red blood phase was transferred into new 50 ml falcon tubes except of the last 3 cm, which contain mostly red blood cells, were discarded. The concentrated blood was diluted with PBS to a final volume of 50 ml in each tube and concentrated again (1400 rpm, 15 min, 18 °C, break off). The clear upper phase was removed except of 1 cm above the red blood phase; the red blood phase was transferred into new 50 ml falcon tubes except of the last 3 cm, which were discarded. The concentrated blood was transferred in two 50 ml falcon tubes and diluted with PBS to a final volume of 50 ml. 25 ml of blood were put on 15 ml of Ficoll Hypaque and centrifuged (30 min, RT, 1800 rpm, break off). In the meanwhile 5 gelatin coated plates are incubated with 10 ml of plasma/PBS per dish for a minimum of 40 minutes in the 37 °C CO2 incubator. After Ficoll density gradient centrifugation, the middle white layer (containing the PBMCs) between the Ficoll and the serum was harvested and transferred into a 50 ml Falcon tube. To wash away the remaining Ficoll and remaining plateles, the PBMCs were diluted with ice cold PBS and pelleted by centrifugation (1400 rpm, 15 min, 4 °C). The PBMCs were washed 2–3 × with ice cold 25 ml PBS until the SN was clear. Monocytes were isolated from PBMCs by adherence. Therefore the plasma was removed from the gelatin plates; the plates were washed once with 10 ml RT PBS (vortex). The PBMCs were resuspended in 47.5 ml of in ice cold RPMI-10% FCS plus 2.5 ml NHS (not heat inactivated, final 5% NHS). 10 ml of the cell suspension were plated on each gelatin plate and incubated for 40–60 minutes in the 37 °C CO2 incubator. After the incubation, the remaining non-adherent lymphocytes were removed by washing the plates 3–5 × with 37 °C warm washing medium (RPMI/PBS 1:1) for 15–20 minutes in the 37 °C CO2 incubator. The adherent monocytes were detached with 10 ml of RMPI/EDTA (500 µl 0.5 M EDTA + 49.5 ml RPMI) and transferred in two precooled 50 ml Falcon tubes (From here on, the cells have to be kept on ice). The plates were washed again with ice cold washing medium (RPMI/PBS 1:1) to collect residual monocytes. Cells were washed twice with ice cold washing medium (1400 rpm, 5 min, 4 °C), resuspended in 10 ml of ice cold RMPI 5% NHS and counted. Monocytes were diluted to a final concentration of 1.5×10^6 cells/ml and 3 ml of cell suspension/well were seeded in 6-well plates. The purity of the monocytes was >80% as verified by FACS analysis. Monocytes differentiate in the presence of NHS to mature macrophages during 7 days. The medium was exchanged every 2–3 days. The monocytes were cultured in RPMI supplemented with 5% NHS and penicillin/streptomycin.

3.2.2.4 Isolation of primary murine peritoneal macrophages

To isolate peritoneal macrophages (PM), mice were sacrificed by cervical dislocation and the abdominal skin was cut below the sternum, without damaging the peritoneum. The skin was peeled longitudinally to both sides, exposing the sternum and the pelvis. A 10 ml syringe with a 26G needle was filled with 5 ml of ice-cold harvest medium (PBS/0.5% BSA) and 3 ml of air. A forceps was used to firmly hold the sternum while the harvest medium and the air were gently filled into the abdominal cavity - with making a smallest possible hole. The needle was removed and the mouse was shaken vigorously 10–15 times.

The sternum was grabbed again with forceps and an air-filled Pasteur pipette was inserted into the peritoneal cavity with a circling movement.

The air was expressed into the peritoneal cavity, and the harvest medium containing the peritoneal cells was aspirated and collected in a precooled 50 ml Falcon tube on ice. Cells were pelleted by centrifugation for 5 minutes at 1000 rpm at 4 °C. Peritoneal cells were resuspended in ice cold RPMI 10% FCS medium, seeded into a 10 cm cell culture dish (2–3 mice per dish) and incubated for 90 minutes at 37 °C in a 7% CO2 incubator.

After incubation, the plate was washed 3 × with 10 ml of 37 °C warm washing medium (RPMI/PBS 1:1) to remove non-adherent and dead cells. PMs were scraped off the plate on ice with ice cold RPMI 5% FCS, counted and immediately used for experiments. The isolated PMs were cultured in RPMI 5% FCS and penicillin/streptomycin and 1 × 10^6 cells/ml/well was seeded in 12-well plates. Only cell preparations containing more than 90% macrophages were used for further experiments (verified by FACS analysis).

3.2.2.5 Isolation of primary murine spleen monocytes

To isolate spleen-derived monocytes (SM), mice were sacrificed by cervical dislocation and opened ventrally. The spleen was cleaned from adherent soft tissues and RPMI was injected with a 26G needle into several parts of the spleen. The two ends of the spleen were cut off with a scalpel and monocytes were squeezed out with the help of the upper part of a plunger of a 2 ml syringe; remaining cells were flushed out of the spleen with the 26G needle syringe.

The spleen cells were filtered through a 70 µm nylon mesh filter (BD Falcon, Heidelberg) in a precooled 50 ml Falcon tube on ice with 10 ml of ice cold RMPI 10% FCS. Tissue fragments, remaining in the strainer, were squeezed through the filter with the help of the upper part of a plunger of a 2 ml syringe. Cells were pelleted by centrifugation for 5 minutes at 1000 rpm at 4 °C. Cells were resuspended in ice cold RPMI 10% FCS medium, seeded into a 10 cm cell culture dish (2–3 spleens per dish) and incubated for 2 hours at 37 °C in a 7% CO2 incubator.

After incubation, the plate was washed 3 × with 10 ml of 37 °C warm washing medium (RPMI/PBS 1:1) to remove non-adherent and dead cells. SMs were scraped off the plate on ice with 3 ml of ice cold RPMI 5% FCS, counted and immediately used for experiments. The isolated SMs were cultured in RPMI 5% FCS and penicillin/streptomycin.

3.2.2.6 Isolation of primary murine bone marrow monocytes

To isolate bone marrow-derived monocytes (BM), mice were sacrificed by cervical dislocation and their femurs and tibiae were carefully cleaned from adherent soft tissue. The tip of each bone was removed with a scalpel, and the marrow was harvested by inserting a 27G syringe needle into one end of the bone and flushing with RPMI through the bone shafts.

The bone marrow cells were filtered through a 70 µm nylon mesh filter (BD Falcon, Heidelberg) in a precooled 50 ml Falcon tube on ice with 10 ml of ice cold RMPI 10% FCS. Tissue fragments, remaining in

the strainer, were squeezed through the filter with the help of the upper part of a plunger of a 2 ml syringe. Cells were pelleted by centrifugation for 5 minutes at 1000 rpm at 4 °C. Bone marrow cells were resuspended in ice cold RPMI 10% FCS medium, seeded into a 10 cm cell culture dish (3–4 bones per dish) and incubated for 2 hours at 37 °C in a 7% CO2 incubator.

After incubation, the plate was washed 3 × with 10 ml of 37 °C warm washing medium (RPMI/PBS 1:1) to remove non-adherent and dead cells. BMs were scraped off the plate on ice with 3 ml of ice cold RPMI 5% FCS, counted and immediately used for experiments. The isolated BMs were cultured in RPMI 5% FCS and penicillin/streptomycin.

3.2.2.7 Treatment of human macrophages with cancer cell conditioned medium

3×10^6 primary human monocytes were seeded into a 6-well immediately after isolation and cultured for three days in 2 ml RPMI 5% NHS. On day three, six, eight and ten after isolation, cells were treated with CM of MDA-MB-231 cells. Therefore the medium was exchanged by 1 ml of RPMI 5% NHS plus 1 ml of CM. On day eleven the 24 hour CM was collected. This medium was used to stimulate SCC9 and MDA-MB-231 cells.

For the cell line screen cells were treated with CM of different cancer cell lines on day three, six and nine after isolation. On day ten the 24 hour CM was collected. This medium was used to stimulate SCC9 and MDA-MB-231 cells.

3.2.2.8 Treatment of murine monocytes/macrophages with cancer cell conditioned medium

Immediately after the monocytes were isolated, 1×10^6 cells/500 µl/well were seeded into a 12-well plate. 500 µl of cancer cell conditioned medium was added per well. After 24 hours the cell culture medium was collected into 1.7 ml tubes, clarified by centrifugation (1200 rpm, 5 min, 4 °C) and assayed in sandwich ELISA for oncostatin M release. For RT-PCR analysis, adherent cells were washed once with PBS, lysed in 300 µl RLT buffer (Qiagen RNA purification kit) and RNA isolation was performed as described in part 2 7.4.

3.2.2.9 Coculture experiment

3×10^6 primary human monocytes were seeded into a 6-well immediately after isolation and cultured for three days in 2 ml RPMI 5% NHS. On day three after isolation 2×10^4 MDA-MB-231 cells/well were added to the macrophages. On day six, eight and ten after isolation, the medium was exchanged by 2 ml of RPMI 5% NHS. On day eleven the 24 hour CM was collected. This medium was used to stimulate SCC9 and MDA-MB-231 cells.

3.2.2.10 Preparation of cell culture conditioned media (CM)

Preparation of CM for stimulation and for ELISA

6×10^4 SCC9, A498, MDA-MB-231, HuH7, Sk-Hep-1, HS680, and HepG2 cells were seeded on 12-well plates and allowed to adhere overnight. On the following day cells were treated with 50 ng/ml HGF for 24 hours. For stimulation experiments, SCC9 cell CM with blocking antibodies against AR or TGFα was used to stimulate untreated SCC9 cells for 5 minutes. In order to ensure the same conditions in ELISA analysis, RPMI 10% FCS was used for all cell lines during HGF treatment.

For ELISA analysis, supernatants were collected clarified by centrifugation (1200 rpm, 5 min, 4 °C), snap-frozen in liquid nitrogen and stored at -80 °C. Frozen samples were thawed on ice before they were assayed in ELISA. Samples were used undiluted or diluted 1:5 or 1:10 with PBS/1% BSA before assayed.

Preparation of MAD-NT CM

MAD-NT cells were cultured on 150 mm cell culture dishes until they were 90% confluent. Adherent cells were washed once with 10 ml of pre-warmed (37 °C) PBS in order to remove most of the non-adherent cells. The adherent cells were grown in 15 ml RPMI 10% FCS for 24 hours. The CM was collected, clarified by centrifugation (1200 rpm, 5 min, 4 °C) and used immediately to treat SCC9 cells or was snap-frozen in liquid nitrogen and stored at -80 °C.

Preparation of CM for primary monocyte/macrophage treatment

5×10^6 cell of human and mouse breast cell lines were seeded per 10 cm dish and allowed to adhere overnight (L8A cells were allowed to adhere for 48 hours). On the following day cells were incubated with RMPI 5% NHS for the treatment of human monocytes and with RPMI 5% FCS for the treatment of mouse macrophages. Supernatants were collected, clarified by centrifugation (1200 rpm, 5 min, RT) and immediately snap-frozen in liquid nitrogen and stored at -80 °C.

3.2.2.11 Treatment of CM with blocking antibodies

The CM were pre-incubated with the blocking antibody or with control IgG at 37 °C for 45 minutes, before cells were stimulated with the CM. Final blocking antibody concentrations were as follows: human AR 2.5 µg/ml, human TGFα 5 µg/ml, human HB-EGF 10 µg/ml, human OSM 5 µg/ml and mouse OSM 20 µg/ml (see table 11).

3.2.2.12 Preparation of human serum

Whole-blood of healthy human donors was transferred into a sterile 15 ml Falcon tube. A sterile 2 ml plastic pipette was put into to blood to induce faster coagulation. The blood in incubated in a laminar

flow for one hour at RT. After one hour the pipette was removed and the coagulated blood was centrifuged (2500 rpm, 10 min, 4 °C). Serum was harvested in a precooled 15 ml Falcon tube. The residual blood was again centrifuged (2500 rpm, 10 min, 4 °C) and the serum was again harvested. 500 µl aliquots of serum were immediately snap-frozen in liquid nitrogen and stored at -80 °C. Around 10 ml of serum were obtained from 20 ml whole-blood.

3.2.2.13 Heat inactivation of human serum

The heat sensitive complement proteins in the serum were inactivated by 30 minutes incubation of the serum at 56 °C. The heat inactivated serum was stored at -20 °C.

3.2.2.14 Preparation of gelatin coated plates

2 gram gelatin plus 100 ml Millipore water were incubated in a water bath at 75–100 °C until gelatin was dissolved. The hot 2% gelatin solution was filtered through a sterile 40 µm pore size filter. 10 ml of the warm gelatin solution per 10 cm cell culture dish were incubated for 2 hours at 37 °C in the CO2 incubator. After discarding the redundant solution, the plates were dried under the laminar flow. With the coated side up, the plates can be stored at RT for several weeks.

3.2.2.15 Transfection of mammalian cells

Transfection of siRNA duplexes

Transfection of 21-nucleotide small interfering RNA (siRNA) duplexes (see table 14) for targeting endogenous genes in SCC9 cells was carried out using 5–8 µl LipofectamineTM RNAiMAX (Invitrogen) and 3–5 µl siRNA duplex /ml Optimem® medium (transfection mix) according to the manufacturer's protocol. The formats, the individual cell numbers seeded and the volume of transfection mix (Optimum plus nucleic acid plus transfection reagent) used are summarized below. Briefly, the transfection mix was incubated for 10-15 minutes on the cell culture plate, before the cells were added. 24 hours post transfection the medium was exchanged with fresh medium containing no antibiotics. For Erk1 and Erk2 knockdowns, the 24 hour HGF treatment was started 72 hours after transfection. For the Mig6 knockdown, the 24 hour HGF treatment was started at around 30 hours after transfection. Specific silencing of targeted genes was confirmed by Western blotting.

format	transfection mix	cell number (examples)
24-well	150 µl	35 000/150 µl
12-well	300 µl	50 000/300 µl

Transfection of plasmids

Transfection of pcDNA3-VSV-proAR or the empty control vector (table 12 and 13) for overexpression of pro-amphiregulin in SCC9 cells was carried out using 10 µl LipofectamineTM 2000 (Invitrogen) and 2 µl of vector DNA /800 µl Optimem® medium (transfection mix). Briefly, 40 000 SCC9 cells were seeded the day before transfection in 24-well plates. On the following day, the transfection mix was prepared and incubated for 30 minutes RT. Cells were washed once with pre-warmed PBS (37 °C) and 150 µl Optimem plus 150 µl raction mix was added per well. 5–6 hours post transfection the medium was exchanged with fresh medium containing no antibiotics. 24 hours after transfection cells were treated for 15 min with BB94 before they were incubated with HGF for 24 hours. On the following day the medium was collected and used to stimulate fresh SCC9 cells.

3.2.3 Protein analytical methods

3.2.3.1 Lysis of cells with Triton X-100 lysis buffer

Prior to lysis cells were washed once with ice cold PBS and then lysed for 15 minutes on ice in lysis buffer containing protease inhibitors (1 mM phenylmethylsulfonyl fluoride, 10 µg/ml aprotinin) and phosphatase inhibitors (2 mM sodium orthovanadate and 10 mM sodium fluoride). Cell lysates were scraped off the plates and precleared by centrifugation at 17 000 g for 10 minutes at 4 °C.

3.2.3.2 Determination of protein concentration in cell lysates

Protein concentration measurement was carried out using the Micro BCA Protein Assay Kit (Pierce, Sankt Augustin) according to the manufacturer's recommendations. The absorption was measured at 570 nm in a BioTek ELISA reader.

3.2.3.3 Immunoprecipitation of proteins

An equal volume of HNTG buffer was added to the precleared cell lysates that had been adjusted for equal protein concentration. Proteins of interest were immunoprecipitated using the respective antibodies (see table 7) and 20 µl of protein A-Sepharose for 4 hours at 4 °C with rotation. Precipitates were washed three times with 700 µl of HNTG buffer 1200 g for 3 minutes at 4 °C, suspended in 30 µl of 3× Laemmli buffer, boiled for 5 minutes and subjected to SDS-PAGE.

3.2.3.4 SDS-polyacrylamide-gelelectrophoresis (SDS-PAGE)

SDS-PAGE was conducted as described previously (Sambrook, 1990). Samples were run on gels consisting of collecting gel and separating gel in an ATTO polyacrylamide gel electrophoresis system. The separating gel contained 7.5% up to 12% acrylamide solution (according to the protein size) After gel polymerization, 20 µl of the protein samples were mixed with 10 µl of 3× Laemmli buffer, boiled for 5 minutes to remove all secondary, tertiary and quaternary structures and were loaded together with the protein marker on the acrylamide gel. Tris-glycine-SDS buffer was used for the electrophoresis and the voltage was set to 22 mA per gel. After protein separation, the gel was transferred to a nitrocellulose membrane for Western blotting.

3.2.3.5 Western Blotting

Western blotting was conducted as described previously (Gershoni and Palade, 1982). The separated proteins in the gel were transferred to a nitrocellulose membrane using a "semidry" Western blot system. Therefore the gel was put on the nitrocellulose membrane and 3 sheets of Whatmann 3MM paper were placed on top of the gel and below of the membrane. Blotting was performed for 2 hours at 80 mA/gel (0.8 mA/cm2) in the presence of transblot-SD buffer. After protein transfer to the membrane, proteins were stained with Ponceau S (2 g/l in 2% TCA) in order to visualize and mark standard protein bands. The membrane was destained in Millipore water.

3.2.3.6 Immunoblot detection

The transferred proteins, bound to the surface of the nitrocellulose membrane, were specifically visualized with immunodetection reagents. Therefore, the membrane was incubated in NET-gelatin for at least 1 hour at room temperature to block unspecific binding sites. The membrane was then probed with primary antibody (see table 6) diluted 1:500 to 1:2 000 in NET-gelatin, overnight. The membrane was washed 3 × for 5 minutes in NET-gelatin, incubated for 1 hour at room temperature with secondary peroxidas conjugated antibody (see table 8) diluted 1:10 000 in NET-gelatin, and washed again 3 × for 15 minutes. Antibody-antigen complexes were visualized using an ECL reagent. Luminescent bands were detected with X-ray films and, if indicated, densitometrically analysed using ImageJ software.

3.2.3.7 Stripping

Membranes were stripped of bound antibody in order to reprobe the membrane with different antibodies. Therefore, the membrane was incubated shaking in stripping buffer for 45 minutes at 52 °C in a closed container. Afterwards the membrane was washed at least 4 × for 20 minutes in NET-gelatin before it was incubated with another antibody overnight.

3.2.3.8 ELISA

To measure the concentration of human AR, human TGFα, human HB-EGF, mouse AR and mouse OSM sandwich ELISAs were performed. In brief, a 96-well plate (MaxiSorpTM flat-bottom, Nunc, Denmark) was coated with 100 µl/well of coating antibody (see table 9) overnight at room temperature. Final coating antibody concentrations were as follows: human AR 1.25 µg/ml, TGFα 0.5 µg/ml, HB-EGF 17 µg/ml, mouse AR 0.32 µg/ml and OSM 2 µg/ml diluted in PBS. On the following day plates were washed 3 × 150 µl/well with washing buffer (PBS/0.05% TW20). Then plates were blocked with PBS/1% BSA for 1 hour at room temperature. The blocking solution was removed from the plates and 100 µl/well of diluted samples and of standard were added to the plate and incubated at room temperature for 2 hours. Samples were diluted 1:10 for human AR, 1:5 for TGFα, HB-EGF and mouse AR in PBS/ 1% BSA; OSM samples were used undiluted. For the standards recombinant ligands (see section 2. 1.6) were diluted in PBS/ 1% BSA containing the same amount of RPMI + FCS as in the samples. The highest concentration of the standards was as follows: human AR 4000 pg/ml, TGFα 1000 pg/ml, HB-EGF 1000 pg/ml, mouse AR 2000pg/ml and OSM 1000 pg/ml. After three washes as above, biotinylated detection antibodies (see table 9) were added in a final concentration of 0.1 µg/ml for 1 hour at room temperature. The detection antibodies were diluted in PBS/1% BSA. The unbound detection antibody was removed by six washes as above and peroxidase-conjugated Streptavidin 1:5 000 (Jackson ImmunoResearch, USA) was added for 15–20 minutes. Plates were washed again 6 × as above before the ELISA was developed using 100 µl/well TMB and absorption was determined with a BioTek ELISA reader at 630 nm or the reaction was stopped with 50 µl/well 1 M H2SO4 and absorption was determined at 405 against 570 nm as a reference. ELISAs were performed in duplicates.

3.2.4 Analysis of whole cell-based assays

3.2.4.1 Migration assay

SCC9 cells were harvested with trypsin and washed with medium containing 10% FCS. Cells were washed again with serum free medium to remove residual FCS. 5×10^4 cells were seeded in 500 µl of serum free medium containing 0.1% BSA into 8 µm pore size polycarbonate transwells (also called boyden chamber, Becton Dickinson, France). The lower well (24-well companion plate) was filled with 700 µl of medium containing 0.1% BSA and TGFα or amphiregulin as chemoattractant. Migration was allowed for 4–6 hours at 37 °C and 7% CO2. Subsequently, migratory cells were washed with PBS and fixed and stained with fixing/staining buffer (0.5% (w/v) crystal violet in 20% methanol). Cells inside the transwell were removed with a cotton swab. Stained cells which have migrated to the bottom part of the chamber were photographed using a Zeiss AxioObserver A1 phase contrast microspcope with MetaVueTM imaging software. Cell migration was deduced by measuring the membrane area covered with migrated cells using Photoshop CS3 Extended Measurement feature.

3.2.4.2 MTT assay

In a 96-well flat bottom plate (Nunc, USA) 1 000 cells/100 µl were seeded. After 2 hours and after 72 hours 20 µl of MTT solution (3-[4,5-dimethylthiazol-2-yl]-2,5-diphenyltetrazolim bromide; thizolyl blue, Sigma, Taufkirchen) was added to each well to a final concentration of 1 mg/ml MTT. Plates were incubated in the presence of MTT for 2 hours. Mitochondrial dehydrogenase activity reduces the yellow MTT to a purple formazan, which was solubilized with MTT stop solution (DMSO, acidic acid, SDS) and absorbance was measured at 570 nm on a micro-plate reader.

3.2.4.3 FACS analyses

FACS analyses of antibody labeled cells

For human and mouse monocyte/macrophage FACS analyses, $2 \times 10^5 – 5 \times 10^5$ cells were harvested on ice, pelleted by centrifugation for 3 minutes at 800 g at 4 °C. The cells were resuspended in ice-cold PBS/1% BSA/10 mM EDTA. For human monocyte/macrophage FACS analyses, cells were incubated with dual color primary monoclonal antibodies against CD14 (FITC-labeled) and CD64 (PE-labeled) or the corresponding isotype control (see table 10). For mouse monocyte/macrophage FACS analyses, cells were incubated with either with primary FITC-labeled monoclonal antibodies against CD14 and F4/80 or the corresponding isotype control (see table 10). The cells were incubated with the antibodies for 45 minutes at 4 °C in the dark. Stained cells were washed once with 500 µl PBS/1% BSA/10 mM EDTA and resuspended in 400 µl PBS/1% BSA/10 mM EDTA. Dead cells were gated out on the basis of their light scatter properties. The analyses were performed using a FACScan flow cytometer and CellQuest software. Cells were gated on FL2 (PE) and FL1 (FITC).

For human SCC9 cell FACS analyses, $2 \times 10^5 – 5 \times 10^5$ differentially treated cells were harvested on ice, resuspended in ice-cold PBS/1% BSA/10 mM EDTA and incubated either with monoclonal antibodies against the EGFR extracellular domain specific mAb (clone 108.1) or the corresponding isotype control (clone 4H1A7) (see table 10) at a concentration of 20 µg/ml for 1 hour at 4 °C. The cells were washed once followed by 45 minutes incubation at 4 °C in the dark with the PE-conjugated secondary donkey anti-mouse IgG antibody (see table 10). Stained cells were washed twice with PBS/1% BSA and resuspended in 400 µl PBS/1% BSA/10 mM EDTA. The analyses were performed using a FACScan flow cytometer and CellQuest software. Cells were gated on FL2 (PE).

FACS analyses using FFC vs. SSC dot blot

FSC (forward scatter) vs. SSC (side scatter) FACS analysis was used to determine the monocyte/ macrophage purity after isolation. The distribution of the dots in the plot can distinguish one type of cell from another and allow gating around one particular population of cells for further analysis. Cells that are more granular are represented as higher values along the x-axis (SSC), while larger cells are represented as higher values along the y-axis (FSC).

$2 \times 10^5 – 5 \times 10^5$ primary human or mouse monocyte/macrophage were harvested on ice by scraping them off the plates and pelleted by centrifugation at 800 g for 3 minutes at 4 °C. Cells were resuspended

in ice-cold PBS/1% BSA/10 mM EDTA and analyzed using FACScan flow cytometer and CellQuest software.

3.2.5 SILAC experiments and MS analysis

3.2.5.1 Cell culture in SILAC medium

SCC9 cells were grown for eleven days in DMEM high glucose/F12 1:1 mix containing either normal L-arginine and L-lysine (Sigma), L-arginine-U-13C6 14N4 and L-lysine 2H4 or L-arginine-U-13C6-15N4 and L-lysine-U-13C6-15N2 (Cambridge Isotope Laboratories, USA), as well as dialyzed FBS (Gibco). After 10 days cells were treated with 50 ng/ml HGF for 24 hours.

3.2.5.2 Stable isotope labeling, cell lysis and anti-EGFR immunoprecipitation for mass spectrometry

After washing once with ice-cold PBS, SILAC labeled cells were lysed for 15 minutes with ice-cold lysis buffer (50 mM Tris, pH 7.5; 150 mM NaCl; 1% NP40; 0.1% sodium deoxycholate; 1 mM EDTA; 1 mM sodium orthovanadate; 1 mM PMSF; 0.1 µg/ml aprotinin; 10 mM NaF). Lysates were precleared by centrifugation at 16 000 g for 10 minutes at 4 °C. The BCA assay (Pierce) was then used to determine the absolute protein amount. For the pooling control 10 µl cell lysate per label were mixed 1:1:1 directly after protein amount determination and 20 µl of NuPAGE® LDS sample buffer (4×) were added. For anti-EGFR immunoprecipitation 8 mg antibody was added together with 80 µl protein A-Sepharose to cell lysates containing 6 mg total protein and incubated for 4 hours at 4 °C. Precipitates were subsequently washed three times with lysis buffer.

3.2.5.3 Mass spectrometry analysis

The samples were pooled and prepared for mass spectrometry as described previously (Selbach et al., 2006). The samples were analyzed by online liquid chromatography-tandem mass spectrometry (LC-MS/MS) on a LTQ-Orbitrap mass spectrometer (Thermo Electron). The identified peptides were assigned to proteins using Mascot (Matrix Science). Data processing was performed using MaxQuant software (version 1.1.1.21). Two biological replicates were analyzed.

4 RESULTS

4.1 HGF-mediated EGFR paracrine crosstalk

4.1.1 HGF-induced EGFR ligand release

To analyze HGF-induced EGFR transactivation pathways the tongue-derived squamous cell carcinoma cell line SCC9 was used as prototypical cell model system. SCC9 cells represent an excellent system to study EGFR signaling because of several reasons: first, they have already been used successfully for EGFR transactivation studies (126, 127); second, SCC9 cells have high EGFR expression levels and low EGFR background phosphorylation, which makes it easy to detect low EGFR ligand doses; and third SCC9 cells grow in epithelial sheets, which makes them an ideal model to study HGF-induced cell scattering.

4.1.1.1 Identification of HGF-induced EGFR ligands in SCC9 cells

SCC9 cells treated with HGF showed elevated mRNA levels of the EGFR ligands amphiregulin (AR), TGFα and HB-EGF. AR and HB-EGF mRNA levels increased by a maximum of 7-fold and TGFα mRNA levels of 2.3-fold at 2 h after stimulation with HGF (Fig. 5A). In ELISA analyses of the cell culture supernatant increased AR and TGFα protein levels could be detected in response to HGF (Fig. 5B). In contrast, HB-EGF protein was not found in the supernatant, but in the cell lysate (Fig. 5C) indicating that HB-EGF was either not released or the released ligand attached to the extracellular matrix or the cell surface and was therefore not available. Although the transcript induction took place early after HGF stimulation, the kinetics of the release was delayed: AR and TGFα accumulation started after 4–8 hours and peaked after 24 hours. To investigate a dose dependency, SCC9 cells were stimulated with a serial dilution of HGF. AR release started at around 5 ng/ml HGF and reached a plateau at 30 ng/ml (Fig. 5D).

However, although EGFR ligands were present in the cell culture medium, the EGF receptor did not become phosphorylated on tyrosine residues after HGF treatment (Fig. 5E)—this blocked EGFR TK-activity will be discussed later in part 4.1.2.

In order to test if the released ligands are capable of EGFR activation, the following two step experimental setup was used: first, SCC9 cells were incubated with HGF for 24 hours; the conditioned medium (CM) was then collected. Second, fresh, untreated SCC9 cells were stimulated for three minutes with this CM before they were subjected to phospho-EGFR immunoblot. If active EGFR ligands were shed, an activation of the EGFR should occur now.

Strong EGFR and HER2 phosphorylation was observed and blocking antibody experiments revealed AR and TGFα to be the major contributors of activation (Fig. 5F).

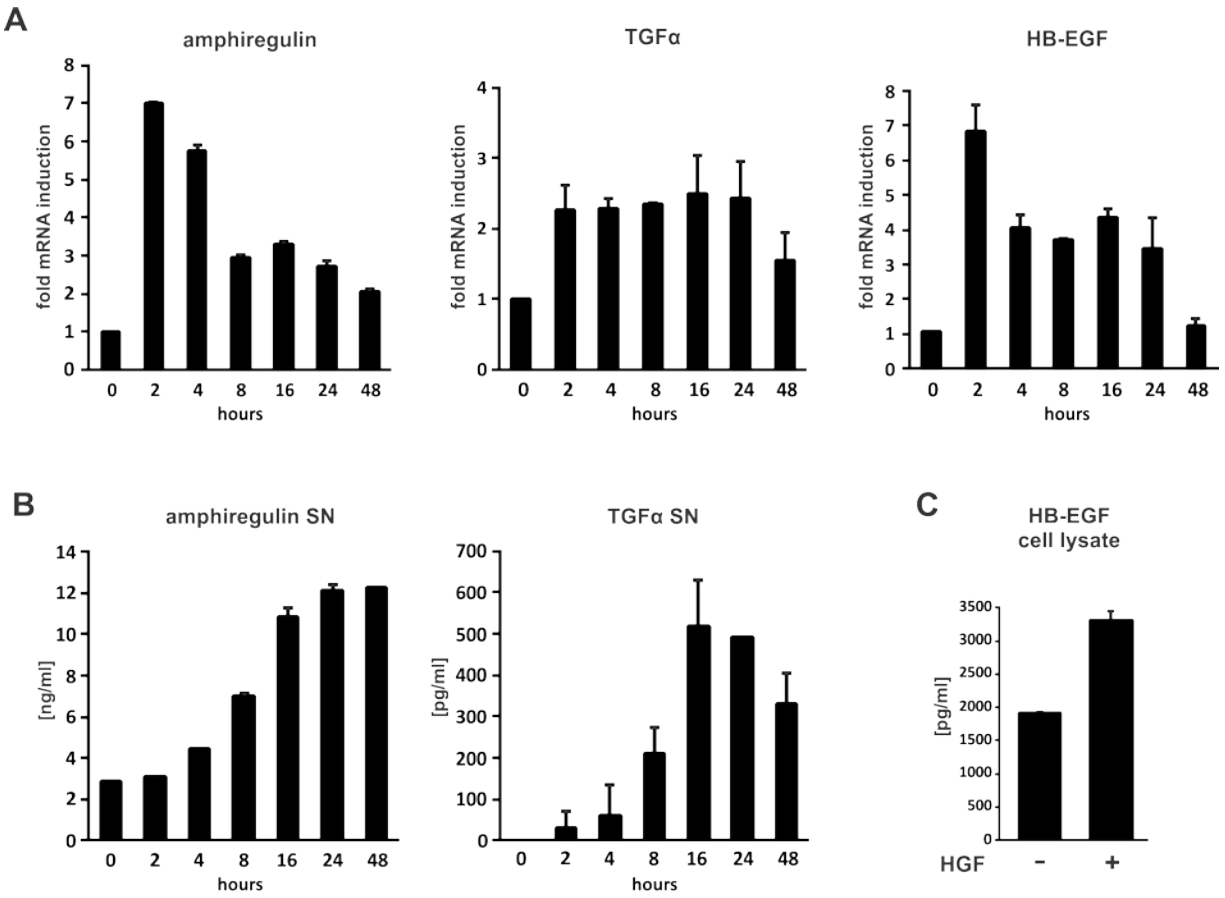

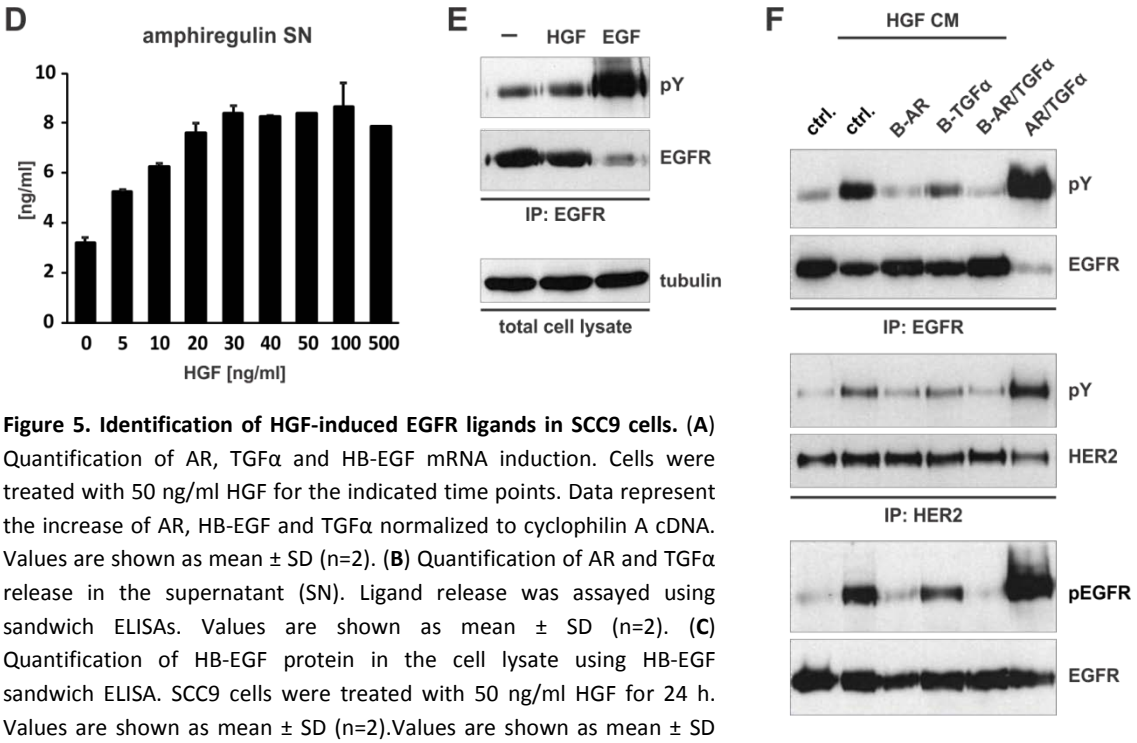

Figure 5. Identification of HGF-induced EGFR ligands in SCC9 cells. (**A**) Quantification of AR, TGFα and HB-EGF mRNA induction. Cells were treated with 50 ng/ml HGF for the indicated time points. Data represent the increase of AR, HB-EGF and TGFα normalized to cyclophilin A cDNA. Values are shown as mean ± SD (n=2). (**B**) Quantification of AR and TGFα release in the supernatant (SN). Ligand release was assayed using sandwich ELISAs. Values are shown as mean ± SD (n=2). (**C**) Quantification of HB-EGF protein in the cell lysate using HB-EGF sandwich ELISA. SCC9 cells were treated with 50 ng/ml HGF for 24 h. Values are shown as mean ± SD (n=2).Values are shown as mean ± SD (n=2). (**D**) Kinetics of AR shedding. AR release was assayed using AR sandwich ELISA. Values are shown as mean ± SD (n=2). (**E**) EGFR IP followed by Western blot analysis of SCC9 cells treated with HGF and EGF for 10 min. Immunoblots for phospho-tyrosine (=pY) and EGFR are shown. Total cell lysate blotted with tubulin was used as loading control. (**F**) EGFR and HER2 IP followed by Western blot analysis. SCC9 cells were stimulated for 5 min with HGF CM in the presence of blocking (B) anti-AR and anti-TGFα antibodies. Immunoblots for pY, EGFR and HER2 are shown. Total cell lysate was blotted for pEGFR and EGFR.

4.1.1.2 HGF-induced EGFR ligand release is a common characteristic of cancer cells and depends on new protein synthesis

Next, various epithelial cancer cell lines, derived from different tissues (breast, kidney and liver) were tested for their capability of HGF-induced EGFR ligand release. As shown in figure 6A the breast cancer cell line MDA-MB-231, the kidney cell line A498 as well as the two liver cancer cell lines HepG2 and Huh7 were capable of releasing AR and/or TGFα, into the cell culture medium within 24 hours. Induction of AR transcripts was observed in all tested cell lines, whereas elevated TGFα transcripts were found only in MDA-MB-231 cells (Fig. 6B).

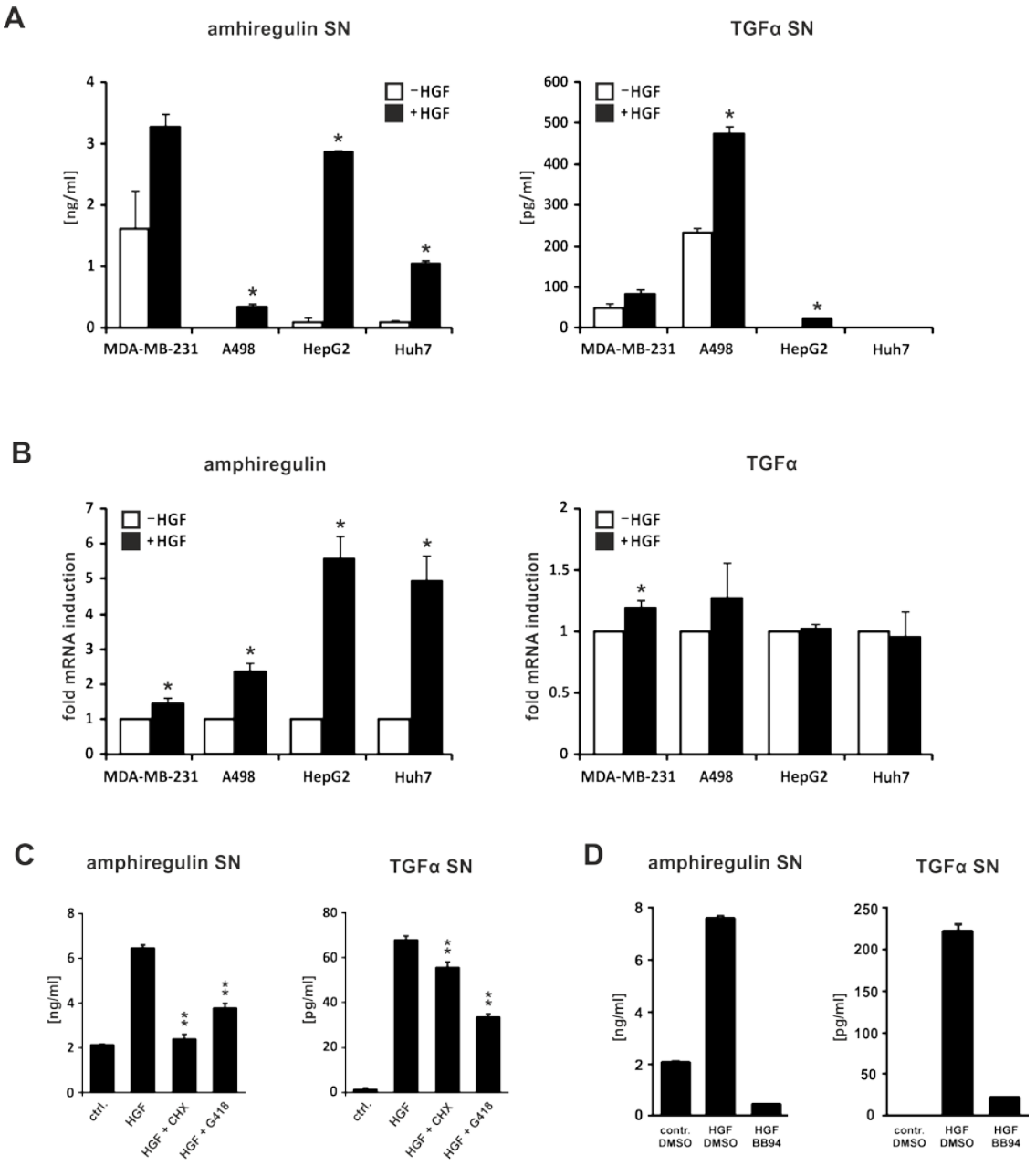

Figure 6. HGF-induced EGFR ligand release is a common characteristic of cancer cells and depends on new protein synthesis. (**A**) Quantification of AR and TGFα release in the supernatant (SN). Different epithelial cancer cell lines, derived from breast (MDA-MB-231), kidney (A498) and liver (HepG2, Huh7), were treated with (black bars) or without (white bars) 50 ng/ml HGF for 24 hours. Ligand release into the SN was assayed using sandwich ELISAs. Error bars indicate SEM of three independent experiments. Asterisk indicate significant changes (p<0.001, unpaired

Student's *t*-test). (**B**) Quantification of AR and TGFα mRNA induction of the same cell lines shown in figure A. Cells were treated with 50 ng/ml HGF for two hours. Error bars indicate SEM of three independent experiments. Asterisk indicate significant changes ($p<0.001$, unpaired Student's *t*-test). (**C**) Quantification of AR and TGFα release. SCC9 cells were treated with HGF and with the translation inhibitors cycloheximide (CHX) and geneticin (G418) for 24 h. Ligand release into the SN was assayed using sandwich ELISAs. Error bars indicate SEM of three independent experiments. Double asterisk indicate significant repression ($p<0.001$, unpaired Student's *t*-test). (**D**) The metalloprotease inhibitor batimastat (BB94) blocked shedding of AR and TGFα from the cell surface. SCC9 cells were treated with BB94 and HGF for 24 hours. Ligand release into the SN was assayed using sandwich ELISAs. Values are shown as mean ± SD (n=2). (**E**) Pro-AR transfected SCC9 cells were treated with HGF and the metalloprotease inhibitor batimastat (BB94) for 24 h. The SN was used to stimulate new (untreated SCC9 cells). Immunoblot for pEGFR is shown. Tubulin served as loading control.

Release of EGFR ligands is induced by proteolytic cleavage of membrane-anchored proforms. To test whether AR and TGFα release depend on new protein synthesis or on shedding of existing proforms, the effect of the translation inhibitors cycloheximide and G418 (=geneticin) was investigated. Both inhibitors abrogated AR release and significantly reduced TGFα release into the SN (Fig. 6C) proving a regulation on the level of transcription.

4.1.1.3 Metalloprotease-dependent shedding of EGFR ligands

EGFR ligands are mainly produced as membrane bound proforms. To test if metalloproteases regulate the shedding from the cell surface, SCC9 cells were treated with the broad band metalloprotease inhibitor batimastat (BB94) during the entire period of HGF treatment. Batimastat completely abrogated the EGFR ligand release into the supernatant (Fig. 6D).

Knowing that EGFR ligand accumulation depends on new protein synthesis, the question, however, still remains if the shedding of the membrane bound proforms is induced in response to HGF. To answer this question pro-AR was overexpressed in SCC9 cells. There were two possible outcomes: first, if HGF stimulation is required to initiate shedding, no AR should be released; or the second possibility, if the presence of AR is already sufficient for its shedding, AR should be released. Overexpressed pro-AR was shed strongly without the need of HGF stimulation—suggesting a HGF independent shedding mechanism. Endogenous as well as exogenous AR shedding was inhibited by batimastat (Fig. 6E).

4.1.1.4 CM of a monocytic cell line induces EGFR ligand induction via HGF/Met

Monocytes, macrophages and fibroblasts are thought to be the major sources of HGF in the tumor stroma (15, 35, 37). It was of interest, whether a complex conditioned medium (CM) derived from a monocytic cell line, is capable to induce EGFR ligand release. Therefore, CM of MAD-NT cells, a subclone of the promyelocytic leukemia cell line HL60, was used. AR and TGFα were released upon MAD-NT CM by SCC9 cells and a blocking HGF antibody abrogated the ligand induction (Fig. 7). Blood-derived cells can be very potent inducers of EGFR ligand release in cancer cells.

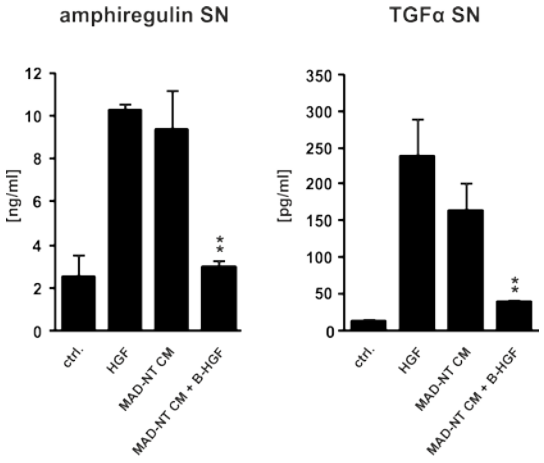

Figure 7. Monocyte-derived HGF induces EGFR ligand release. SCC9 cells incubated with the CM of the monocytic cell line MAD-NT release AR and TGFα into the SN. MAD-NT CM pretreated with a blocking (B) anti-HGF antibody before it was used to treat SCC9 cells, did not induce EGFR ligand release in SCC9 cells. Ligand release was assayed using sandwich ELISAs. Error bars indicate SEM of three independent experiments. Double asterisk indicate significant decrease ($p<0.005$, unpaired Student's t-test).

4.1.1.5 Identification of the pathway underlying EGF ligand induction

To investigate which signal transducers downstream of HGF mediate the upregulation of EGFR ligands, SCC9 cells were stimulated with HGF or MAD-NT CM and assayed in immunoblot analysis for the activation of the downstream signal transducers Erk1/2, Akt, p38 MAPK and SAPK/JNK. All tested signal transducers got activated by HGF and by MAD-NT CM. A blocking HGF antibody reduced activation of Erk1/2, Akt, p38 MAPK and SAPK/JNK (Fig. 8A). In a next step, SCC9 cells were cultured in the presence of the PI3 kinase inhibitor wortmannin and with the MEK inhibitor UO126 during the 24 hour HGF treatment and their effects on AR and TGFα transcript induction and protein accumulation was examined. Full inhibition of EGFR ligand induction was achieved with the MEK inhibitor, whereas the PI3

kinase inhibitor showed no effect (Fig. 8B and C). This experiment reveals a MAPK pathway underlying the EGFR ligand transcript induction.

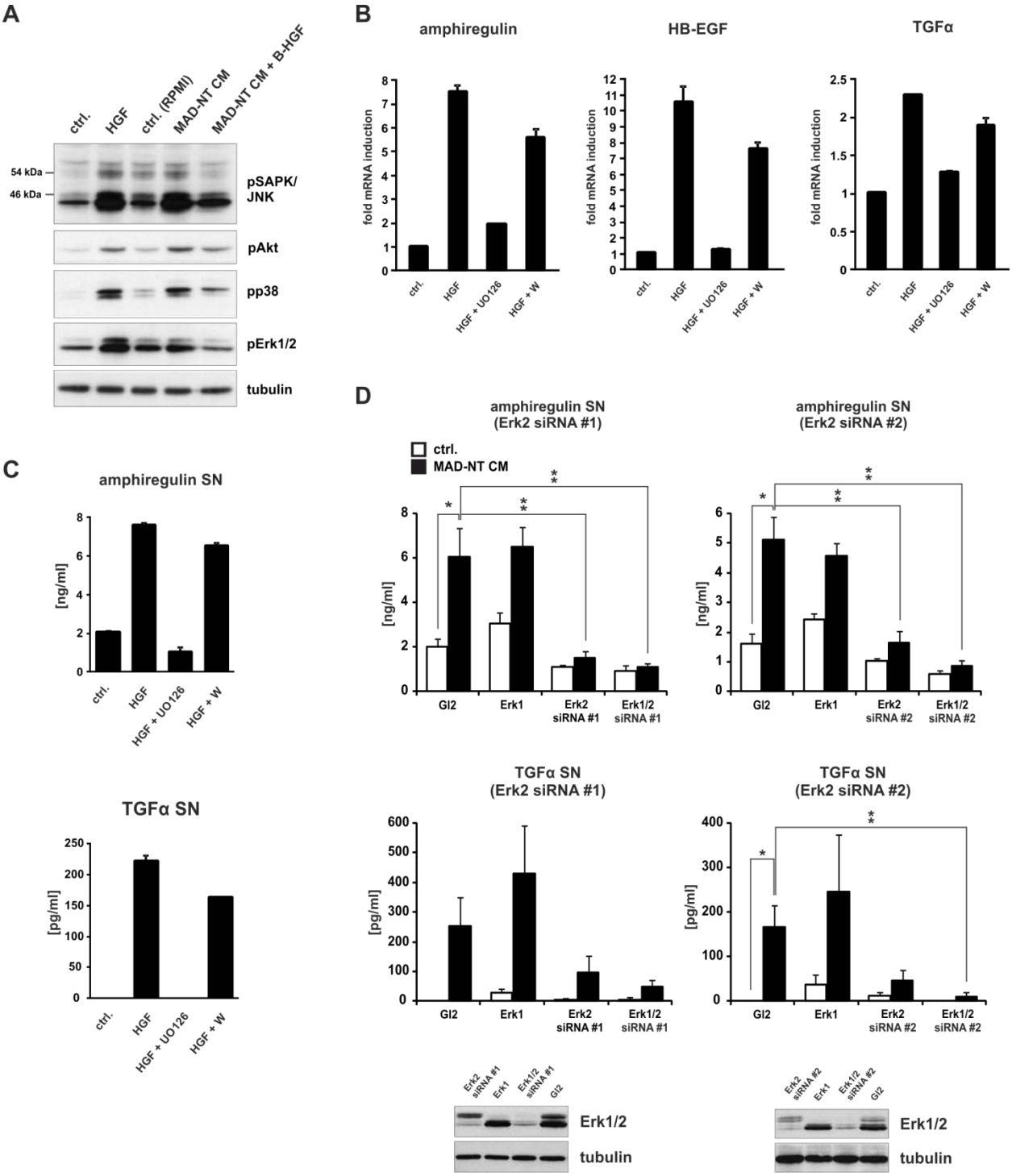

Figure 8. Erk2 is required for HGF-induced EGFR ligand production. (A) Western blot analysis of SCC9 cells stimulated with HGF, MAD-CM or MAD-CM+blocking (B) anti-HGF antibody for 10 min. Immunoblots for pSAPK/JNK (JNK1 (SAPK gamma) = 46 kDa; JNK2 (SAPK alphaII) = 54 kDa), pAkt, pp38 MAPK and pErk1/2 are shown. Tubulin served as loading control. (**B**) Quantification of AR, HB-EGF and TGFα mRNA induction of SCC9 cells pretreated with the MEK inhibitor UO126 and the PI3K inhibitor wortmannin (W) for 15 min before 2 h HGF treatment. Values are shown as mean ± SD (n=2). (**C**) Quantification of AR and TGFα release of SCC9 cells treated with UO126 and wortmannin (W) for 15 min prior to 24 h HGF treatment. Ligand release was assayed using sandwich ELISAs. Values are shown as mean ± SD (n=2). (**D**) Erk1 and Erk2 knockdown (KD) in SCC9 cells. AR and TGFα release was measured with sandwich ELISAs. MAD-NT CM was used as HGF source. Error bars indicate SEM of three independent experiments. Single asterisk indicate significant increase; double asterisk indicate significant decrease ($p<0.05$, unpaired Student's t-test). KD was verified with Erk1/2 immunoblot; tubulin served as loading control.

To evaluate which MAPK is responsible for the EGFR ligand induction, siRNA knockdown experiments of Erk1 and Erk2 were performed. A Knockdown of Erk2 dramatically reduced the release of AR and TGFα, whereas a knockdown of Erk1 showed no effect. Interestingly a double knockdown of Erk1 and Erk2 further reduced the production of the EGFR ligands, indicating, that Erk1 could partly compensate for the loss of Erk2 (Fig. 8D).

4.1.1.6 TGFα is a strong inducer of directed cell migration in SCC9 cells

Next we evaluated the migratory effect of the induced EGFR ligands AR and TGFα on SCC9 cells. AR and TGFα concentrations with a similar potency in activating the EGF receptor as well as the downstream signal transducers Akt and Erk1/2 (Fig. 9A) were used for the transwell experiments. Surprisingly, although EGFR, Akt and Erk1/2 were activated by both ligands, TGFα seems to be a much stronger (two-fold and 25-fold, respectively) chemoattractant for SCC9 cells (Fig. 9B).

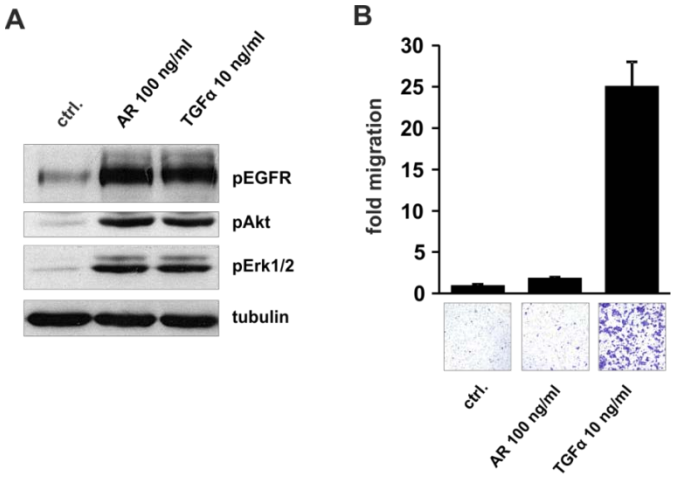

Figure 9. TGFα is a strong inducer of directed cell migration in SCC9 cells. (**A**) Western blot analysis of SCC9 cells stimulated with AR and TGFα for 5 min. Immunoblots for pEGFR, pAkt and pErk1/2 are shown. Tubulin served as loading control. (**B**) In vitro transwell migration assay with SCC9 cells. Cells were seeded on to a membrane with 8 µM pores of a modified boyden chamber containing 500 µl serum-free medium. The lower chamber was filled with 700 µl medium containing AR and TGFα as chemoattractants. The cells were allowed to migrate for 6 h through the pores.

4.1.2 HGF-induced EGFR negative regulation

4.1.2.1 HGF is a paracrine inhibitor of classical EGFR activation

As mentioned above, HGF-induced EGFR ligands do not phosphorylate the EGF receptor on tyrosine residues of the same cell, although these ligands are very potent in activating new (HGF-untreated) cells. Interestingly, the EGFR of HGF-treated SCC9 cells cannot even be activated by stimulation with recombinant amphiregulin (AR) (Fig. 10A).

To investigate whether this inhibitory effect of HGF on EGFR TK activity represents a common characteristic of cancer cells, 12 human carcinoma cell lines originating from breast, kidney, liver and tongue—tissues which were found to express functional Met as well as EGFR in primary tumors—were examined. In all tested cell lines HGF-mediated inhibition of EGFR activation after AR stimulation was observed (Fig. 10B).

To further assess the impact of the loss of EGFR TK activity on downstream signaling events, we investigated the phosphorylation of EGFR co-immunoprecipitated EGFR interactors. We found a complete inhibition of EGFR signal transducer activity upon ligand stimulation (Fig. 10C).

4.1.2.2 Loss of EGFR TK activity is independent of an autocrine EGFR feedback loop

Protein internalization and degradation is a common negative feedback mechanism to attenuate growth factor receptor signaling. In order to determine whether the HGF-induced release of active amphiregulin into the cell culture medium leads to an EGFR negative feedback loop, total EGFR protein as well as cell surface EGFR was analyzed via Western blot and FACS analyses, respectively. Interestingly no changes in total EGFR protein amount were observed in EGFR immunoblot (Fig. 10B, EGFR reblot) nor were there relevant differences in cell surface EGFR levels detected by FACS analysis (Fig. 10D). To further verify these findings, shedding of the EGFR ligands from the cell membrane was blocked by treatment of SCC9 cells with the metalloprotease inhibitor batimastat (BB94) during the entire period of HGF treatment, before the cells were stimulated with amphiregulin (Fig. 10E and Fig. 6D). It could be confirmed that the observed inhibition of EGFR TK activity is independent of the HGF-induced release of endogenous EGFR ligands.

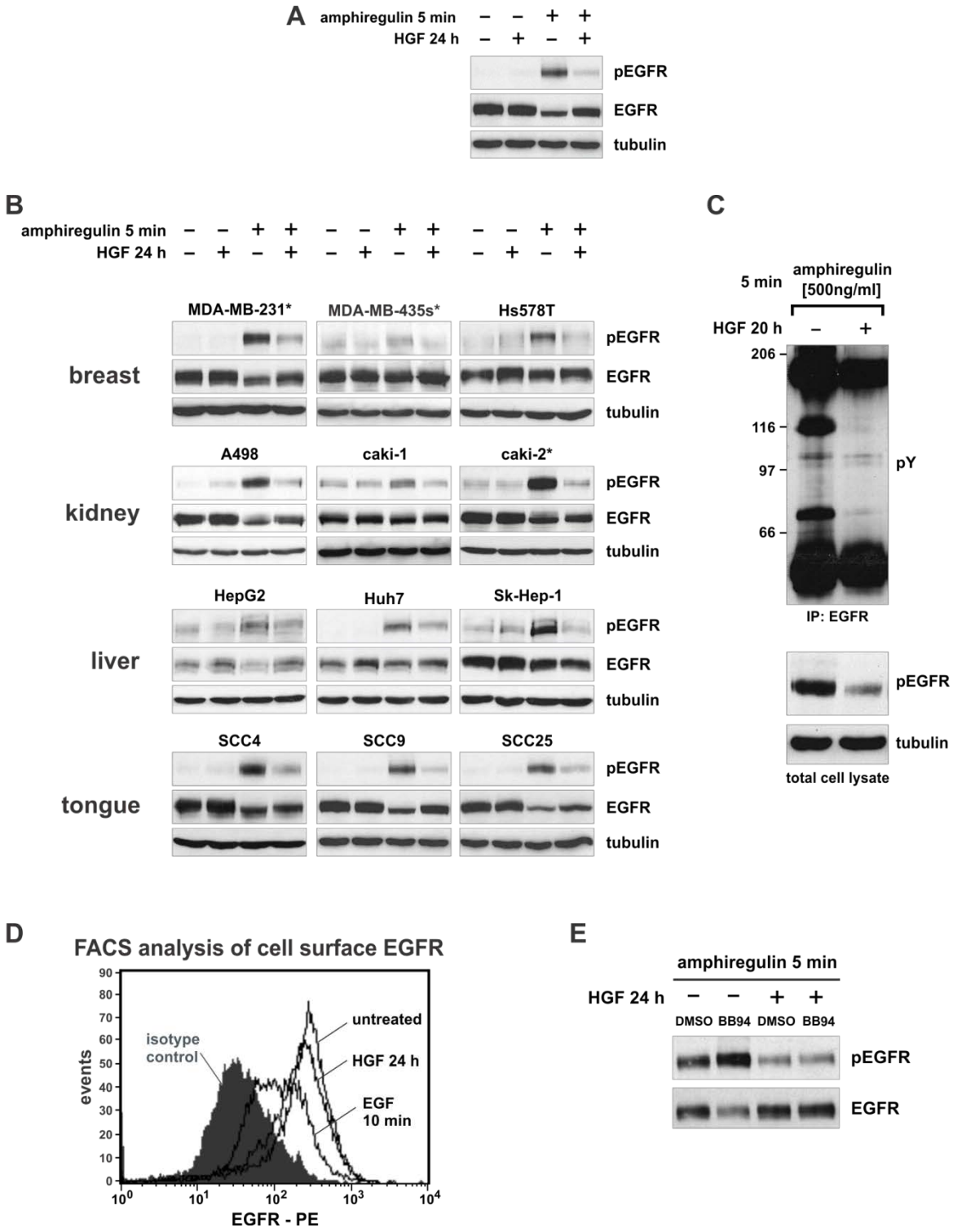

Figure 10. Inhibition of EGFR ligand-induced EGFR phosphorylation after HGF treatment. (**A**) Western blot analysis of SCC9 cells pretreated with HGF for 24 h before stimulation with 50 ng/ml amphiregulin. (**B**) Western blot analysis of different cancer

cell lines pretreated with HGF for 24 h before stimulation with either 50 ng/ml or *500 ng/ml amphiregulin. (**C**) Western blot analysis of EGFR downstream signaling after HGF treatment. 20 h HGF-treated SCC9 cells were stimulated with amphiregulin. Total cell lysate and EGFR co-immunoprecipitation were immunoblotted for phospho-tyrosine (=pY), pEGFR Y1173 and tubulin. (**C**) Flow cytometric analysis of cell surface EGFR in SCC9 cells. EGF-stimulated cells were used as positive control for receptor internalization. Note that HGF-treated cells express the same level of cell surface EGFR compared to untreated cells. (**E**) Western blot analysis of SCC9 cells pretreated with HGF in the presence of batimastat (BB94) or DMSO (negative control) for 24 h before stimulation with amphiregulin.

4.1.2.3 Pathway underlying EGFR TK blockage

To investigate which signal transducers downstream of HGF mediate the non-responsiveness to the EGFR ligand stimulation, we cultured SCC9 cells in the presence of an inhibitor against the HGF receptor Met (PHA665752), a PI3 kinase inhibitor (wortmannin) and two MEK inhibitors (UO126 and PD98059) during the 24 hour HGF treatment, and examined their effects on amphiregulin-induced EGFR activation.

Notably, full recovery of EGFR responsiveness was achieved with the Met and both MEK inhibitors, whereas the PI3 kinase inhibitor showed no effect (Fig. 11A). Two different MEK inhibitors showing the same effect, argues for specific involvement of MEK rather than off-target effects of these inhibitors. This experiment reveals a MAPK pathway underlying the EGFR suppression.

4.1.2.4 Loss of EGFR TK activity is independent of the EGFR negative regulator Mig6

Overexpression and siRNA knockdown studies revealed that Mig6 is a negative regulator of EGF receptor signaling (128). Mig6 can be induced in response to HGF/Met signaling (129). Therefore it was of interest to explore whether a Mig6 induction upon HGF treatment accounts for the observed loss of EGFR TK activity in SCC9 cells. Thus we evaluated if a siRNA knockdown of Mig6 could reverse the loss of EGFR TK activity. SCC9 cells were transfected with siRNAs specific for firefly luciferase (ctrl.) or Mig6, before they were treated with HGF for 24 hours and stimulated with AR. Western blot analysis of pEGFR revealed that Mig6 is not responsible for the suppressed EGFR TK activity (Fig. 11B).

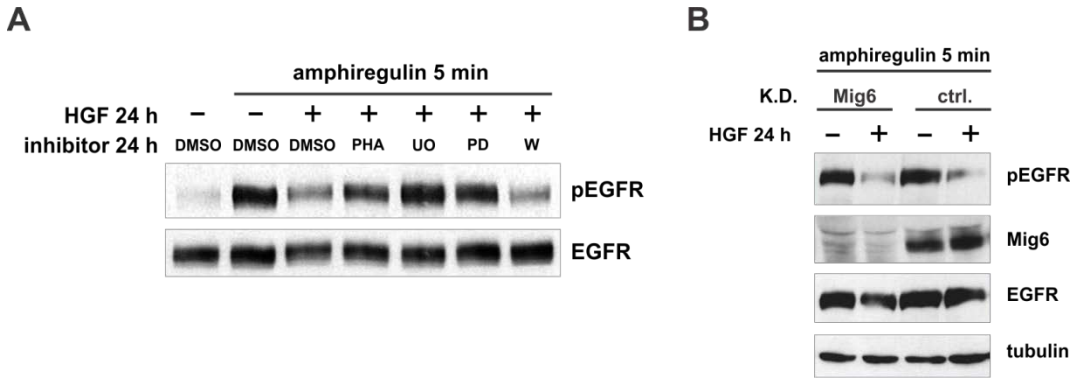

Figure 11. Rescue of EGFR TK blockage depends on MAPK signaling, but is independent of Mig6. (**A**) Western blot analysis of SCC9 cells pretreated with HGF in the presence of Met inhibitor PHA665752 (=PHA), MEK inhibitors UO126 (=UO) and PD98059 (=PD), PI3K inhibitor wortmannin (=W) or DMSO for 24 h before stimulation with 50 ng/ml amphiregulin. (**B**) Mig6 knockdown SCC9 cells. The cells were transfected with Mig6 or control siRNAs as described in Material and Methods. 30 h after transfection, cells were incubated with HGF for 24 h before stimulation with AR. Cell lysates were subjected to Western blot analysis. Immunoblots for pEGFR, Mig6, EGFR and tubulin are shown.

4.1.2.5 HGF leads to impaired EGFR-mediated migration

Next, it was investigated whether the HGF-mediated inhibition of EGFR TK activity has a functional consequence on the migratory behavior of SCC9 cells. In line with the widely accepted effect of HGF on cell scattering, an undirected scattering of SCC9 cells could be detected after 24 hours of HGF treatment (Fig. 12A). Due to the fact that HGF-treated cells scatter and are in a scatterlike morphology already, it would be expected that they migrate faster towards chemoattractants compared to cells, which are in a resting mode. Surprisingly, directed migration towards the EGFR ligand TGFα was found to be 2.3-fold reduced in HGF-pretreated SCC9 cells compared to untreated cells (5.4-fold and 12.6-fold, respectively (Fig. 12B). In support of this, the binding and activation of signal transducers to EGFR upon ligand stimulation is completely abolished in cells pretreated with HGF (Fig. 10C). Thus, HGF incubation results in enhanced scattering but impaired EGFR-mediated migration.

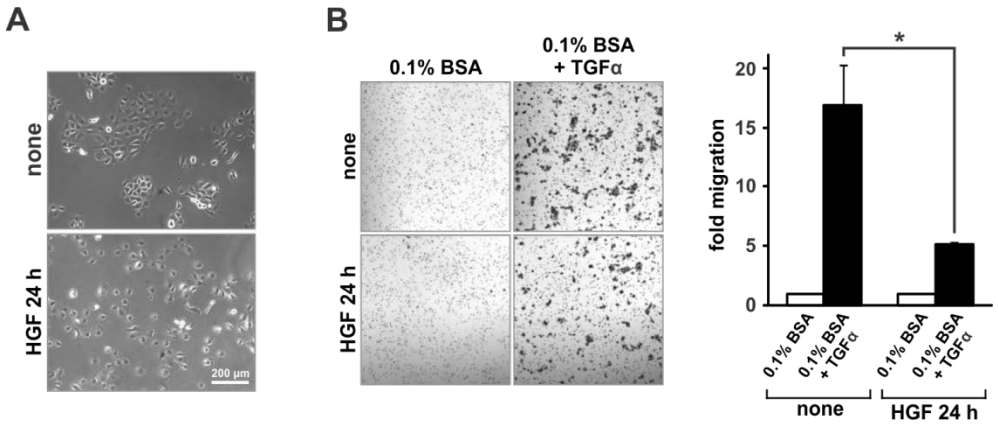

Figure 12. Inhibition of EGFR ligand-induced cell migration after HGF treatment. (**A**) Pictures of undirected migrating SCC9 cells. Cells were treated with or without HGF and scattering was evaluated after 24 h. Pictures were taken with a Zeiss Axio Observer.A1 microscope. (**B**) In vitro transwell migration assay with SCC9 cells. Cells were treated with HGF for 24 h and subjected to the chemoattractant TGFα. The cells were allowed to migrate for 4 h through the pores. Results were plotted in each case as fold migration relative to background migration (10× magnification). Error bars indicate SEM (n=3). Asterisk indicates significant reduction ($P < 0.050$, unpaired Student's *t*-test).

4.1.2.6 HGF induces various EGFR interactions

The finding that classical EGFR signaling is abrogated after HGF treatment although the EGFR cell surface expression level is unchanged, prompted us to search for an alternative mode of EGFR action or for an EGFR modification. In order to identify potential HGF-induced EGFR binding partners, total lysate from SCC9 cells treated with or without HGF was subjected to EGFR co-IP followed by mass spectrometric analysis. Therefore SCC9 cells were metabolically SILAC-labeled with either normal arginine and lysine (Arg0 and Lys0) or with combinations of isotopic variants of the two amino acids (Arg6 and Lys4, or Arg10 and Lys8). To distinguish between specific EGFR binders and non-specific binders, SCC9 total lysate was subjected to control beads (no antibody). In addition, HGF-treated and untreated cells were stimulated with amphiregulin, since possible EGFR interaction partners should also be present in this originally used setting of figure 10A. Precipitated proteins were resolved by SDS-PAGE. Coomassie staining of the gel visualized protein bands, which were excised from the gel and digested with trypsin followed by subsequent MS analysis (Fig. 13A-C). Fig. 14A provides an overview of all HGF reduced ($r \leq 0.67$; left side of left dashed line) and induced ($r \geq 1.5$; right side of right dashed line) EGFR binding partners. EGFR interactors specifically induced by HGF were further selected using the following criteria:

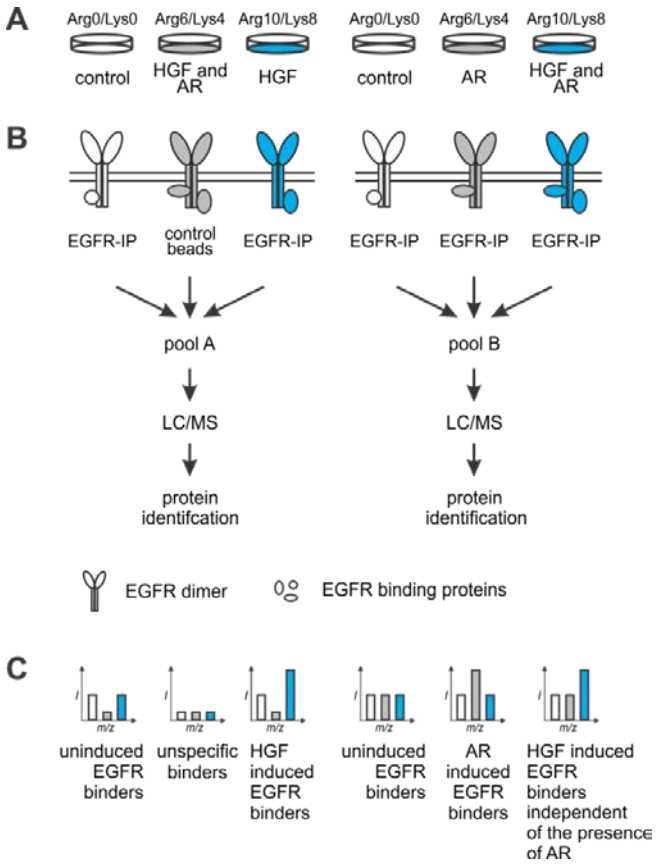

Figure 13. Strategy to detect HGF-induced EGFR binding partners by quantitative proteomics. (**A**) Experimental workflow showing SILAC labeling and stimulation schemes. Six SILAC-labeled SCC9 cell-populations were treated with HGF and/or amphiregulin (AR). (**B**) Cell lysates were subjected to immunoprecipitation (IP) with a monoclonal anti-EGFR antibody or were incubated with control beads (no antibody). To allow the comparison of five different conditions with only three different labels, sample Arg0/Lys0 of pool A and pool B was used as reference sample. The three elution fractions of pool A and pool B were analyzed by quantitative liquid-chromatography mass-spectrometry (LC-MS). (**C**) Identification of HGF-induced EGFR binding partners based on peptide ratios determined for target proteins. Schematic representations of the main response patterns observed in SILAC mass spectra of EGFR binders are shown. *m/z*, mass to charge ratio; *I*, intensity.

first, to discriminate EGFR binders from background binders, average ratios of the two biological replicates of EGFR retained peptides should be at least two-fold enriched compared to control beads (no antibody), indicated by cuts of r ≤ 0.5 for Arg6/Lys4 *versus* Arg0/Lys0 (pool A) and r ≥ 2 for Arg0/Lys0 (pool B) *versus* Arg6/Lys4 (pool A); second, HGF-induced EGFR binders should be 1.5-fold enriched compared to cells without HGF treatment with (Arg10/Lys8 *versus* Arg6/Lys4 of pool B) or without (Arg10/Lys8 *versus* Arg0/Lys0 of pool A) amphiregulin stimulation; and finally, HGF-induced EGFR binders, induced in the presence of amphiregulin, should not be affected by amphiregulin stimulation—indicated by a cut of r ~1 for Arg6/Lys4 *versus* Arg0/Lys0 of pool B (table 17). Interestingly, binding capacity of the EGFR signaling molecules CBL, CBLB, SHC, SOS2, PI3K subunits p85 and p110 is abrogated or even down regulated after HGF or HGF plus AR treatment (Fig. 14B).

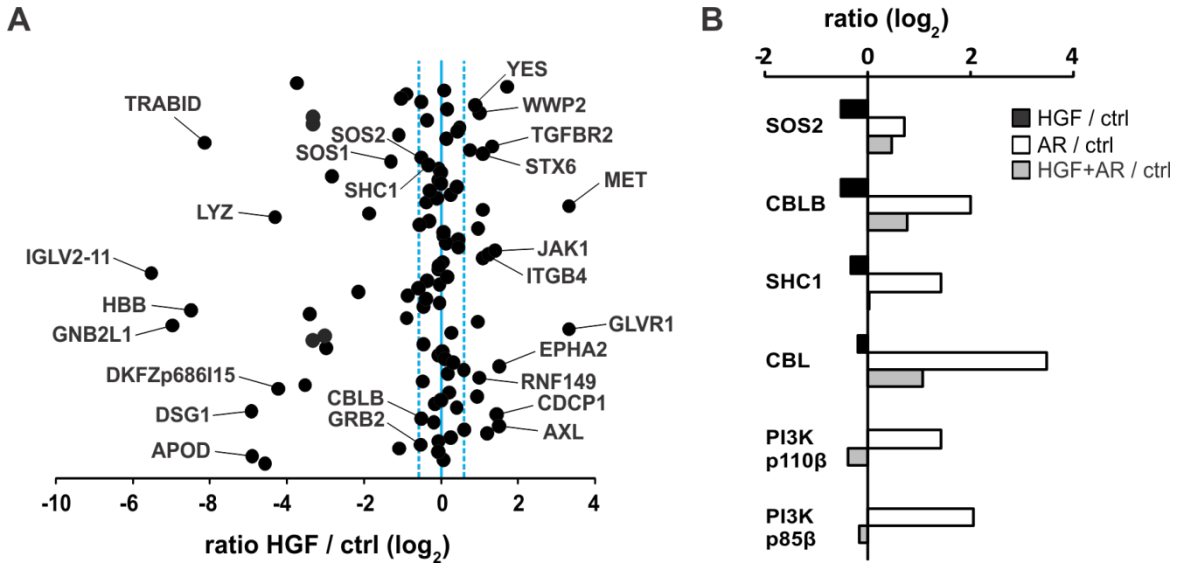

Figure 14. HGF-induced and reduced EGFR interactors. (**A**) Overview of HGF-induced and reduced EGFR interactors of pool A. Average ratios of two biological replicates were analyzed and the log2 ratio of HGF stimulated cells *versus* non-stimulated cells are shown. HGF-induced (ratio (log2) ≥ 0.58) and reduced (ratio (log2) ≤ -0.58) EGFR binders are indicated by dashed lines, unaltered (ratio (log2) ~ 0) EGFR binders are indicated by a solid line. Several EGFR interactors are reduced upon HGF treatment, indicating not only a blocked but also a negative regulated EGFR signaling. (**B**) Selected targets of AR-induced (ratio (log2) ≥ 0.58) HGF reduced (ratio (log2) ≤ -0.58) EGFR interactors. Note that HGF treatment is already enough for down regulated binding of relevant downstream signaling molecules to EGFR.

To validate the MS data, we performed EGFR co-IP followed by Western blot analysis. SCC9 cells were treated for 24 hours with HGF, lysed and subjected to EGFR co-IP. Immunoblots of the trapped proteins could prove Axl, CDCP1, EphA2, integrin beta-4 and JAK1 as specifically HGF-induced EGFR interaction partners (Fig. 15A, left part). In addition, increased levels of Axl, CDCP1, EphA2 and integrin beta-4 were found in total protein lysates subjected to Western blot analysis (Fig. 15A, right part)—suggesting HGF-induced stabilization or upregulation. To check whether the same changes in protein levels occur in the cell lines which we tested for loss of EGFR TK activity in figure 10B (plus the colon cell line HT29), cells were treated with or without HGF for 24 hours and subjected to Western blot analysis. Changes in protein expression between control treatment and HGF treatment were then densitometrically measured (ImageJ software) and represented as a heat map (Fig. 15B). An upregulation of at least two interaction partners was found in seven out of ten cell lines.

4.1.2.7 HGF leads to enhanced survival upon gefitinib treatment

Knowing that HGF blocks EGFR TK activity, it was examined if gefitinib, a selective inhibitor of the EGFR tyrosine kinase domain, can still function and induce apoptosis. SCC9 cells were subjected to different concentrations of gefitinib in the presence or absence of HGF and cell growth was measured after 72 hours. Growth inhibition was much stronger in untreated cells than in HGF-treated cells (Fig. 16A), indicating that HGF-treated cancer cells became more independent of EGFR-induced cell proliferation.

Table 17. HGF-induced EGFR binding partners.

protein ID	gene name	ratio after HGF treatment [a)]	ratio after HGF treatment in the presence of AR [b)]
proteins enriched independent of AR stimulation			
IPI00290039	CDCP1	2.7	1.8
IPI00398272	COL17A1	2.8	2.4
IPI00021267	EPHA2	2.9	2.0
IPI00022624	GPCR5A	1.9	1.9
IPI00061780	ITCH	2.1	1.5
IPI00027422	ITGB4	2.4	1.7
IPI00175092	RNF149	2.0	1.5
IPI00299086	SDCBP	2.1	1.5
IPI00023035	SLC20A1	>10 [c)]	2.0
IPI00164934	TGFBR2	2.5	1.7
IPI00022462	TFRC	1.7	1.3
IPI00013010	WWP2	2.0	1.3
proteins enriched solely by HGF treatment			
IPI00296992	AXL	2.3	
IPI00000643	BAG2	1.5	
IPI00784013	JAK1	2.6	
IPI00294528	MET	>10 [c)]	
IPI00107831	PTPRF	1.9	
IPI00013930	STX6	2.1	
IPI00004413	TNFRSF21	1.5	
IPI00170752	TNS4	1.9	

a) represents the ratio of Arg10/Lys8 *versus* Arg0/Lys0 labeled cells of pool A; b) represents the ratio of Arg10/Lys8 *versus* Arg6/Lys4 labeled cells of pool B. c) peptide ratios with un-detecable signals in the setting without HGF were indicated as >10.

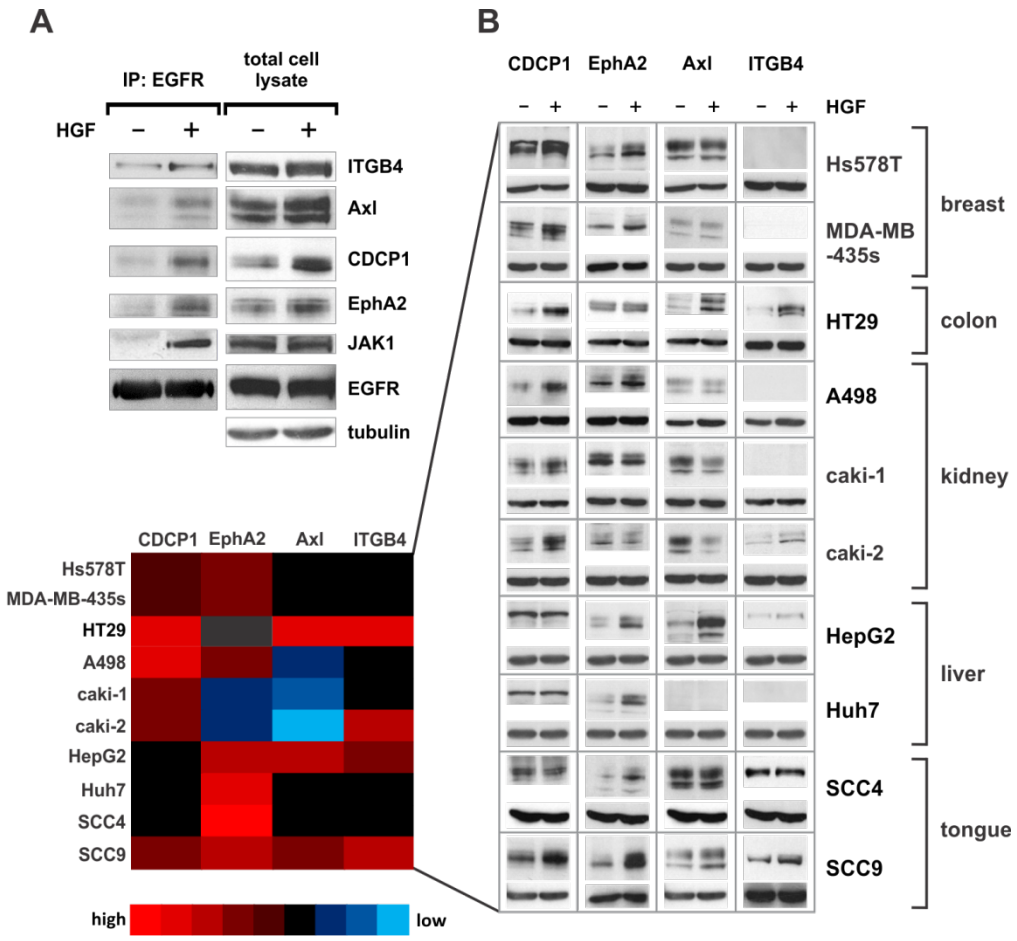

Figure 15. Validation of HGF-induced EGFR binding partners identified by mass spectrometry and EGFR binding partner upregulation in different cell lines. (**A**) Western blot analysis of EGFR co-immunoprecipitation (IP) and total cell lysate of SCC9 cells treated with HGF for 24 h. (**B**) Total cell lysate of different cell lines treated with HGF for 24 h. Immunoblots are shown for CDCP1, EphA2, Axl, ITGB4 and tubulin. The Western blots were densitometrically analyzed and illustrated as a heat map.

4.1.2.8 HGF-induced EGFR interactions are resistant to gefitinib treatment

As shown in table 17 HGF-induced EGFR interactions are completely independent of EGFR ligand-induced phosphorylation of the EGFR. Based on this finding it was of interest to determine whether an inhibition of phosphorylation by gefitinib can block the interreceptor crosstalk. This is of great importance, because it might implicate a mechanism of primary resistance to EGFR inhibitors. We therefore subjected long term HGF-treated SCC9 cells for the last two hours of the treatment to gefitinib and then stimulated them with amphiregulin. In gefitinib-treated cells the level of pEGFR Y1173 was

completely blocked compared to cells solely treated with HGF or untreated cells—confirming the efficiency of gefitinib in blocking EGFR phosphorylation in our model (Fig. 16B, upper part). However, binding capacity of the EGFR interaction partners integrin beta-4, Axl, CDCP1 and EphA2 was unchanged or even higher in the presence of gefitinib (Fig. 16B, lower part).

4.1.2.9 Met TK-inhibition restores gefitinib sensitivity

Having found that HGF-induced Met activation very efficiently conveys resistance to EGFR TKI treatment in cancer cells, we wondered if pretreatment with a Met TKI restores gefitinib sensitivity. Therefore we incubated SCC9 cells with the Met TKI AMG-458 derivate 1 before the cells were treated with gefitinib and HGF. Pretreatment with AMG-458 completely blocked HGF-induced cell scattering (Fig. 16C) and fully recovered the antiproliferative effects of gefitinib (Fig. 16D).

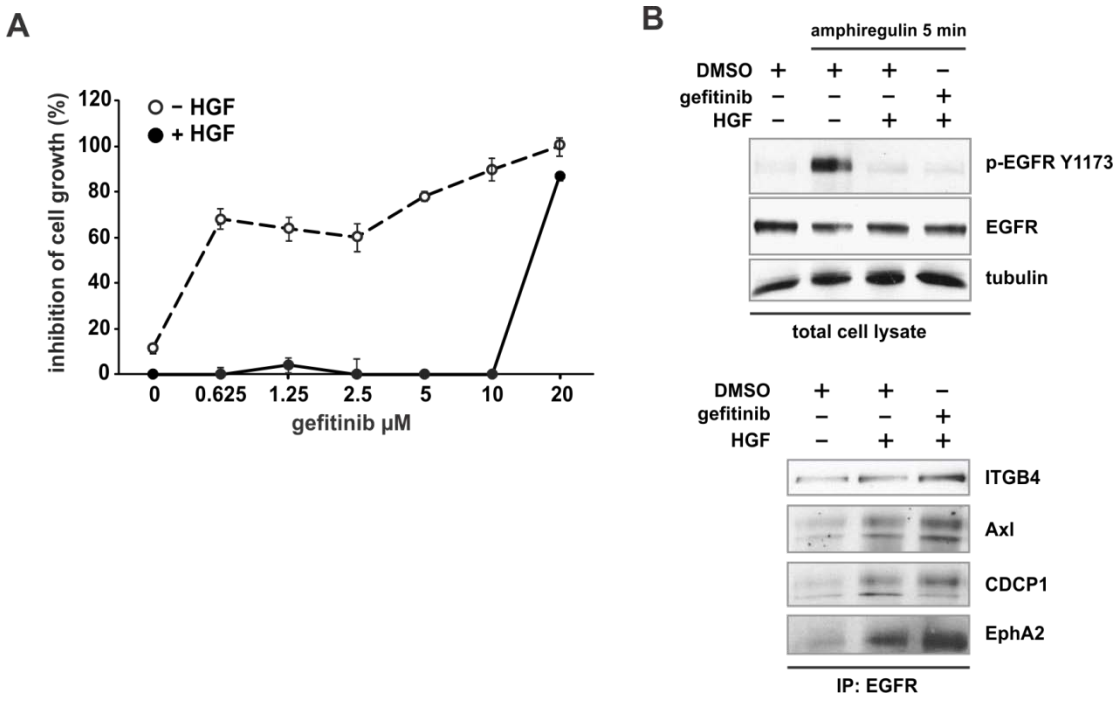

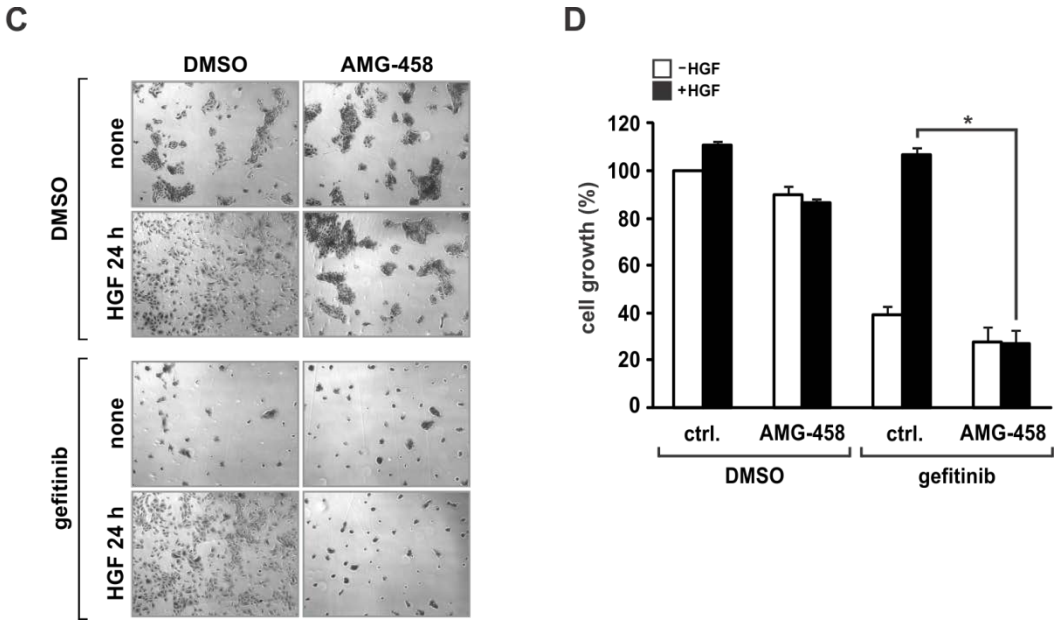

Figure 16. Effect of gefitinib on binding capacity of EGFR interactors and rescue of gefitinib sensitivity upon Met TKI treatment. (**A**) Proliferation assay with SCC9 cells. Cells were treated for 72 h with different concentrations of gefitinib in the absence or presence of HGF. Mean ± SD is shown. (**B**) Western blot analysis of EGFR co-immunoprecipitation (IP) and total cell lysate of SCC9 cells pretreated with HGF for 24 h and with gefitinib or DMSO for 2 h before stimulation with 50 ng/ml AR. (**C**) Pictures of SCC9 cells treated for 1 h with 4 µM AMG-458 derivate 1 before treatment for 72 h with 2 µM gefitinib in the absence or presence of HGF. Pictures were taken with a Zeiss Axio Observer.A1 microscope. (**D**) Proliferation assay with SCC9 cells. Cells were incubated for 1 h with 4 µM AMG-458 derivate 1 before treatment for 72 h with 2 µM gefitinib in the absence or presence of HGF. Error bars indicate SEM (n=3). Asterisk indicates significant inhibition ($P < 0.001$, unpaired Student's *t*-test).

4.1.2.10 HGF-induced EGFR TK blockage is a characteristic of cancer cells

As shown above, the EGF receptor of different epithelial cancer cells becomes TK-inactive upon HGF treatment. To investigate whether normal, untransformed epithelial cells show the same response to HGF/Met activation, we incubated the two untransformed mammary cell lines Ac745 and MCF10A with HGF and stimulated them with AR. None of the untransformed cell lines showed EGFR TK blockage upon HGF treatment (Fig. 17A).

4.1.2.11 Similar to EGFR, also HER2 and HER3 activation is blocked upon HGF treatment

In order to test whether HGF can also block other HER family members, we analyzed activation of HER2 and HER3 after HGF treatment. We incubated SCC9 cells with HGF for 24 h before they were stimulated with either AR or heregulin beta-1 (HRGβ1). AR activates HER2/EGFR heterodimers, whereas HRGβ1 activates HER2/HER3 heterodimers. Surprisingly HGF can also block HER2 and HER3 activation (Fig. 17B).

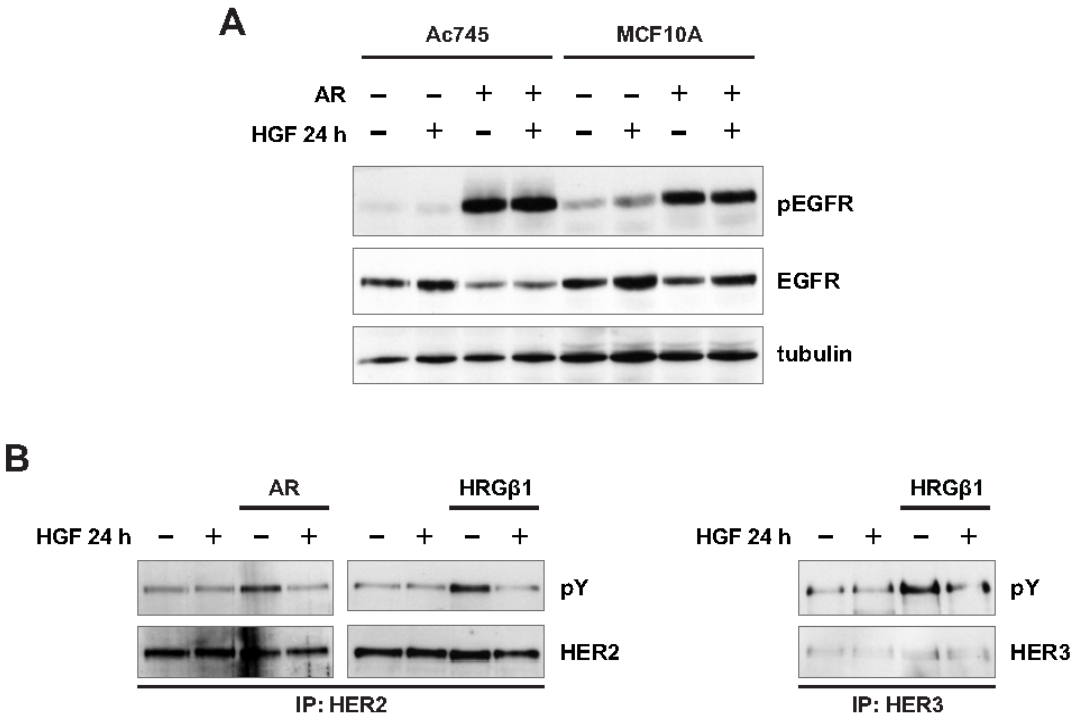

Figure 17. HGF-induced EGFR TK blockage is a characteristic of cancer cells and besides EGFR, also HER2 and HER3 activity is blocked. (**A**) Western blot analysis of the untransformed cell lines Ac745 and MCF10A pretreated with HGF for 24 h before stimulation with either 50 ng/ml AR. Immunoblots for pEGFR, EGFR and tubulin are shown. (**B**) Western blot analysis of HER2 and HER3 immunoprecipitation (IP) of SCC9 cells pretreated with HGF for 24 h before stimulation with 50 ng/ml AR or 10 ng/ml heregulin beta-1 (HRGβ1). Immunoblots for phospho-tyrosine (=pY), HER2 and HER3 are shown.

4.2 Interaction pathways between breast cancer cells and macrophages in human and mouse

4.2.1 Interaction pathways between breast cancer cells and human macrophages

4.2.1.1 Characterization of human macrophages

Human blood-derived monocytes were differentiated into macrophages by culturing them in the presence of normal human serum. During this maturation time cell size increased around four-fold (Fig. 18A). On day five after isolation, macrophages were characterized by FACS analysis. Therefore cells were stained with the cell surface marker CD14, which is expressed on monocytes, macrophages and activated granulocytes and with CD64, which is expressed on monocytes and macrophages (Fig. 18B). The isolated monocytes expressed high levels of CD14 as well as CD64 on their cell surface.

4.2.1.2 HB-EGF and OSM release in tumor-educated macrophages

Tumor-associated macrophages are known to promote tumor progression through several mechanisms. Two examples of tumor-promoting pathways are the EGFR pathway and the STAT3 pathway. To examine their role in tumor stroma crosstalk, primary human macrophages were educated to the conditioned medium (CM) of the MDA-MB-231 breast cancer cell line. And in addition, in the case that cell-cell contact is required, a coculture of MDA-MB-231 cells and primary human macrophages was setup. To assess a possible release of EGFR ligands, SCC9 cells were used as reporter cell line and to assess a release of STAT3 activators, MDA-MB-231 cells were used. Therefore SCC9 cells and MDA-MB-231 cells were stimulated with the supernatants of tumor-educated macrophages for three minutes and for ten minutes, respectively. Macrophages treated with the CM of MDA-MB-231 cells released EGFR ligands and STAT3 activators within 24 hours, whereas untreated macrophages and macrophages which were cocultured with MDA-MB-231 cells showed neither EGFR ligand nor STAT3 activator accumulation in the supernatant (Fig. 19A).

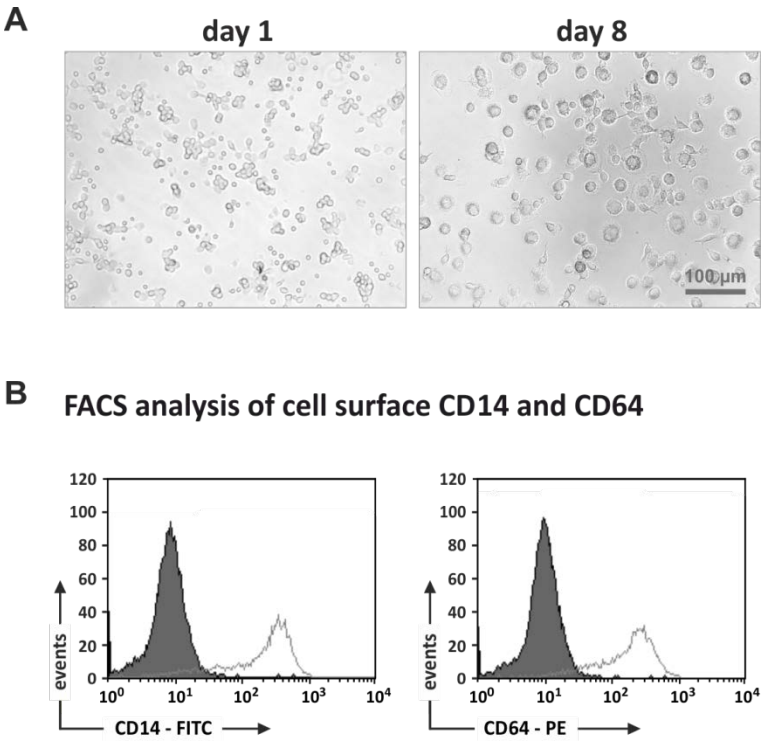

Figure 18. Characterization of primary human macrophages. (**A**) Pictures of human monocytes and macrophages. Blood-derived monocytes mature within 10 days to mature macrophages. Brightfield pictures were taken with a Zeiss Axio Observer.A1 microscope (20x magnification). (**B**) Flow cytometric analysis of CD14 and CD64 antigen expression on primary human macrophages.

To further investigate, whether this MDA-MB-231 CM-induced EGFR ligand and STAT3 activator release represents a general mechanism of cancer cells, different CM of cancer cells and of nontransformed cell lines were analyzed. The CM were generated from the following cell lines: four breast cancer cell lines MDA-MB-231, T47D, MCF7, MDA-MB-468; two nontransformed breast cell lines HMEC and MCF10A; and finally the squamous cell carcinoma cell line SCC9. EGFR phosphorylation and STAT3 phosphorylation was achieved with CM of MDA-MB-231, T47D, MCF7 and SCC9 cells. None of the nontransformed cell lines was capable of EGFR or STAT3 activation. Notably activating CM always induced both signaling pathways (Fig. 19B).

Having found that various cancer cell CM are capable of inducing the release of EGFR and of STAT3 activating ligands in macrophages, next the ligands accountable for the receptor activations were identified. Therefore the CM were pre-incubated with blocking antibodies against HB-EGF and oncostatin M (OSM) before they were used to stimulate SCC9 cells and MDA-MB-231 cells, respectively. Blocking HB-EGF completely inhibited activation of EGFR (Fig. 19C) and blocking OSM completely inhibited activation of STAT3 (Fig. 19D).

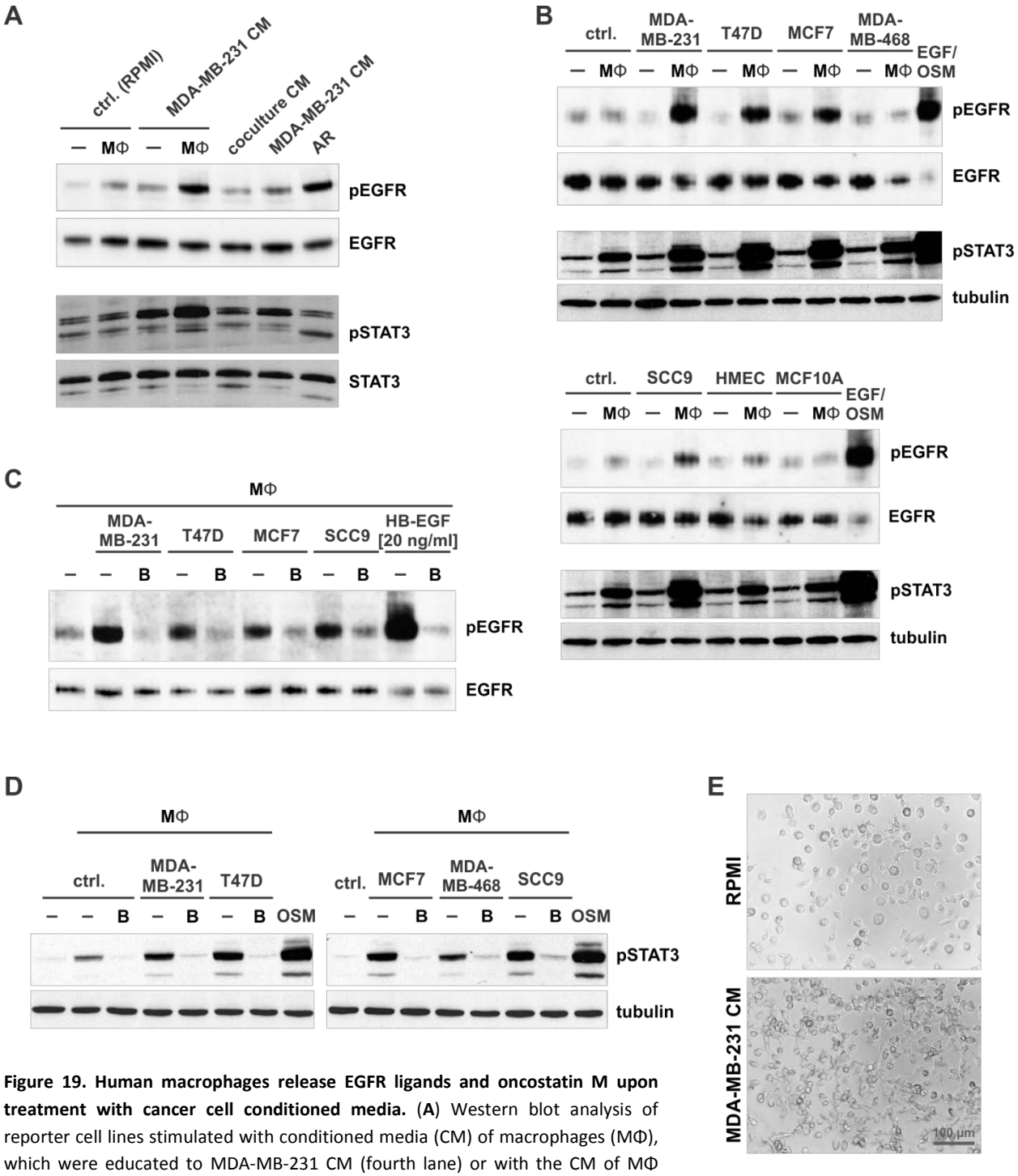

Figure 19. Human macrophages release EGFR ligands and oncostatin M upon treatment with cancer cell conditioned media. (**A**) Western blot analysis of reporter cell lines stimulated with conditioned media (CM) of macrophages (MΦ), which were educated to MDA-MB-231 CM (fourth lane) or with the CM of MΦ cocultured with MDA-MB-231 cells (fifth lane). Amphiregulin (AR) stimulation served as positive control for the pEGFR immunoblot. (**B**) Western blot analysis of reporter cell lines stimulated with CM of MΦ educated to cancer cell CM of different breast (MDA-MB-231, T47D, MCF7, MDA-MB-468) cell lines and the squamous cell carcinoma (SCC9) cell line as well as with CM of two nontransformed cell lines (HMEC, MCF10A). EGF and OSM stimulation served as positive control for the pEGFR and the pSTAT3 immunoblot, respectively. (**C**) Western blot analysis of reporter cells stimulated with CM of differentially educated MΦ in the presence of a blocking (B) anti-HB-EGF antibody and (**D**) in the

presence of a blocking (B) anti-OSM antibody. (**E**) Pictures of human macrophages treated for 5 days with MDA-MB-231 CM or with RMPI 5% NHS were taken with a Zeiss Axio Observer.A1 microscope at a 20x magnification.

4.2.1.3 Morphology change of human macrophages after treatment with cancer cell CM

Human macrophages that had been cultured in the presence of MDA-MB-231 CM for 5 days changed their morphology. In the presence of CM the macrophages become more stretched and developed spiny membrane protrusions compared to those cultured in the absence of CM (Fig. 19E).

4.2.2 Generating an in vitro mouse model

In the following study it was investigated if a similar EGFR and STAT3 activating mechanism occurs in a mouse breast cancer model. For this study, female 8-9 week old C57BL mice were used.

4.2.2.1 Screen for mouse reporter cell lines

In a first step several mouse cell lines were screened for their capability as reporter system for EGFR and STAT3 activation. The cell lines were as follows: four breast cancer cell lines Mm2mt, Mm5mt, L8A and RIIImt; one polyomavirus middle T antigen transgenic mouse breast cell line 1209-Pmt-T, two nontransformed mammary epithelial cell lines EpH4 and NMUMG and finally wild-type primary mouse embryonic fibroblasts (MEFs). The cell lines with the weakest pEGFR and pSTAT3 background but with a strong pEGFR and pSTAT3 signal after stimulation with EGF and OSM, respectively, were chosen for further experiments. The best signal to background ratio for EGFR activation was observed in MEFs and for STAT3 activation in EpH4 cells (Fig. 20A). To further assess the optimal time point for STAT3 and EGFR activation, MEFs and EpH4 cells were stimulated for 3, 5, 10 and 20 minutes with EGF and OSM, respectively. The optimal EGFR activation in MEFs occurred after 3 minutes and the optimal STAT3 activation occurred after 10 minutes (Fig. 20B). These two stimulation times where further used. To investigate the capability of low EGF and OSM dose responses, MEFs and EpH4 cells were stimulated

with a serial dilution of EGF and OSM. The lowest ligand dose for visible receptor activation was for EGF around 1 ng/ml and for OSM around 10 pg/ml (Fig. 20C). MEFs and EpH4 cells were used as reporter cell lines for EGFR and STAT3 signaling, respectively.

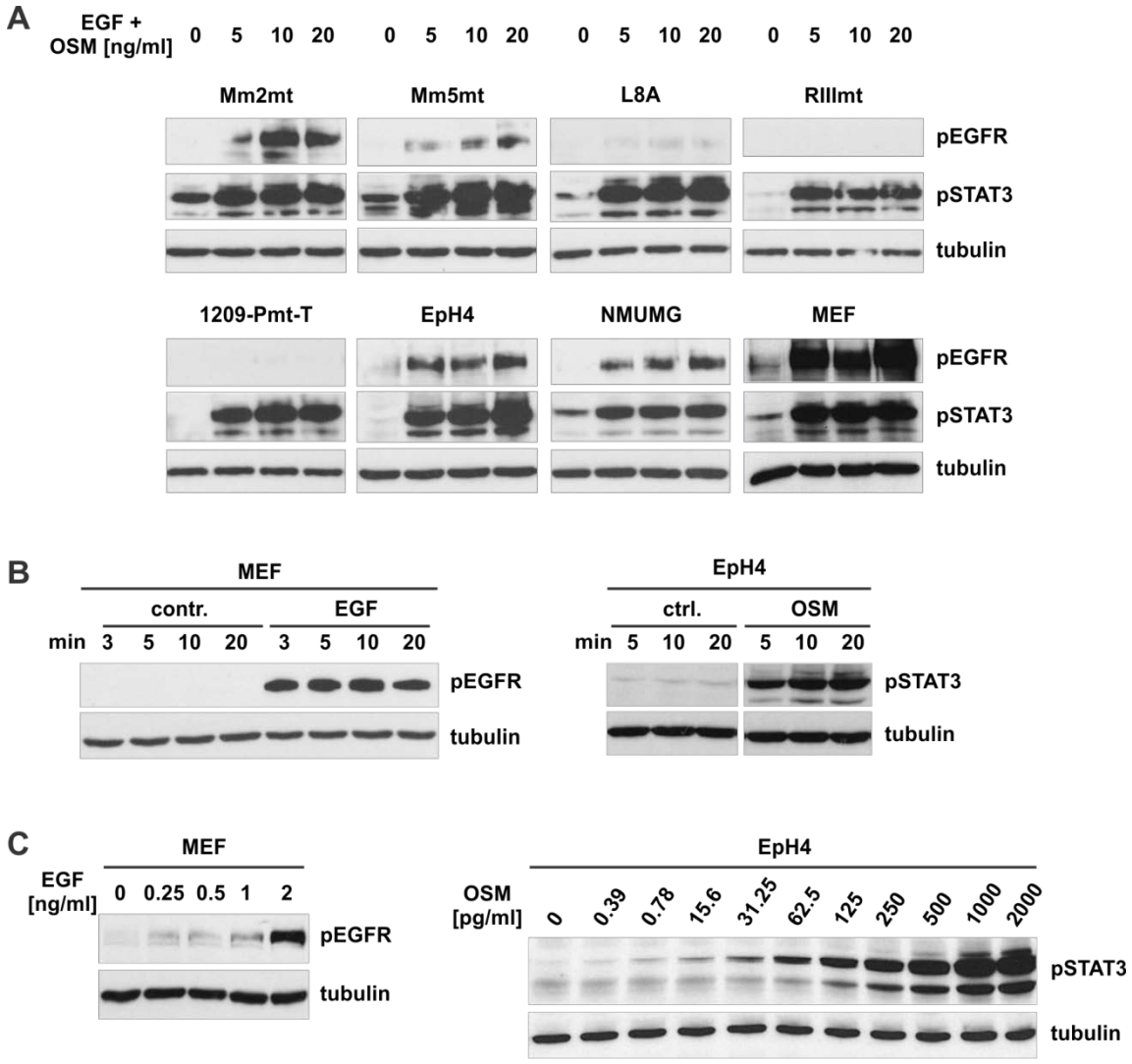

Figure 20. Screen for mouse reporter cell lines. (**A**) Western blot analysis of mouse breast cell lines, stimulated with different concentrations of EGF and OSM. (**B**) Western blot analysis of mouse embryonic fibroblasts (MEFs) and EpH4 cells stimulated with EGF or OSM for the indicated time points or (**C**) with different concentrations of EGF and OSM.

4.2.2.2 Characterization of mouse peritoneal macrophages

Isolated peritoneal macrophages were characterized by FACS analysis. Therefore cells were stained immediately after isolation with the cell surface marker F4/80, which is restricted to macrophages and with the cell surface marker CD14, which is expressed on monocytes, macrophages and activated granulocytes (Fig. 21A). Gate 1 contains CD14+, F4/80+ and a small portion of F4/80- cells; gate 2 comprises non-monocytic cells (F480-, CD14-); gate 3 contains F4/80+ and CD14+ cells and finally gate 4 contains CD14+ and F4/80+ as well as some F4/80- cells. Although a small portion of gate 4 was F4/80 negative, it was concluded that cells of gate 1 (= 88.5% of the isolated cells) were mature macrophages.

4.2.2.3 Morphology change of mouse macrophages after treatment with cancer cell CM

Peritoneal macrophages that had been cultured in the presence of L8A CM for 18 hours exhibited dramatic morphological changes. These cells were more stretched and developed spiny membrane protrusions compared to those cultured in the absence of CM (Fig. 21B). As described above, a similar morphology change was observed with human monocytes.

4.2.2.4 OSM release in tumor-educated mouse macrophages

Next, the release of EGFR ligands and STAT3 activators by peritoneal macrophages (MΦ) upon breast cancer cell line CM treatment was assessed. Therefore peritoneal MΦ were educated to the CM of the following cell lines: five mouse breast cancer cell lines Mmt060562, L8A, Mm2mt, Mm5mt, RIIImt; one nontransformed mammary epithelial cell line EpH4; and finally the human breast cancer cell line MDA-MB-231 was used as positive control, because of its strong effects in the human system. The macrophage conditioned medium (MΦ-CM) was then used to stimulate the reporter cell line EpH4 and MEFs to analyze their capability to activate EGFR or STAT3.

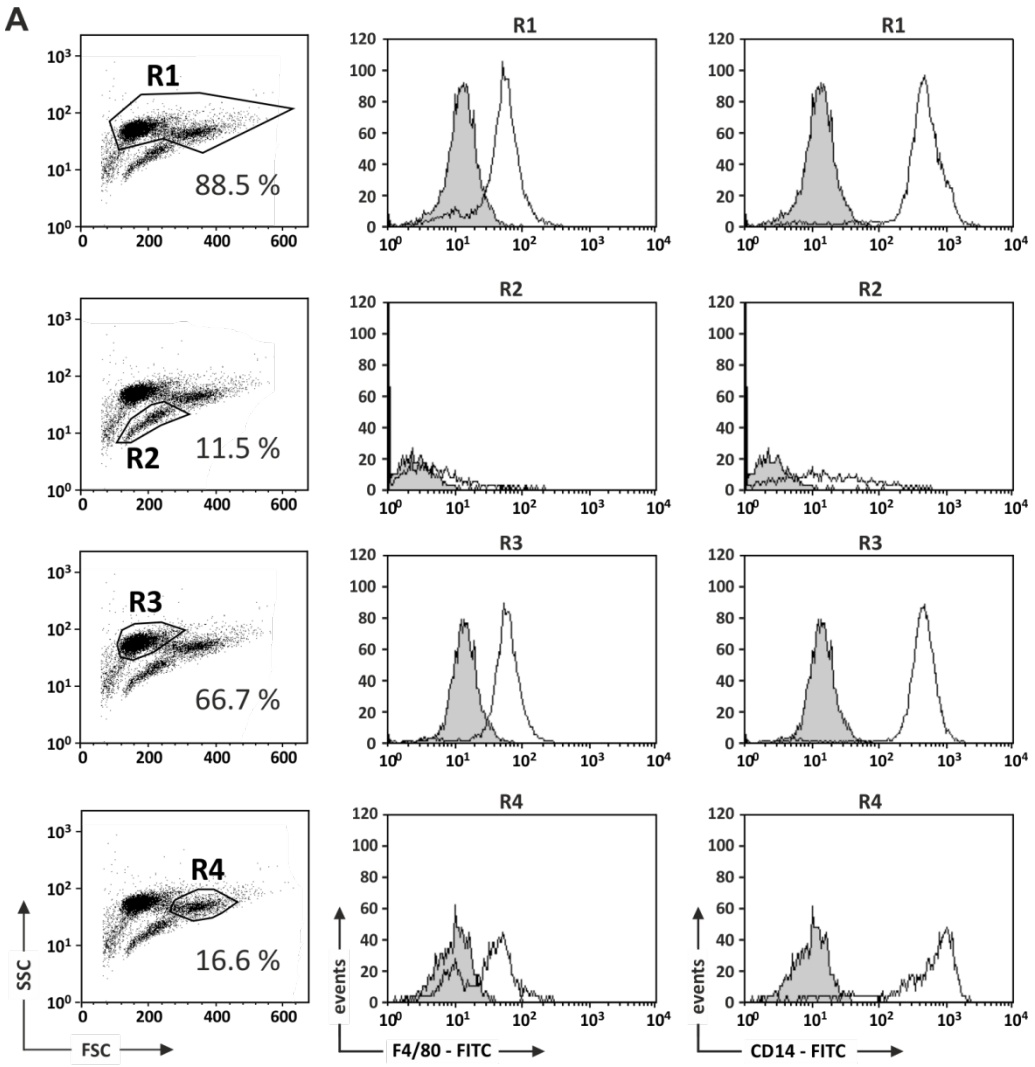

Figure 21. Characterization of mouse peritoneal macrophages. (**A**) Flow cytometric analysis of F4/80 and CD14 antigen expression on primary mouse peritoneal MΦ. (**B**) Pictures of mouse peritoneal MΦ treated for 18 h with CM of the mouse breast cancer cell line L8A or with RMPI 5% FCS. Brightfield pictures were taken with a Zeiss Axio Observer.A1 microscope (20x magnification).

The mouse cell lines Mmt060562, Mm5mt, RIIImt, L8A, as well as the human cell line MDA-MB-231 were capable to induce a release of STAT3 activators in mouse macrophages. This induction was much lower

in the case of EpH4 and Mm2mt cells (Fig. 22A). However, none of the breast cancer cell line conditioned media was capable of EGFR activation in EpH4 cells (data not shown).

To prove whether the released STAT3 activator was OSM, like in the human system, a blocking OSM antibody was used (Fig. 22B). Indeed, a reduction of STAT3 phosphorylation could be observed, but the signal was not completely abolished. This remaining signal was most likely caused by other STAT3 activating ligands. To quantify the OSM release, a sandwich ELISA was established and the MΦ-CM were analyzed (Fig. 22C). The released OSM was up to three-fold increased as compared to untreated MΦ (604 and 211 pg/ml respectively). Cancer cell CM-treated MΦ released OSM, and this released OSM was capable of STAT3 activation.

4.2.2.5 OSM transcript and EGFR ligand transcript induction in tumor-educated macrophages

To further characterize the underlying mechanism of the OSM release in macrophages, a possible transcriptional upregulation of OSM was analyzed. In addition transcript induction of the EGFR ligands amphiregulin, EGF, HB-EGF and TGFα was examined. OSM as well as the EGFR ligands amphiregulin and HB-EGF were found to be transcriptionally upregulated in MΦ treated with CM of L8A cells (**Fig. 23A**). To assess if a same effect could be observed with other mammary cancer cell lines, peritoneal MΦ were

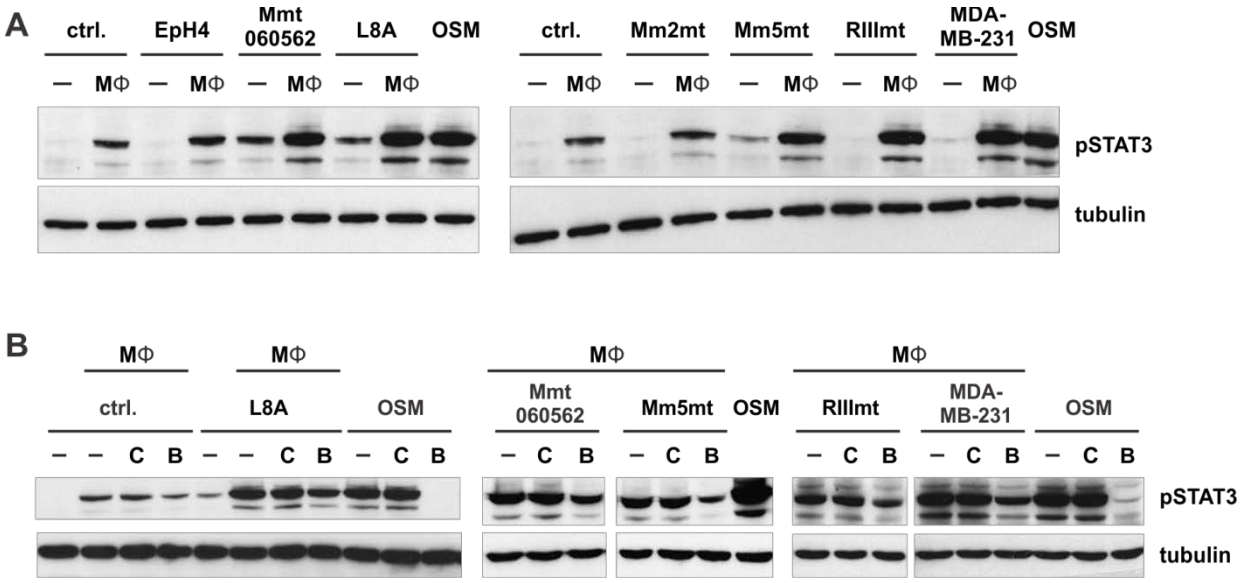

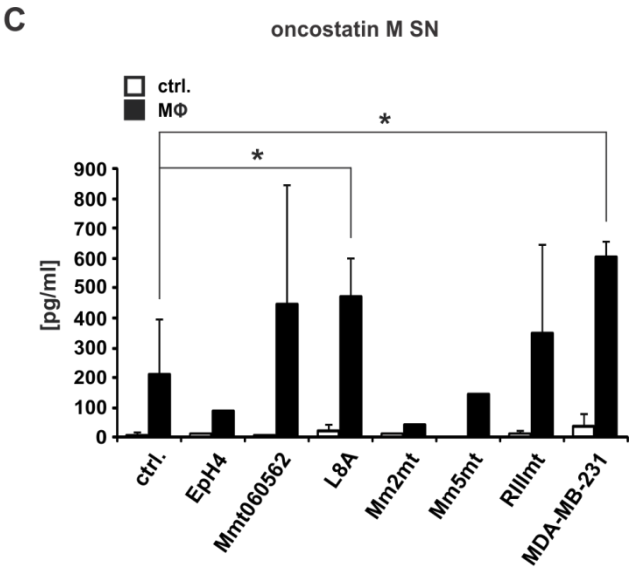

Figure 22. OSM induction upon treatment with breast cancer cell conditioned media. (**A**) Western blot analysis of reporter cells stimulated with CM of peritoneal MΦ which were educated to cancer cell CM of different mouse (Mmt060562, L8A, Mm2mt, Mm5mt, RIIImt,) and human (MDA-MB-231) breast cell lines as well as to CM of the nontransformed breast cell line EpH4. OSM stimulation served as positive control for the pSTAT3 immunoblot. (**B**) Western blot analysis of reporter cells stimulated with CM of differentially educated peritoneal MΦ in the presence of a blocking (B) anti-OSM antibody or of control (C) IgG. (**C**) Quantification of OSM release by peritoneal MΦ. Different cancer cell and nontransformed cell CM were incubated with (black bars) or without (white bars) macrophages for 24 hours. OMS release in the SN was assayed using OSM sandwich ELISA. Error bars indicate SEM of experimental triplicates. Asterisks indicate significant change ($P < 0.05$, unpaired Student's *t*-test).

treated with CM of Mmt060562, Mm2mt, Mm5mt, RIIImt and MDA-MB-231 cells. The nontransformed cell line EpH4 served as negative control. Mmt060562 and RIIImt cells strongly induced transcript upregulation of amphiregulin and OSM (Fig. 23B), the latter confirming the Western blot and ELISA results of figure 22A and C, where these two cell lines were also highly effective in triggering OSM release by MΦ. These data show that cancer cells are capable to prompt MΦ to induce EGFR ligand and OSM transcript induction.

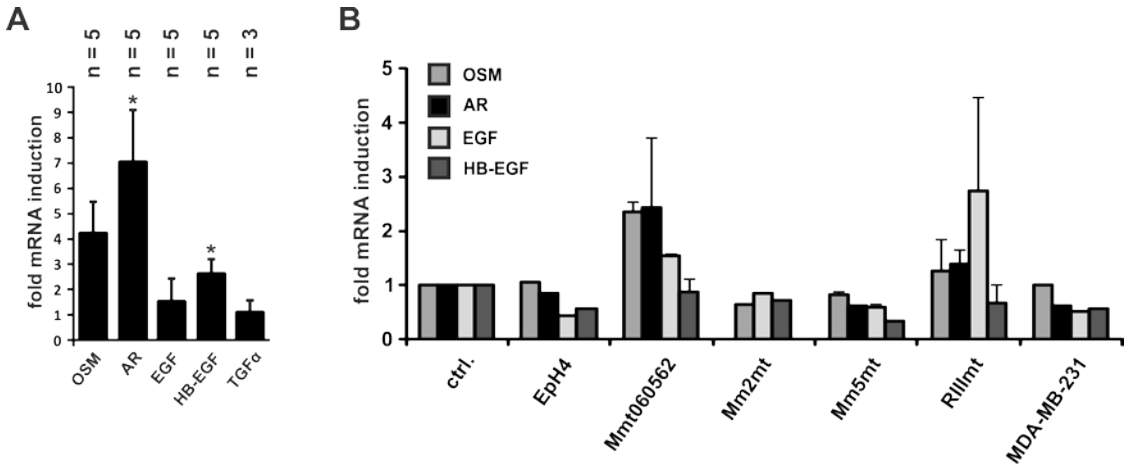

Figure 23. OSM and EGFR ligand transcript induction upon treatment with breast cancer CM. (**A**) Quantification of OSM, AR, TGFα and HB-EGF mRNA induction in peritoneal MΦ treated with L8A CM for 24 hours. Data represent the increase compared to the untreated control and were normalized to β-actin. Error bars indicate SEM of 3–5 independent experiments. Asterisks indicate significant change (*P*< 0.05, unpaired Student's *t*-test). (**B**) OSM, AR, EGF and HB-EGF mRNA induction in peritoneal MΦ treated with different breast cancer CM for 24 hours. Data represent the increase compared to the untreated control and were normalized to β-actin. Values are shown as mean ± SD (n=2).

4.2.2.6 OSM release in bone marrow and spleen-derived monocytes

Having found that mature MΦ release OSM after treatment with breast cancer cell CM, next an OSM release by early monocytes was assessed. Therefore, spleen and bone marrow-derived monocytes were educated to breast cancer CM and assayed, as described above for STAT3 activators. L8A CM-treated early monocytes released OSM (Fig. 24A), and the released OSM amounts were capable of STAT3 activation (Fig. 24B).

Spleen monocytes that had been cultured in the presence of L8A CM for 1 day show no morphological differences compared to the untreated cells. However, after 5 days, L8A CM-treated monocytes underwent dramatic morphological changes. These cells become much more stretched compared to those cultured in the absence of CM (Fig. 24C).

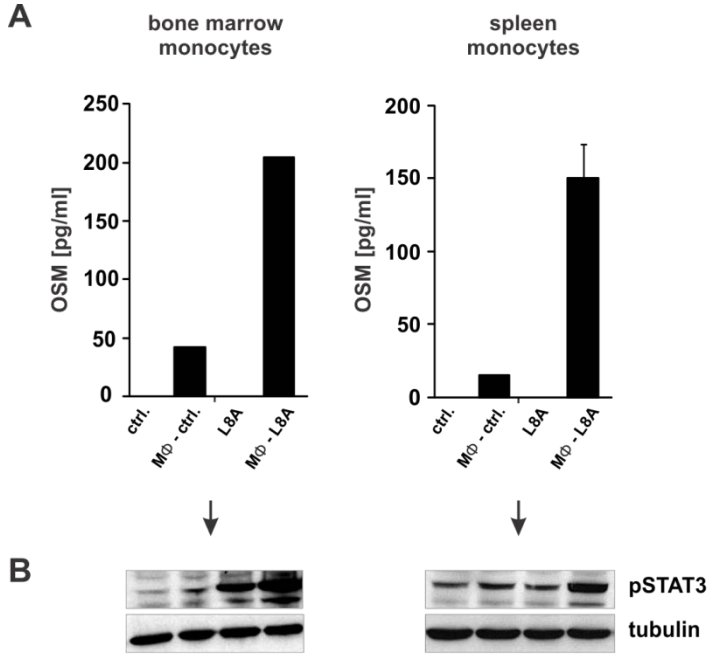

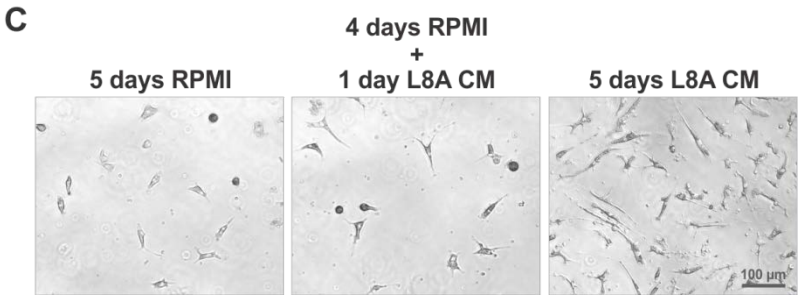

Figure 24. OSM and EGFR ligand induction by bone marrow and spleen-derived monocytes. (**A**) Quantification of OSM release by bone marrow and spleen-derived monocytes (MΦ). L8A CM was incubated with or without MΦ for 24 hours. OMS release in the SN was assayed using OSM sandwich ELISA. Values are shown as mean ± SD (n=2). (**B**) Western blot analysis of reporter cells stimulated with CM of bone marrow or spleen educated MΦ from figure A. (**C**) Pictures of spleen-derived MΦ educated for the indicated time points to L8A CM or to RMPI 5% FCS. Brightfield pictures were taken with a Zeiss Axio Observer.A1 microscope at a 20x magnification.

5 DISCUSSION

5.1 HGF-mediated EGFR paracrine crosstalk

5.1.1 HGF is a potent paracrine inducer of EGFR ligands

HGF is a frequently found ligand in the tumor stroma and is produced by tumor-associated macrophages (TAMs) and by stromal fibroblasts. Met activation upon HGF binding, was shown to trigger several protumorigenic pathways. However, the complex crosstalk between tumor cells and stromal cells is yet poorly understood. In the first part of this study we aimed to investigate HGF/Met-mediated EGFR crosstalk in human epithelial cancer cell lines.

Several studies have shown multiple mechanisms of transactivation between Met and EGFR. Scheving et al. (130) demonstrated that inhibition of EGFR TK blocks HGF-induced DNA synthesis in primary hepatocytes, indicating that the proliferative actions of HGF may be secondary via new synthesis or processing of EGFR ligands. Similarly, Spix et al. (131) blocked HGF-induced scattering of human corneal limbal epithelial cells with an EGFR TKI. And finally Reznik and coworkers (132) demonstrated that HGF stimulation of glioblastoma cells induces EGFR activation via new transcription of EGFR ligands. Furthermore this receptor transactivation can also occur the other way around. EGFR activation was found to result in constitutive activation of Met in several cancer cell lines. The mechanisms underlying this Met activation involves prostaglandins and the production of reactive oxygen species (124, 133).

The role of Met/EGFR receptor crosstalk in epithelial cancers remained largely elusive. We show here, that different epithelial cancer cell lines, derived from breast, kidney, liver and tongue, produce the EGFR ligands amphiregulin and/or TGFα upon HGF stimulation. These ligands are induced via transcriptional upregulation and are released from the cell membrane by metalloprotease dependent shedding. In addition, we demonstrate the ability of a monocytic cell line to induce EGFR ligand release in a HGF/Met-dependent manner. Furthermore, we identified MAPK signaling as the underlying pathway for new EGFR ligand DNA syntheses. We intended to specifically inhibit Erk1 and 2 by siRNA knockdown and could demonstrate that Erk2 but not Erk1 is responsible for ligand upregulation.

However Erk1 can partly compensate for the loss of Erk2. Interestingly, Erk2 was recently described to play a key role in cancer cell proliferation in an in vivo mouse model (134).

Although HGF induces EGFR phosphorylation via the transcription of EGFR ligands in human corneal limbal epithelial (131) and glioblastoma (132) cells, our present study, using epithelial cancer cell lines, could not show EGFR tyrosine kinase phosphorylation. Indeed, in our study, we were neither able to detect pEGFR signals, nor could we block HGF-induced cell migration using EGFR TKIs or blocking antibodies, in the way Spix et al. (131) demonstrated. However, the use of recombinant amphiregulin and TGFα per se, were strong inducers of EGFR phosphorylation, of downstream signal transduction (Erk1/2, Akt) and of migration in the epithelial cancer cell lines we used. This discrepancy between the presence of EGFR ligands in the cell culture medium and the unresponsive EGFR will be discussed in the second part of the discussion (5.1.2).

We speculate that the released EGFR ligands could be provided for distant tumor cells, which did not get in contact with HGF before. Another possibility is that these ligands induce recruitment and proliferation of stromal cells like endothelial cells and fibroblasts. The latter idea is supported by the fact that the EGFR of untransformed cells cannot be inactivated by HGF (Fig. 17A). Interestingly Amin et al. (65) compared tumor-associated endothelial cells and normal endothelial cells and found tumor-derived endothelial cells express EGFR, HER2 and HER4, whereas their normal counterparts express HER2, HER3 and HER4. As a consequence of the gain of EGFR and the loss of HER3, tumor vasculature responds to EGFR ligands. They suggest in their study that this receptor exchange promotes tumor angiogenesis (65).

In summary, we have shown in this study that HGF is a strong inducer of EGFR ligands in epithelial cancer cells and that the released ligands are potent activators of EGFR of new cells, but not of the HGF stimulated cells. Therefore it is likely, that the produced EGFR ligands are provided for other cells of the tumor stroma (Fig. 25).

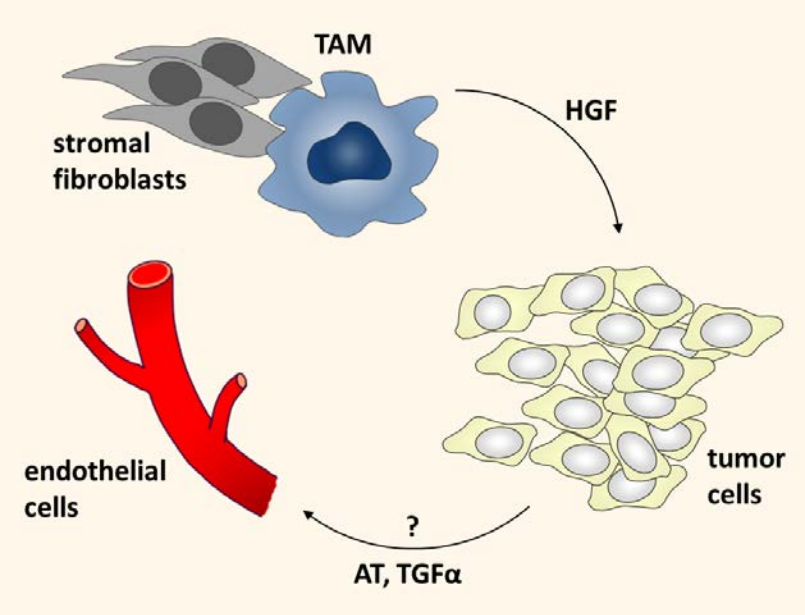

Figure 25. Paracrine interaction model between TAM, tumor cells and endothelial cells. TAMs and tumor-associated stromal fibroblasts release a variety of factors that support tumor growth and progression. HGF, one of these factors, prompts tumor cells to produce the EGFR ligands amphiregulin (AR) and transforming growth factor α (TGFα). Importantly, once the tumor cells are activated by HGF, their EGF receptor cannot be activated by EGFR ligands anymore. However, tumor-associated endothelial cells express high levels of EGFR and have been shown to respond to EGFR activation. Therefore, we propose, that the tumor vasculature represent a possible target for the produced EGFR ligands.

5.1.2 HGF-induced EGFR negative regulation

Activation of EGFR has been frequently reported to promote tumor progression. However, expression levels of EGFR in human cancers do not correlate with responsiveness to EGFR TKI treatment and the rate of complete tumor regression is very low. The expression and activation of Met has been implicated in resistance to EGFR-targeted therapies in breast cancer, colon cancer and NSCLC patients (70, 81, 83, 84). Engelman et al. (70) reported that MET amplification causes gefitinib resistance in lung cancer cell lines by circumventing the blocked EGFR activity via a HER3-dependent activation of the PI3K-Akt pathway. Additionally, in vitro studies in EGFR mutated NSCLC cell lines show that exposure to HGF induces EGFR TKI resistance and inhibition of Met/HGF restores gefitinib sensitivity. However, the differences in the mode of action between a normal EGFR and EGFR after HGF stimulation remain elusive so far.

Here we show that human epithelial cancer cell lines stimulated with HGF are no longer susceptible for EGFR ligand stimulation nor for EGFR TK-targeted drugs, like gefitinib. Importantly, untransformed "normal" epithelial cells do not respond to this HGF-induced EGFR TK blockage. This suggests that HGF-

mediated EGFR TK inhibition is characteristic for cancer cells. Similar to EGFR, also HER2 and HER3 activation is blocked upon HGF treatment.

To identify potential HGF-induced EGFR interaction partners we performed mass spectrometry in SCC9 cells. Interestingly, several specifically HGF-induced EGFR binding partners could be identified. In the presence of HGF the EGFR directly interacts with several cytoplasmic proteins, as well as with transmembrane proteins like CDCP1, EphA2 and Axl. CDCP1, a 135 kDa glycoprotein, is overexpressed in breast, gastric, kidney and lung cancers and was shown to be associated with high invasiveness (135-138). Consistent with its role in metastatic spread, silencing of CDCP1 reduced the migratory behavior and anchorage-independent growth in gastric cancer cell lines (139). Therefore, CDCP1 seems to be a potential therapeutic target although its signaling mechanism is still unknown. Besides their well described tumor-associated functions, the RTKs EphA2 and Axl were both recently shown to confer acquired resistance to anti-HER2 treatment in breast cancer cells (140, 141). A similar resistance mechanism probably contributes to our observed EGFR TKI resistance. In this study, we not only found higher expression-levels of EphA2 and Axl upon HGF treatment, but also a direct interaction with EGFR—indicating a TK-independent role of EGFR in stabilization of these receptors, thereby maybe empowering cancer cells with the ability to receive further tumor-promoting signals from the tumor microenvironment.

In addition to the well known prosurvival and proproliferative roles of EGFR, which are mediated via activation of the EGFR tyrosine kinase domain and further downstream PI3K, MAPK and STAT signaling cascades, the EGFR seems to function in another dimension of complexity: a kinase-independent stabilization of cancer-associated proteins.

Taken together, we demonstrate here that in the presence of HGF the EGFR TK becomes inactive, and that this inactive TK leads to primary resistance to EGFR-targeted drugs and at the same time induces interactions of the EGFR with various tumor relevant proteins (as described in figure 26). These novel functions of EGFR may endow tumor cells with an increased survival capacity even in the presence of targeted anti-cancer therapeutics, including tyrosine kinase inhibitors. Thus, pretreatment with HGF/Met inhibitors before EGFR-targeted therapy as well as targeting HGF/Met-induced EGFR interactors may both be necessary for elimination of epithelial cancers.

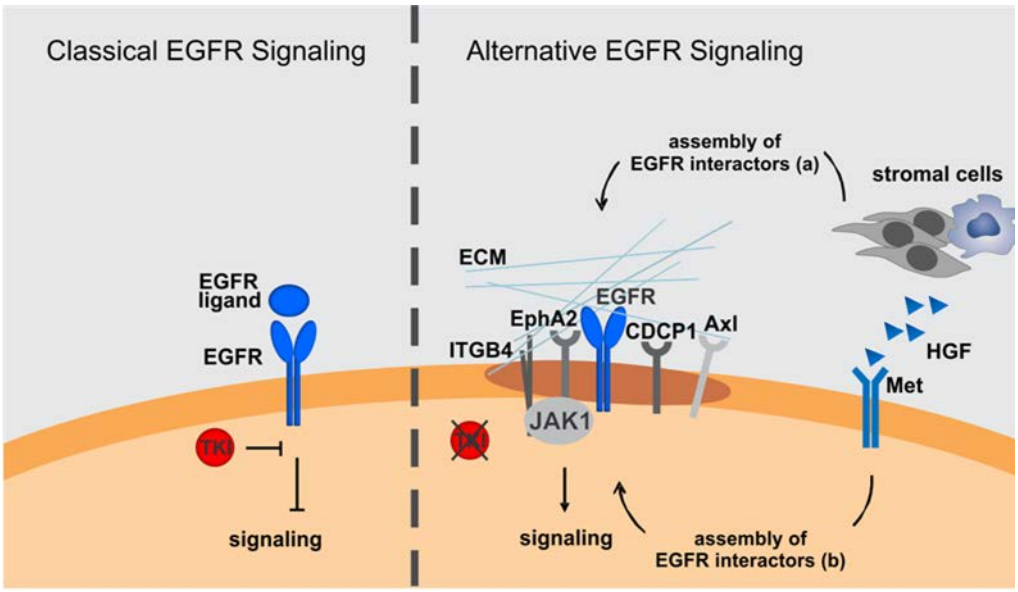

Figure 26. Proposed model for an alternative EGFR mechanism. Classical EGFR signaling which includes EGFR ligand binding, receptor autophosphorylation and activation of downstream signaling cascades can be blocked by EGFR TKIs (left side). However upon activation of Met by its ligand HGF, which is provided by stromal cells, EGFR signaling gets dramatically altered (right side): HGF confers EGFR TKI resistance and at the same time induces interreceptor crosstalk with integrin beta-4 (ITGB4), EphA2, CDCP1, Axl and JAK1. Binding of these interactors may provide alternative signaling mechanism for EGFR, thereby circumventing TKI resistance. This interactor assembly may be either mediated via extracellular crosslinking, involving the extracellular matrix (ECM) (a) or via intracellular signaling mechanisms (b).

5.2 Interaction pathways between breast cancer cells and macrophages in human and mouse

Tumor cells influence stromal cells in order to escape from host defense, to induce angiogenesis and to produce factors that promote growth, survival, and metastases (42). Tumor educated macrophages are known to facilitate tumor growth and spread of several different cancers, including breast cancer. Importantly, in mammary tumors the abundance of TAMs is associated with a poorer prognosis (35, 142). Considering the enormous protumorigenic potential of the two signaling pathways EGFR and STAT3, we aimed to investigate a possible link between TAMs and the activation of these two pathways in mammary tumors.

In mammary tumors the EGF receptor and its ligands have been described to be frequently expressed and are associated with higher proliferation and poorer prognosis (143, 144). Several EGFR-targeted drugs are currently in clinical trials for the treatment of advanced breast cancer (145-147). The EGFR ligand HB-EGF was shown to increase the growth rate of human bladder carcinoma cells in vivo and enhance colony-formation, as well as VEGF expression in vitro (148). Moreover, it was shown that HB-EGF induces the expression of several metalloproteases, thus leading to enhanced cell motility (148). A siRNA knock down of HB-EGF in a nude mouse model blocked tumor formation of ovarian cancer cell lines (149).

In our in vitro breast cancer model, we were able to induce HB-EGF production in human primary macrophages upon treatment with breast cancer cell conditioned medium. Interestingly, Rigo et al. (64) demonstrated recently a possible GM-CSF/HB-EGF loop between human cancer cells and macrophages. Using a neutralizing HB-EGF antibody, they were able to abolish proliferation of cervical cancer cells and colorectal adenocarcinoma cells in vitro (64). It would be critical to elucidate the exact mechanism of HB-EGF induction and whether a similar loop, like the one proposed by Rigo et al. (64), exists in our human breast cancer model. Such experiments could be performed in future studies and might help to extend our understanding about macrophage/tumor cell crosstalk mechanism. The idea of synergistic interactions between macrophages and breast cancer cells is not new: in 2004, Wyckoff and colleagues (150) reported, using a polyoma middle T antigen-induced mammary tumor model in mice, that TAMs and tumor cells migrate via a CSF-1/EGF paracrine loop between the two cell types; in 2005 Goswami and coworkers (63) showed the same CSF-1/EGF paracrine loop between melanoma cancer cells and macrophages. In contrast to the murine system, where macrophage-derived EGF seems to mediate cancer cell motility, the macrophage released EGFR ligand in human cancers seems to be mainly HB-EGF.

We found in our macrophage/breast cancer model that breast cancer cell conditioned medium promotes the formation of elongated protrusions in macrophages. This change in the morphology is probably indicating enhanced cell motility and would fit to the theory of a paracrine loop, which increases motility of TAMs as well as tumor cells.

In addition to the production of an EGFR ligand, we were able to induce a STAT3 activator in tumor-educated macrophages. The STAT3 activating ligand was identified as OSM. OSM belongs to the IL-6 family and was reported to be produced by several immune cells, including macrophages (151), neutrophils (152) and activated T lymphocytes (153, 154), as well as from some tumor cells including

breast cancer epithelial cells (155). It has been shown that OSM plays a significant role in breast cancer metastasis. Besides the induction of cell migration and invasion, OSM triggers also the expression of the proangiogenic factor VEGF (152, 156). As we showed here with a blocking antibody experiment, out of the complex medium of tumor-educated macrophages, it was mainly OSM that induced STAT3 activation. Thus, OSM may represent an attractive target, and an alternative to STAT3 inhibitors, for cancer therapy.

Notably, both HB-EGF and OSM release were coinduced, suggesting a common mediator in the upstream pathway of.

To investigate the TAM-induced protumorigenic pathways EGFR and STAT3 in a mouse breast cancer model, we performed preliminary in vitro experiments. We were able to induce OSM release in primary mouse macrophages as well as in monocytes. Contrary to the human system, no EGFR ligands were released by murine tumor-educated macrophages. However, we were able to detect transcriptional upregulation of OSM as well as of the EGFR family ligands amphiregulin, EGF and HB-EGF. It will be an aim of future experiments to test whether the cell lysate of educated macrophages contains EGFR ligands. Their presence in the cell lysate would indicate that metalloproteases have to be produced or activated, since they are essential for the shedding of the membrane bound proforms of EGFR ligands. An optimization of the in vitro mouse model will be critical in order to perform future in vivo experiments.

In summary our data provide evidence that macrophages are strongly involved in the activation of two critical tumor-promoting pathways. And therefore tumor-associated macrophages themselves as well as their released ligands HB-EGF and OSM could be attractive targets for the treatment of mammary tumors.

6 SUMMARY

Macrophages of the tumor stroma support and enable proliferation, survival and migration of malignant cells by direct interactions, or by supplying soluble paracrine factors. In this thesis we studied the effect of the macrophage produced ligand HGF on tumor cell EGFR activity. Additionally we examined the capability of tumor cells to educate macrophages, so that they produce protumorigenic ligands.

The first part of this study demonstrates that the Met ligand HGF induces transcriptional upregulation and release of HER ligands in different epithelial cancer cells. In a squamous cell carcinoma (SCC) cell line we found that amphiregulin and TGFα are the predominantly produced EGFR ligands. Moreover, we show that the conditioned medium of a monocytic cell line induces amphiregulin and TGFα release in a HGF/Met dependent manner. Notably, although EGFR ligands are present in the cell culture medium, the EGFR does not get phosphorylated. In order to characterize the TK blocked EGFR, we subjected SCC cell lysate to EGFR co-immunoprecipitation followed by quantitative mass spectrometry, and identified several HGF-induced EGFR binders, including Axl, EphA4, CUB domain containing protein 1 (CDCP1) and integrin beta-4—each of them highly associated with cancer progression. Recent studies showed a correlation between Met activity and EGFR TKI resistance. In line with this observation, we demonstrate that in the presence of HGF, EGFR TK activity as well as the classical downstream signaling events are not only unavailable but also unnecessary for tumor growth.

In the second part of the thesis we demonstrate that tumor-educated human macrophages activate two crucial tumorigenic signaling pathways: STAT3 and EGFR. We identified OSM as the STAT3 activating factor and HB-EGF as the EGFR activating factor. In addition, we show in an in vitro mouse model the release of OSM in TAMs as well as transcriptional upregulation of OSM and of different HER family ligands.

7 ZUSAMMENFASSUNG

Makrophagen im Tumorstroma unterstützen und ermöglichen Proliferation, Überleben und Migration von malignen Zellen durch direkte Interaktionen oder durch das Zurverfügungstellen von löslichen parakrinen Faktoren. In dieser Arbeit untersuchten wir den Effekt von HGF, das von Makrophagen produziert werden kann, auf den EGFR der Tumorzellen. Zusätzlich erforschten wir das Potential von Tumorzellen Makrophagen auszubilden, sodass diese dann tumorfördernde Liganden produzieren.

Der erste Teil dieser Arbeit zeigt, dass der Met-Ligand HGF sowohl die Transkription als auch die Freisetzung von HER-Liganden in verschiedenen epithelialen Krebszellen induziert. Bei der untersuchten *squamous cell carcinoma* (SCC) Zelllinie handelt es sich bei den induzierten Liganden vor allem um Amphiregulin und TGFα. Auch das konditionierte Medium einer monozytären Zelllinie kann diese Freisetzung von Amphiregulin und TGFα in einer HGF/Met-abhängigen Weise bewirken. Obwohl sich EGFR-Liganden im Zellkulturmedium befinden, wird der EGFR nicht phosphoryliert. Um den TK-gehemmten EGFR zu charakterisieren, wurde der EGFR aus SCC-Zelllysat immunopräzipitiert und massenspektrometrisch untersucht. Dabei konnten verschiedene HGF-induzierte EGFR-Interaktoren identifiziert werden, wie unter anderem Axl, EphA4, *CUB domain containing protein 1* (CDCP1) und Integrin-beta 4. Jeder dieser Faktoren wird mit Krebsentwicklung in Zusammenhang gebracht. Neuere Studien zeigen eine Korrelation zwischen Met-Aktivität und EGFR-TKI-Resistenz. Damit übereinstimmend zeigt diese Arbeit, dass in Anwesenheit von HGF die EGFR-TK-Aktivität und die dadurch ausgelösten klassischen *downstream* Signalwege nicht nur unverfügbar werden, sondern auch gar nicht mehr für das Tumorwachstum erforderlich sind.

Im zweiten Teil dieser Arbeit konnte gezeigt werden, dass von Tumorzellen ausgebildete Makrophagen die zwei tumorfördernden Signalwege STAT3 und EGFR aktivieren. Die dafür verantwortlichen Liganden wurden mit OSM für die STAT3-Aktivierung beziehungsweise mit HB-EGF für die EGFR-Aktivierung identifiziert. In einem in vitro Maus-Model wurde in Tumor-assoziierten Makrophagen sowohl die Freisetzung von OSM, als auch die Transkription von OSM und verschiedener Liganden der HER-Familie nachgewiesen.

8 REFERENCES

1. DePinho RA. The age of cancer. Nature. 2000;408(6809):248-54. Epub 2000/11/23.

2. Malvezzi M, Arfe A, Bertuccio P, Levi F, La Vecchia C, Negri E. European cancer mortality predictions for the year 2011. Annals of oncology : official journal of the European Society for Medical Oncology / ESMO. 2011;22(4):947-56. Epub 2011/02/10.

3. Hanahan D, Weinberg RA. The hallmarks of cancer. Cell. 2000;100(1):57-70. Epub 2000/01/27.

4. Albertson DG, Collins C, McCormick F, Gray JW. Chromosome aberrations in solid tumors. Nature genetics. 2003;34(4):369-76. Epub 2003/08/19.

5. Tlsty TD, Coussens LM. Tumor stroma and regulation of cancer development. Annu Rev Pathol. 2006;1:119-50. Epub 2007/11/28.

6. Mueller MM, Fusenig NE. Friends or foes - bipolar effects of the tumour stroma in cancer. Nat Rev Cancer. 2004;4(11):839-49. Epub 2004/11/02.

7. Campbell I, Qiu W, Haviv I. Genetic changes in tumour microenvironments. The Journal of pathology. 2011;223(4):450-8. Epub 2011/02/05.

8. Alberts B. Molecular biology of the cell. 4th ed. New York: Garland Science; 2002. xxxiv, 1548 p. p.

9. Egeblad M, Rasch MG, Weaver VM. Dynamic interplay between the collagen scaffold and tumor evolution. Current opinion in cell biology. 2010;22(5):697-706. Epub 2010/09/09.

10. Schedin P, Keely PJ. Mammary gland ECM remodeling, stiffness, and mechanosignaling in normal development and tumor progression. Cold Spring Harbor perspectives in biology. 2011;3(1):a003228. Epub 2010/10/29.

11. Whiteside TL. The tumor microenvironment and its role in promoting tumor growth. Oncogene. 2008;27(45):5904-12. Epub 2008/10/07.

12. Kalluri R, Zeisberg M. Fibroblasts in cancer. Nature reviews Cancer. 2006;6(5):392-401. Epub 2006/03/31.

13. Sappino AP, Schurch W, Gabbiani G. Differentiation repertoire of fibroblastic cells: expression of cytoskeletal proteins as marker of phenotypic modulations. Laboratory investigation; a journal of technical methods and pathology. 1990;63(2):144-61. Epub 1990/08/01.

14. Chang HY, Sneddon JB, Alizadeh AA, Sood R, West RB, Montgomery K, et al. Gene expression signature of fibroblast serum response predicts human cancer progression: similarities between tumors and wounds. PLoS biology. 2004;2(2):E7. Epub 2004/01/23.

15. Bhowmick NA, Neilson EG, Moses HL. Stromal fibroblasts in cancer initiation and progression. Nature. 2004;432(7015):332-7. Epub 2004/11/19.

16. Spaeth EL, Dembinski JL, Sasser AK, Watson K, Klopp A, Hall B, et al. Mesenchymal stem cell transition to tumor-associated fibroblasts contributes to fibrovascular network expansion and tumor progression. PloS one. 2009;4(4):e4992. Epub 2009/04/09.

17. Mahadevan D, Von Hoff DD. Tumor-stroma interactions in pancreatic ductal adenocarcinoma. Molecular cancer therapeutics. 2007;6(4):1186-97. Epub 2007/04/05.

18. Wang W, Li Q, Yamada T, Matsumoto K, Matsumoto I, Oda M, et al. Crosstalk to stromal fibroblasts induces resistance of lung cancer to epidermal growth factor receptor tyrosine kinase inhibitors. Clin Cancer Res. 2009;15(21):6630-8. Epub 2009/10/22.

19. Bergers G, Benjamin LE. Tumorigenesis and the angiogenic switch. Nature reviews Cancer. 2003;3(6):401-10. Epub 2003/06/05.

20. Folkman J. Tumor angiogenesis: therapeutic implications. The New England journal of medicine. 1971;285(21):1182-6. Epub 1971/11/18.

21. Dirkx AE, Oude Egbrink MG, Wagstaff J, Griffioen AW. Monocyte/macrophage infiltration in tumors: modulators of angiogenesis. Journal of leukocyte biology. 2006;80(6):1183-96. Epub 2006/09/26.

22. de Visser KE, Eichten A, Coussens LM. Paradoxical roles of the immune system during cancer development. Nature reviews Cancer. 2006;6(1):24-37. Epub 2006/01/07.

23. Grivennikov SI, Karin M. Inflammation and oncogenesis: a vicious connection. Current opinion in genetics & development. 2010;20(1):65-71. Epub 2009/12/29.

24. Pardoll D. Does the immune system see tumors as foreign or self? Annual review of immunology. 2003;21:807-39. Epub 2003/03/05.

25. Dranoff G. Coordinated tumor immunity. The Journal of clinical investigation. 2003;111(8):1116-8. Epub 2003/04/17.

26. Bingle L, Brown NJ, Lewis CE. The role of tumour-associated macrophages in tumour progression: implications for new anticancer therapies. The Journal of pathology. 2002;196(3):254-65. Epub 2002/02/22.

27. Condeelis J, Pollard JW. Macrophages: obligate partners for tumor cell migration, invasion, and metastasis. Cell. 2006;124(2):263-6. Epub 2006/01/28.

28. Murdoch C, Muthana M, Coffelt SB, Lewis CE. The role of myeloid cells in the promotion of tumour angiogenesis. Nature reviews Cancer. 2008;8(8):618-31. Epub 2008/07/18.

29. Solinas G, Germano G, Mantovani A, Allavena P. Tumor-associated macrophages (TAM) as major players of the cancer-related inflammation. Journal of leukocyte biology. 2009;86(5):1065-73. Epub 2009/09/11.

30. Loberg RD, Ying C, Craig M, Yan L, Snyder LA, Pienta KJ. CCL2 as an important mediator of prostate cancer growth in vivo through the regulation of macrophage infiltration. Neoplasia. 2007;9(7):556-62. Epub 2007/08/22.

31. Leek RD, Lewis CE, Whitehouse R, Greenall M, Clarke J, Harris AL. Association of macrophage infiltration with angiogenesis and prognosis in invasive breast carcinoma. Cancer research. 1996;56(20):4625-9. Epub 1996/10/15.

32. Scholl SM, Pallud C, Beuvon F, Hacene K, Stanley ER, Rohrschneider L, et al. Anti-colony-stimulating factor-1 antibody staining in primary breast adenocarcinomas correlates with marked inflammatory cell infiltrates and prognosis. Journal of the National Cancer Institute. 1994;86(2):120-6. Epub 1994/01/19.

33. Lewis CE, Pollard JW. Distinct role of macrophages in different tumor microenvironments. Cancer research. 2006;66(2):605-12. Epub 2006/01/21.

34. Ryder M, Ghossein RA, Ricarte-Filho JC, Knauf JA, Fagin JA. Increased density of tumor-associated macrophages is associated with decreased survival in advanced thyroid cancer. Endocrine-related cancer. 2008;15(4):1069-74. Epub 2008/08/23.

35. Pollard JW. Tumour-educated macrophages promote tumour progression and metastasis. Nature reviews Cancer. 2004;4(1):71-8. Epub 2004/01/07.

36. White JR, Harris RA, Lee SR, Craigon MH, Binley K, Price T, et al. Genetic amplification of the transcriptional response to hypoxia as a novel means of identifying regulators of angiogenesis. Genomics. 2004;83(1):1-8. Epub 2003/12/12.

37. Coffelt SB, Hughes R, Lewis CE. Tumor-associated macrophages: effectors of angiogenesis and tumor progression. Biochimica et biophysica acta. 2009;1796(1):11-8. Epub 2009/03/10.

38. Lin EY, Nguyen AV, Russell RG, Pollard JW. Colony-stimulating factor 1 promotes progression of mammary tumors to malignancy. The Journal of experimental medicine. 2001;193(6):727-40. Epub 2001/03/21.

39. Nowicki A, Szenajch J, Ostrowska G, Wojtowicz A, Wojtowicz K, Kruszewski AA, et al. Impaired tumor growth in colony-stimulating factor 1 (CSF-1)-deficient, macrophage-deficient op/op mouse: evidence for a role of CSF-1-dependent macrophages in formation of tumor stroma. International journal of cancer Journal international du cancer. 1996;65(1):112-9. Epub 1996/01/03.

40. Grivennikov SI, Greten FR, Karin M. Immunity, inflammation, and cancer. Cell. 2010;140(6):883-99. Epub 2010/03/23.

41. Ben-Neriah Y, Karin M. Inflammation meets cancer, with NF-kappaB as the matchmaker. Nature immunology. 2011;12(8):715-23. Epub 2011/07/21.

42. Coussens LM, Werb Z. Inflammation and cancer. Nature. 2002;420(6917):860-7. Epub 2002/12/20.

43. Mantovani A, Allavena P, Sica A, Balkwill F. Cancer-related inflammation. Nature. 2008;454(7203):436-44. Epub 2008/07/25.

44. Demaria S, Pikarsky E, Karin M, Coussens LM, Chen YC, El-Omar EM, et al. Cancer and inflammation: promise for biologic therapy. Journal of immunotherapy. 2010;33(4):335-51. Epub 2010/04/14.

45. Allavena P, Sica A, Garlanda C, Mantovani A. The Yin-Yang of tumor-associated macrophages in neoplastic progression and immune surveillance. Immunological reviews. 2008;222:155-61. Epub 2008/03/28.

46. Dvorak HF. Tumors: wounds that do not heal. Similarities between tumor stroma generation and wound healing. The New England journal of medicine. 1986;315(26):1650-9. Epub 1986/12/25.

47. Schafer M, Werner S. Cancer as an overhealing wound: an old hypothesis revisited. Nature reviews Molecular cell biology. 2008;9(8):628-38. Epub 2008/07/17.

48. Sparmann A, Bar-Sagi D. Ras-induced interleukin-8 expression plays a critical role in tumor growth and angiogenesis. Cancer cell. 2004;6(5):447-58. Epub 2004/11/16.

49. Ammirante M, Luo JL, Grivennikov S, Nedospasov S, Karin M. B-cell-derived lymphotoxin promotes castration-resistant prostate cancer. Nature. 2010;464(7286):302-5. Epub 2010/03/12.

50. Zhang B, Bowerman NA, Salama JK, Schmidt H, Spiotto MT, Schietinger A, et al. Induced sensitization of tumor stroma leads to eradication of established cancer by T cells. The Journal of experimental medicine. 2007;204(1):49-55. Epub 2007/01/11.

51. Vecchione L, Jacobs B, Normanno N, Ciardiello F, Tejpar S. EGFR-targeted therapy. Experimental cell research. 2011;317(19):2765-71. Epub 2011/09/20.

52. El-Rayes BF, LoRusso PM. Targeting the epidermal growth factor receptor. British journal of cancer. 2004;91(3):418-24. Epub 2004/07/09.

53. Prenzel N, Fischer OM, Streit S, Hart S, Ullrich A. The epidermal growth factor receptor family as a central element for cellular signal transduction and diversification. Endocrine-related cancer. 2001;8(1):11-31. Epub 2001/05/15.

54. Gherardi E, Birchmeier W, Birchmeier C, Woude GV. Targeting MET in cancer: rationale and progress. Nature reviews Cancer. 2012;12(2):89-103. Epub 2012/01/25.

55. de Bono JS, Yap TA. c-MET: an exciting new target for anticancer therapy. Therapeutic advances in medical oncology. 2011;3(1 Suppl):S3-5. Epub 2011/12/01.

56. Darnell JE. Validating Stat3 in cancer therapy. Nature medicine. 2005;11(6):595-6. Epub 2005/06/07.

57. Olayioye MA, Neve RM, Lane HA, Hynes NE. The ErbB signaling network: receptor heterodimerization in development and cancer. EMBO J. 2000;19(13):3159-67. Epub 2000/07/06.

58. Yarden Y, Sliwkowski MX. Untangling the ErbB signalling network. Nat Rev Mol Cell Biol. 2001;2(2):127-37. Epub 2001/03/17.

59. Hynes NE, Lane HA. ERBB receptors and cancer: the complexity of targeted inhibitors. Nature reviews Cancer. 2005;5(5):341-54. Epub 2005/05/03.

60. Citri A, Yarden Y. EGF-ERBB signalling: towards the systems level. Nat Rev Mol Cell Biol. 2006;7:505-16.

61. Salomon DS, Brandt R, Ciardiello F, Normanno N. Epidermal growth factor-related peptides and their receptors in human malignancies. Crit Rev Oncol Hematol. 1995;19(3):183-232. Epub 1995/07/01.

62. Normanno N, Bianco C, De Luca A, Maiello MR, Salomon DS. Target-based agents against ErbB receptors and their ligands: a novel approach to cancer treatment. Endocrine-related cancer. 2003;10(1):1-21. Epub 2003/03/26.

63. Goswami S, Sahai E, Wyckoff JB, Cammer M, Cox D, Pixley FJ, et al. Macrophages promote the invasion of breast carcinoma cells via a colony-stimulating factor-1/epidermal growth factor paracrine loop. Cancer research. 2005;65(12):5278-83. Epub 2005/06/17.

64. Rigo A, Gottardi M, Zamo A, Mauri P, Bonifacio M, Krampera M, et al. Macrophages may promote cancer growth via a GM-CSF/HB-EGF paracrine loop that is enhanced by CXCL12. Molecular cancer. 2010;9:273. Epub 2010/10/16.

65. Amin DN, Hida K, Bielenberg DR, Klagsbrun M. Tumor endothelial cells express epidermal growth factor receptor (EGFR) but not ErbB3 and are responsive to EGF and to EGFR kinase inhibitors. Cancer research. 2006;66(4):2173-80. Epub 2006/02/21.

66. De Luca A, Carotenuto A, Rachiglio A, Gallo M, Maiello MR, Aldinucci D, et al. The role of the EGFR signaling in tumor microenvironment. Journal of cellular physiology. 2008;214(3):559-67. Epub 2007/09/27.

67. Fornaro L, Lucchesi M, Caparello C, Vasile E, Caponi S, Ginocchi L, et al. Anti-HER agents in gastric cancer: from bench to bedside. Nature reviews Gastroenterology & hepatology. 2011;8(7):369-83. Epub 2011/06/08.

68. NationalCancerInstitute. Cancer Drug Information. National Institutes of Health; 2012; Available from: http://www.cancer.gov/cancertopics/druginfo/alphalist.

69. Balak MN, Gong Y, Riely GJ, Somwar R, Li AR, Zakowski MF, et al. Novel D761Y and common secondary T790M mutations in epidermal growth factor receptor-mutant lung adenocarcinomas with acquired resistance to kinase inhibitors. Clin Cancer Res. 2006;12(21):6494-501. Epub 2006/11/07.

70. Engelman JA, Zejnullahu K, Mitsudomi T, Song Y, Hyland C, Park JO, et al. MET amplification leads to gefitinib resistance in lung cancer by activating ERBB3 signaling. Science. 2007;316(5827):1039-43. Epub 2007/04/28.

71. Pao W, Miller VA, Politi KA, Riely GJ, Somwar R, Zakowski MF, et al. Acquired resistance of lung adenocarcinomas to gefitinib or erlotinib is associated with a second mutation in the EGFR kinase domain. PLoS Med. 2005;2(3):e73. Epub 2005/03/02.

72. Birchmeier C, Gherardi E. Developmental roles of HGF/SF and its receptor, the c-Met tyrosine kinase. Trends in cell biology. 1998;8(10):404-10. Epub 1998/10/28.

73. Huh CG, Factor VM, Sanchez A, Uchida K, Conner EA, Thorgeirsson SS. Hepatocyte growth factor/c-met signaling pathway is required for efficient liver regeneration and repair. Proceedings of the National Academy of Sciences of the United States of America. 2004;101(13):4477-82. Epub 2004/04/09.

74. Birchmeier C, Birchmeier W, Gherardi E, Vande Woude GF. Met, metastasis, motility and more. Nature reviews Molecular cell biology. 2003;4(12):915-25. Epub 2003/12/20.

75. Nakamura T, Sakai K, Nakamura T, Matsumoto K. Hepatocyte growth factor twenty years on: Much more than a growth factor. Journal of gastroenterology and hepatology. 2011;26 Suppl 1:188-202. Epub 2011/01/14.

76. Ohmichi H, Koshimizu U, Matsumoto K, Nakamura T. Hepatocyte growth factor (HGF) acts as a mesenchyme-derived morphogenic factor during fetal lung development. Development. 1998;125(7):1315-24. Epub 1998/05/09.

77. Trusolino L, Comoglio PM. Scatter-factor and semaphorin receptors: cell signalling for invasive growth. Nature reviews Cancer. 2002;2(4):289-300. Epub 2002/05/11.

78. Rong S, Segal S, Anver M, Resau JH, Vande Woude GF. Invasiveness and metastasis of NIH 3T3 cells induced by Met-hepatocyte growth factor/scatter factor autocrine stimulation. Proceedings of the National Academy of Sciences of the United States of America. 1994;91(11):4731-5. Epub 1994/05/24.

79. Takayama H, LaRochelle WJ, Sharp R, Otsuka T, Kriebel P, Anver M, et al. Diverse tumorigenesis associated with aberrant development in mice overexpressing hepatocyte growth factor/scatter factor. Proceedings of the National Academy of Sciences of the United States of America. 1997;94(2):701-6. Epub 1997/01/21.

80. Weidner KM, Behrens J, Vandekerckhove J, Birchmeier W. Scatter factor: molecular characteristics and effect on the invasiveness of epithelial cells. J Cell Biol. 1990;111(5 Pt 1):2097-108. Epub 1990/11/01.

81. Shattuck DL, Miller JK, Carraway KL, 3rd, Sweeney C. Met receptor contributes to trastuzumab resistance of Her2-overexpressing breast cancer cells. Cancer research. 2008;68(5):1471-7. Epub 2008/03/05.

82. Mueller KL, Yang ZQ, Haddad R, Ethier SP, Boerner JL. EGFR/Met association regulates EGFR TKI resistance in breast cancer. Journal of molecular signaling. 2010;5:8. Epub 2010/07/14.

83. Suda K, Murakami I, Katayama T, Tomizawa K, Osada H, Sekido Y, et al. Reciprocal and complementary role of MET amplification and EGFR T790M mutation in acquired resistance to kinase inhibitors in lung cancer. Clinical cancer research : an official journal of the American Association for Cancer Research. 2010;16(22):5489-98. Epub 2010/11/11.

84. Liska D, Chen CT, Bachleitner-Hofmann T, Christensen JG, Weiser MR. HGF rescues colorectal cancer cells from EGFR inhibition via MET activation. Clinical cancer research : an official journal of the American Association for Cancer Research. 2011;17(3):472-82. Epub 2010/11/26.

85. Wang R, Ferrell LD, Faouzi S, Maher JJ, Bishop JM. Activation of the Met receptor by cell attachment induces and sustains hepatocellular carcinomas in transgenic mice. The Journal of cell biology. 2001;153(5):1023-34. Epub 2001/05/31.

86. Cohen M, Marchand-Adam S, Lecon-Malas V, Marchal-Somme J, Boutten A, Durand G, et al. HGF synthesis in human lung fibroblasts is regulated by oncostatin M. American journal of physiology Lung cellular and molecular physiology. 2006;290(6):L1097-103. Epub 2006/05/11.

87. Matsumoto K, Okazaki H, Nakamura T. Novel function of prostaglandins as inducers of gene expression of HGF and putative mediators of tissue regeneration. Journal of biochemistry. 1995;117(2):458-64. Epub 1995/02/01.

88. Burke B, Giannoudis A, Corke KP, Gill D, Wells M, Ziegler-Heitbrock L, et al. Hypoxia-induced gene expression in human macrophages: implications for ischemic tissues and hypoxia-regulated gene therapy. The American journal of pathology. 2003;163(4):1233-43. Epub 2003/09/26.

89. NationalCancerInstitute. HGF and c-Met Targeted Drug Development for Oncology. 2012; Available from: https://ccrod.cancer.gov/confluence/display/CCRHGF/Home.

90. Rawlings JS, Rosler KM, Harrison DA. The JAK/STAT signaling pathway. Journal of cell science. 2004;117(Pt 8):1281-3. Epub 2004/03/17.

91. Schindler C, Levy DE, Decker T. JAK-STAT signaling: from interferons to cytokines. The Journal of biological chemistry. 2007;282(28):20059-63. Epub 2007/05/16.

92. Heinrich PC, Behrmann I, Muller-Newen G, Schaper F, Graeve L. Interleukin-6-type cytokine signalling through the gp130/Jak/STAT pathway. The Biochemical journal. 1998;334 (Pt 2):297-314. Epub 1998/08/26.

93. Gao SP, Bromberg JF. Touched and moved by STAT3. Science's STKE : signal transduction knowledge environment. 2006;2006(343):pe30. Epub 2006/07/13.

94. Yu H, Pardoll D, Jove R. STATs in cancer inflammation and immunity: a leading role for STAT3. Nature reviews Cancer. 2009;9(11):798-809. Epub 2009/10/24.

95. Yu H, Kortylewski M, Pardoll D. Crosstalk between cancer and immune cells: role of STAT3 in the tumour microenvironment. Nature reviews Immunology. 2007;7(1):41-51. Epub 2006/12/23.

96. Yu H, Jove R. The STATs of cancer--new molecular targets come of age. Nature reviews Cancer. 2004;4(2):97-105. Epub 2004/02/18.

97. Yu CL, Meyer DJ, Campbell GS, Larner AC, Carter-Su C, Schwartz J, et al. Enhanced DNA-binding activity of a Stat3-related protein in cells transformed by the Src oncoprotein. Science. 1995;269(5220):81-3. Epub 1995/07/07.

98. Bromberg JF, Wrzeszczynska MH, Devgan G, Zhao Y, Pestell RG, Albanese C, et al. Stat3 as an oncogene. Cell. 1999;98(3):295-303. Epub 1999/08/24.

99. Leeman RJ, Lui VW, Grandis JR. STAT3 as a therapeutic target in head and neck cancer. Expert opinion on biological therapy. 2006;6(3):231-41. Epub 2006/03/01.

100. Bromberg J. Stat proteins and oncogenesis. The Journal of clinical investigation. 2002;109(9):1139-42. Epub 2002/05/08.

101. Numasaki M, Watanabe M, Suzuki T, Takahashi H, Nakamura A, McAllister F, et al. IL-17 enhances the net angiogenic activity and in vivo growth of human non-small cell lung cancer in SCID mice through promoting CXCR-2-dependent angiogenesis. Journal of immunology. 2005;175(9):6177-89. Epub 2005/10/21.

102. Zorn E, Nelson EA, Mohseni M, Porcheray F, Kim H, Litsa D, et al. IL-2 regulates FOXP3 expression in human CD4+CD25+ regulatory T cells through a STAT-dependent mechanism and induces the expansion of these cells in vivo. Blood. 2006;108(5):1571-9. Epub 2006/04/29.

103. Takeda K, Clausen BE, Kaisho T, Tsujimura T, Terada N, Forster I, et al. Enhanced Th1 activity and development of chronic enterocolitis in mice devoid of Stat3 in macrophages and neutrophils. Immunity. 1999;10(1):39-49. Epub 1999/02/19.

104. Kinjyo I, Inoue H, Hamano S, Fukuyama S, Yoshimura T, Koga K, et al. Loss of SOCS3 in T helper cells resulted in reduced immune responses and hyperproduction of interleukin 10 and transforming growth factor-beta 1. The Journal of experimental medicine. 2006;203(4):1021-31. Epub 2006/04/12.

105. Turkson J. STAT proteins as novel targets for cancer drug discovery. Expert opinion on therapeutic targets. 2004;8(5):409-22. Epub 2004/10/08.

106. Mankan AK, Greten FR. Inhibiting signal transducer and activator of transcription 3: rationality and rationale design of inhibitors. Expert opinion on investigational drugs. 2011;20(9):1263-75. Epub 2011/07/15.

107. Lee H, Pal SK, Reckamp K, Figlin RA, Yu H. STAT3: a target to enhance antitumor immune response. Current topics in microbiology and immunology. 2011;344:41-59. Epub 2010/06/03.

108. NationalCancerInstitute. Clinical Trails: STAT3 inhibitor OPB-31121. National Institutes of Health; 2012; Available from: http://www.cancer.gov/clinicaltrials/search/results?protocolsearchid=8751122.

109. NationalCancerInstitute. STAT3 inhibitors. National Institutes of Health; 2012; Available from: http://www.cancer.gov/drugdictionary.

110. Verstovsek S, Kantarjian H, Mesa RA, Pardanani AD, Cortes-Franco J, Thomas DA, et al. Safety and efficacy of INCB018424, a JAK1 and JAK2 inhibitor, in myelofibrosis. The New England journal of medicine. 2010;363(12):1117-27. Epub 2010/09/17.

111. Ostojic A, Vrhovac R, Verstovsek S. Ruxolitinib: a new JAK1/2 inhibitor that offers promising options for treatment of myelofibrosis. Future oncology. 2011;7(9):1035-43. Epub 2011/09/17.

112. Santos FP, Verstovsek S. JAK2 inhibitors: what's the true therapeutic potential? Blood reviews. 2011;25(2):53-63. Epub 2010/11/26.

113. Hedvat M, Huszar D, Herrmann A, Gozgit JM, Schroeder A, Sheehy A, et al. The JAK2 inhibitor AZD1480 potently blocks Stat3 signaling and oncogenesis in solid tumors. Cancer cell. 2009;16(6):487-97. Epub 2009/12/08.

114. Colombo MP, Mantovani A. Targeting myelomonocytic cells to revert inflammation-dependent cancer promotion. Cancer research. 2005;65(20):9113-6. Epub 2005/10/19.

115. Albini A, Sporn MB. The tumour microenvironment as a target for chemoprevention. Nature reviews Cancer. 2007;7(2):139-47. Epub 2007/01/16.

116. Dineen SP, Lynn KD, Holloway SE, Miller AF, Sullivan JP, Shames DS, et al. Vascular endothelial growth factor receptor 2 mediates macrophage infiltration into orthotopic pancreatic tumors in mice. Cancer research. 2008;68(11):4340-6. Epub 2008/06/04.

117. Melani C, Sangaletti S, Barazzetta FM, Werb Z, Colombo MP. Amino-biphosphonate-mediated MMP-9 inhibition breaks the tumor-bone marrow axis responsible for myeloid-derived suppressor cell expansion and macrophage infiltration in tumor stroma. Cancer research. 2007;67(23):11438-46. Epub 2007/12/07.

118. Giraudo E, Inoue M, Hanahan D. An amino-bisphosphonate targets MMP-9-expressing macrophages and angiogenesis to impair cervical carcinogenesis. The Journal of clinical investigation. 2004;114(5):623-33. Epub 2004/09/03.

119. Coussens LM, Tinkle CL, Hanahan D, Werb Z. MMP-9 supplied by bone marrow-derived cells contributes to skin carcinogenesis. Cell. 2000;103(3):481-90. Epub 2000/11/18.

120. Kenny PA, Lee GY, Bissell MJ. Targeting the tumor microenvironment. Frontiers in bioscience : a journal and virtual library. 2007;12:3468-74. Epub 2007/05/09.

121. Chan AT, Ogino S, Fuchs CS. Aspirin use and survival after diagnosis of colorectal cancer. JAMA : the journal of the American Medical Association. 2009;302(6):649-58. Epub 2009/08/13.

122. Denardo DG, Brennan DJ, Rexhepaj E, Ruffell B, Shiao SL, Madden SF, et al. Leukocyte Complexity Predicts Breast Cancer Survival and Functionally Regulates Response to Chemotherapy. Cancer discovery. 2011;1:54-67. Epub 2011/11/01.

123. Filardo EJ. Epidermal growth factor receptor (EGFR) transactivation by estrogen via the G-protein-coupled receptor, GPR30: a novel signaling pathway with potential significance for breast cancer. The Journal of steroid biochemistry and molecular biology. 2002;80(2):231-8. Epub 2002/03/19.

124. Fischer OM, Giordano S, Comoglio PM, Ullrich A. Reactive oxygen species mediate Met receptor transactivation by G protein-coupled receptors and the epidermal growth factor receptor in human carcinoma cells. J Biol Chem. 2004;279(28):28970-8. Epub 2004/05/05.

125. Gschwind A, Zwick E, Prenzel N, Leserer M, Ullrich A. Cell communication networks: epidermal growth factor receptor transactivation as the paradigm for interreceptor signal transmission. Oncogene. 2001;20(13):1594-600. Epub 2001/04/21.

126. Singh B, Schneider M, Knyazev P, Ullrich A. UV-induced EGFR signal transactivation is dependent on proligand shedding by activated metalloproteases in skin cancer cell lines. International journal of cancer Journal international du cancer. 2009;124(3):531-9. Epub 2008/11/13.

127. Gschwind A, Hart S, Fischer OM, Ullrich A. TACE cleavage of proamphiregulin regulates GPCR-induced proliferation and motility of cancer cells. The EMBO journal. 2003;22(10):2411-21. Epub 2003/05/14.

128. Hackel PO, Gishizky M, Ullrich A. Mig-6 is a negative regulator of the epidermal growth factor receptor signal. Biological chemistry. 2001;382(12):1649-62. Epub 2002/02/15.

129. Pante G, Thompson J, Lamballe F, Iwata T, Ferby I, Barr FA, et al. Mitogen-inducible gene 6 is an endogenous inhibitor of HGF/Met-induced cell migration and neurite growth. The Journal of cell biology. 2005;171(2):337-48. Epub 2005/10/26.

130. Scheving LA, Stevenson MC, Taylormoore JM, Traxler P, Russell WE. Integral role of the EGF receptor in HGF-mediated hepatocyte proliferation. Biochemical and biophysical research communications. 2002;290(1):197-203. Epub 2002/01/10.

131. Spix JK, Chay EY, Block ER, Klarlund JK. Hepatocyte growth factor induces epithelial cell motility through transactivation of the epidermal growth factor receptor. Exp Cell Res. 2007;313(15):3319-25. Epub 2007/07/24.

132. Reznik TE, Sang Y, Ma Y, Abounader R, Rosen EM, Xia S, et al. Transcription-dependent epidermal growth factor receptor activation by hepatocyte growth factor. Mol Cancer Res. 2008;6(1):139-50. Epub 2008/02/01.

133. Pai R, Nakamura T, Moon WS, Tarnawski AS. Prostaglandins promote colon cancer cell invasion; signaling by cross-talk between two distinct growth factor receptors. FASEB J. 2003;17(12):1640-7. Epub 2003/09/06.

134. Bessard A, Fremin C, Ezan F, Fautrel A, Gailhouste L, Baffet G. RNAi-mediated ERK2 knockdown inhibits growth of tumor cells in vitro and in vivo. Oncogene. 2008;27(40):5315-25. Epub 2008/06/04.

135. Ikeda JI, Morii E, Kimura H, Tomita Y, Takakuwa T, Hasegawa JI, et al. Epigenetic regulation of the expression of the novel stem cell marker CDCP1 in cancer cells. The Journal of pathology. 2006;210(1):75-84. Epub 2006/07/11.

136. Scherl-Mostageer M, Sommergruber W, Abseher R, Hauptmann R, Ambros P, Schweifer N. Identification of a novel gene, CDCP1, overexpressed in human colorectal cancer. Oncogene. 2001;20(32):4402-8. Epub 2001/07/24.

137. Awakura Y, Nakamura E, Takahashi T, Kotani H, Mikami Y, Kadowaki T, et al. Microarray-based identification of CUB-domain containing protein 1 as a potential prognostic marker in conventional renal cell carcinoma. Journal of cancer research and clinical oncology. 2008;134(12):1363-9. Epub 2008/05/17.

138. Ikeda J, Oda T, Inoue M, Uekita T, Sakai R, Okumura M, et al. Expression of CUB domain containing protein (CDCP1) is correlated with prognosis and survival of patients with adenocarcinoma of lung. Cancer science. 2009;100(3):429-33. Epub 2008/12/17.

139. Uekita T, Tanaka M, Takigahira M, Miyazawa Y, Nakanishi Y, Kanai Y, et al. CUB-domain-containing protein 1 regulates peritoneal dissemination of gastric scirrhous carcinoma. The American journal of pathology. 2008;172(6):1729-39. Epub 2008/05/10.

140. Zhuang G, Brantley-Sieders DM, Vaught D, Yu J, Xie L, Wells S, et al. Elevation of receptor tyrosine kinase EphA2 mediates resistance to trastuzumab therapy. Cancer research. 2010;70(1):299-308. Epub 2009/12/24.

141. Liu L, Greger J, Shi H, Liu Y, Greshock J, Annan R, et al. Novel mechanism of lapatinib resistance in HER2-positive breast tumor cells: activation of AXL. Cancer research. 2009;69(17):6871-8. Epub 2009/08/13.

142. Lin EY, Pollard JW. Macrophages: modulators of breast cancer progression. Novartis Foundation symposium. 2004;256:158-68; discussion 68-72, 259-69. Epub 2004/03/19.

143. Giltnane JM, Ryden L, Cregger M, Bendahl PO, Jirstrom K, Rimm DL. Quantitative measurement of epidermal growth factor receptor is a negative predictive factor for tamoxifen response in hormone receptor positive premenopausal breast cancer. Journal of clinical oncology : official journal of the American Society of Clinical Oncology. 2007;25(21):3007-14. Epub 2007/07/20.

144. Rimawi MF, Shetty PB, Weiss HL, Schiff R, Osborne CK, Chamness GC, et al. Epidermal growth factor receptor expression in breast cancer association with biologic phenotype and clinical outcomes. Cancer. 2010;116(5):1234-42. Epub 2010/01/19.

145. Dennison SK, Jacobs SA, Wilson JW, Seeger J, Cescon TP, Raymond JM, et al. A phase II clinical trial of ZD1839 (Iressa) in combination with docetaxel as first-line treatment in patients with advanced breast cancer. Investigational new drugs. 2007;25(6):545-51. Epub 2007/06/15.

146. Ciardiello F, Troiani T, Caputo F, De Laurentiis M, Tortora G, Palmieri G, et al. Phase II study of gefitinib in combination with docetaxel as first-line therapy in metastatic breast cancer. British journal of cancer. 2006;94(11):1604-9. Epub 2006/05/11.

147. Twelves C, Trigo JM, Jones R, De Rosa F, Rakhit A, Fettner S, et al. Erlotinib in combination with capecitabine and docetaxel in patients with metastatic breast cancer: a dose-escalation study. European journal of cancer. 2008;44(3):419-26. Epub 2008/02/06.

148. Ongusaha PP, Kwak JC, Zwible AJ, Macip S, Higashiyama S, Taniguchi N, et al. HB-EGF is a potent inducer of tumor growth and angiogenesis. Cancer research. 2004;64(15):5283-90. Epub 2004/08/04.

149. Miyamoto S, Hirata M, Yamazaki A, Kageyama T, Hasuwa H, Mizushima H, et al. Heparin-binding EGF-like growth factor is a promising target for ovarian cancer therapy. Cancer research. 2004;64(16):5720-7. Epub 2004/08/18.

150. Wyckoff J, Wang W, Lin EY, Wang Y, Pixley F, Stanley ER, et al. A paracrine loop between tumor cells and macrophages is required for tumor cell migration in mammary tumors. Cancer research. 2004;64(19):7022-9. Epub 2004/10/07.

151. Kastl SP, Speidl WS, Katsaros KM, Kaun C, Rega G, Assadian A, et al. Thrombin induces the expression of oncostatin M via AP-1 activation in human macrophages: a link between coagulation and inflammation. Blood. 2009;114(13):2812-8. Epub 2009/08/05.

152. Queen MM, Ryan RE, Holzer RG, Keller-Peck CR, Jorcyk CL. Breast cancer cells stimulate neutrophils to produce oncostatin M: potential implications for tumor progression. Cancer research. 2005;65(19):8896-904. Epub 2005/10/06.

153. Brown TJ, Lioubin MN, Marquardt H. Purification and characterization of cytostatic lymphokines produced by activated human T lymphocytes. Synergistic antiproliferative activity of transforming growth factor beta 1, interferon-gamma, and oncostatin M for human melanoma cells. Journal of immunology. 1987;139(9):2977-83. Epub 1987/11/01.

154. Boniface K, Diveu C, Morel F, Pedretti N, Froger J, Ravon E, et al. Oncostatin M secreted by skin infiltrating T lymphocytes is a potent keratinocyte activator involved in skin inflammation. Journal of immunology. 2007;178(7):4615-22. Epub 2007/03/21.

155. Crichton MB, Nichols JE, Zhao Y, Bulun SE, Simpson ER. Expression of transcripts of interleukin-6 and related cytokines by human breast tumors, breast cancer cells, and adipose stromal cells. Molecular and cellular endocrinology. 1996;118(1-2):215-20. Epub 1996/04/19.

156. Jorcyk CL, Holzer RG, Ryan RE. Oncostatin M induces cell detachment and enhances the metastatic capacity of T-47D human breast carcinoma cells. Cytokine. 2006;33(6):323-36. Epub 2006/05/23.

9 APPENDIX

9.1 Abbreviations

Abl	Abelson leukemia
AP-1	activator protein 1
APS	ammonium persulfate
AR	amphiregulin
ATCC	American type culture collection, USA
Axl	tyrosine-protein kinase receptor UFO
B	blocking antibody
BAG2	BCL2-associated athanogene 2
Bcr	breakpoint-cluster region
Bcr-Abl	fusion of the breakpoint-cluster region (Bcr) and Abelson leukemia (Abl) proteins
bFGF	basic fibroblast growth factor
BSA	bovine serum albumin
C	control IgG
CAF	cancer-associated fibroblast
CBL	casitas B-lineage lymphoma
CBLB	casitas B-lineage lymphoma B
CCL	C-C motif chemokine ligand 2
CD	cluster of differentiation
CD14	cluster of differentiation 14
CD64	cluster of differentiation 64
CDCP1	CUB domain containing protein
cDNA	complementary DNA
CO2	carbon dioxide
COL17A	collagen, type XVII, alpha 1
COX-2	cyclooxygenase 2
CM	conditioned medium
ctrl.	control
DMEM	Dulbecco's modified eagle medium
DNA	deoxyribonucleic acid
dNTP	deoxyribonucleoside triphosphate
DMSO	dimethylsulfoxide
ECL	enhanced chemiluminescence
ECM	extracellular matrix
E.coli	Escherichia coli
EDTA	ethylenediaminetetraacetic acid
EGF	epidermal growth factor
EGFR	epidermal growth factor receptor

ELISA	enzyme-linked immunosorbent assay
EphA2	ephrin type-A receptor 2
Erk	extracellular signal-regulated kinase
F4/80	mouse homolog of the human epidermal growth factor-like module containing mucin-like hormone receptor-like 1 (EMR1)
FACS	fluorescence-activated cell sorting
FCS	fetal calf serum
FGF	fibroblast growth factor
FITC	fluorescein isothiocyanate
GPCR5A	G-protein coupled receptor family C group 5 member A
HB-EGF	heparin-binding EGF-like growth factor
HEPES	4-(2-hydroxyethyl)-1-piperazineethanesulfonic acid
HER2, 3, 4	human EGF Receptor 2, 3, 4
HGF	hepatocyte growth factor
HMEC	human mammary epithelial cells
HNTG	HEPES-, NaCl-, Triton X-100- and glycerol-containing buffer
HRGβ1	heregulin beta-1
HRP	horseradish peroxidase
I	intensity
IL-	interleukin-
IP	immunoprecipitation
IPI	international protein index
ITCH	E3 ubiquitin-protein ligase
ITGB4	integrin beta-4
JAK1	janus kinase 1
JNK	jun N-terminal kinase
LC	liquid chromatography
LIF	leukemia inhibitory factor
MAD-NT	macrophage differentiation, non-terminal
MAPK	mitogen-activated protein kinase
MEK	MAPK kinase
Met	hepatocyte growth factor receptor
Mig6	mitogen-inducible gene 6
MMP	matrix metalloprotease
MΦ	macrophage/monocyte
MS	mass spectrometry
MW	molecular weight
m/z	mass to charge ratio
NET	NaCl-, EDTA- and Tris-containing buffer
NFκB	nuclear factor κB
OSM	oncostatin M
PAGE	polyacrylamide gel electrophoresis
PBMCs	peripheral blood monocytes
PBS	phosphate buffered saline
PCR	polymerase chain reaction
PE	phycoerythrin
PI3K	phosphatidylinositol 3-kinase

PI3K p110β	phosphatidylinositol 3-kinase 110 kilodalton catalytic subunit beta
PI3K p85β	phosphatidylinositol 3-kinase 85 kilodalton regulatory subunit beta
PMSF	phenylmethanesulfonylfluoride
PTPRF	protein tyrosine phosphatase, receptor type, F
qPCR	quantitative polymerase chain reaction
RNA	ribonucleic acid
RNF149	ring finger protein 149, E3 ubiquitin-protein ligase
rpm	rounds per minute
RPMI	Roswell Park Memorial Institute medium
RT	room temperature
SAPK	stress-activated protein kinase
SCC	squamous cell carcinoma
SD	standard deviation
SDCBP	syndecan binding protein
SDS	sodium dodecyl sulfate
SEM	standard error of the mean
SHC1	src homology 2 domain containing transforming protein 1
SILAC	stable isotope labeling by amino acids in cell culture
siRNA	small interfering ribonucleic acid
SLC20A1	solute carrier family 20 (phosphate transporter), member 1
SN	supernatant
SOS2	son of sevenless 2
Src	homologue to v-src (sarcoma viral oncogene)
STAT	signal transducer and activator of transcription
STX6	syntaxin 6
TAE	tris base-, acetic acid- and EDTA-containing buffer
TAM	tumor-associated macrophage
TEMED	N, N, N‘, N‘-tetramethyletylendiamine
TFRC	transferrin receptor
TGFα	transforming growth factor alpha
TGFβ	Transforming growth factor beta
TGFBR2	transforming growth factor, beta receptor II
TK	tyrosine kinase
TKI	tyrosine kinase inhibitor
TNFRSF21	tumor necrosis factor receptor superfamily, member 21
TNS4	tensin 4
Treg	T regulatory cell
VEGF	vascular endothelial growth factor
WWP2	WW domain containing E3 ubiquitin protein ligase 2

Units

A	Ampere
bp	base pairs
°C	degree Celsius
Da	Dalton
g	gravitational force
h	hour
kDa	kilodalton
kb	kilobase
l	liter
M	molar
min	minute
m	milli
ml	milliliter
mM	millimolar
mA	milliampere
n	nano
ng	nanogram
p	pico
pg	picogram
µ	micro
µg	microgram
µl	microliter
µM	micromolar
V	Volt

9.2 Acknowledgements

I especially want to thank my supervisor Prof. Axel Ullrich for all his great support, ideas and guidance throughout my work in the department of molecular biology at the Max Planck Institute of Biochemistry. Thank you for a great atmosphere, for keeping an outstanding team spirit between the department members and for supporting many parties!

In particular, I am very grateful to Prof. Claus Schwechheimer for supervising and promoting this thesis at the Technical University of Munich.

My thanks go to all the present and former members of the Ullrich department who made my years at the MPI such a joyful time. Thank you Martin, Matthias, Robert, Caro, Pavlos, Mathias, Michaela, Philipp, Torsten, Claus, Philip, Thomas, Jacqui, Nina, Markus, Pawan, Hamid, Yasuyuki, Kinga, Zoltan, Vijey, Emanuele, Chitra, Jingui, Pjotr, Tatjana, Laura, Dmitry, Stephan, Thiemo, Christoph, Felix, Kathrin, Susanne B, Verena, Isabella, Silvia, Bianca, Renate G., Renate H., Judith, Susanne W. and Attilio for a lot of fun during an ordinary working day.

My special thanks go to Tatjana and Pjotr for help, fruitful discussion and for their outstanding humor.

Many thanks to Michaela for all the advice in the mass-spectrometry experiment, to Philip for the collaboration in the human primary macrophage project and finally to Martin and Yasuyuki for many valuable discussions, suggestions and advice in different aspects of this work.

I want to especially thank Laura, Martin, Robert, Yasuyuki, Pavlos, Dmitry, Bianca and Thiemo for their support and friendship.

Abschließend möchte ich ganz herzlich meiner Familie für die Unterstützung und Motivation sowie für die erholsamen Aufenthalte zu Hause während der Zeit dieser Doktorarbeit danken.